

Lift of non-equilibrium Quantum dynamics: an inverse Adiabatic elimination Approach

Zexi Fan* Bowen Li† Jianfeng Lu‡

22nd November 2025

We extend the mathematical framework of “lifting” in [LL25, EL24a] to accelerate convergence to Nonequilibrium Steady States (NESS), a regime where the breaking of Detailed Balance Condition (DBC) renders traditional methods ineffective. We focus on NESS generated by a weak non-conservative perturbation. Our approach formally analyzes the full system generator $\mathcal{L} = \gamma\mathcal{R} + \mathcal{V}$ as a hypocoercive lift of its own effective slow, non-reversible generator \mathcal{L}_O . To analyze its convergence, we introduce the *Adiabatic Embedding (Ad Embed)* structure, which employs an Approximate Quadratic Form Condition to rigorously capture the non-equilibrium perturbation as an explicitly bounded error. By adapting the Flow Poincaré inequality framework [EGH⁺25, LL24] to this structure, we establish an explicit connection between the convergence rates $\nu(\mathcal{L})$ and $s(\mathcal{L}_O)$. We prove that under appropriate structural conditions and an asymptotic regime where the non-equilibrium perturbation is subdominant to the slow dynamics gap ($\eta \ll s(\mathcal{L}_O)^2$), the optimal “diffusive-to-ballistic” speedup, $\nu(\mathcal{L}) = \Theta(\sqrt{s(\mathcal{L}_O)})$, known for equilibrium lifts, is also achievable in this NESS setting. We validate our theoretical framework with numerical experiments on both classical nonequilibrium Langevin and quantum boundary-driven Zeno spin chain systems.

Keywords: Lift; Adiabatic elimination; Nonequilibrium dynamics; Open quantum system; Hypocoercivity.

*School of Mathematics, Peking University. E-Mail: 2200010816@stu.pku.edu.cn

†Department of Mathematics, City University of Hong Kong. E-Mail: boweli4@cityu.edu.hk

‡Department of Mathematics, Department of Physics, Department of Chemistry, Duke University.
E-Mail: jianfeng@math.duke.edu

1. Introduction

The dynamics of open quantum systems, describing entities interacting with uncontrollable environments, are fundamental to virtually all areas of modern quantum physics. When the environment is large and memoryless, the system’s evolution is often well-approximated by a quantum Markov semigroup (QMS), generated by a Lindbladian \mathcal{L} [GKS76]. A central question concerns the long-time behavior: Does the system relax, and if so, how quickly does it approach its stationary state(s)? For systems coupled to a single thermal bath, the dynamics typically relaxes towards thermal equilibrium, characterized by a Gibbs state σ_{eq} [HJLZ23, GHC⁺25]. The generator often satisfies a detailed balance condition (DBC) with respect to σ_{eq} , rendering the dynamics effectively “reversible” [DOvdH25, RLC21]. Convergence analysis in this setting is relatively well-developed, leveraging tools like spectral gap estimates derived from DBC [Pav14, FPSU24] or entropy decay methods like modified logarithmic Sobolev inequalities (MLSI) [APS22, SS21].

However, many crucial scenarios involve systems driven out of equilibrium. Examples include quantum transport setups with boundary reservoirs held at different temperatures or chemical potentials [LPS22], driven-dissipative systems realizing novel quantum phases [LB15], and autonomously stabilized quantum states achieved via reservoir engineering [Sel24, RRS24, Nas25]. In such cases, the system typically evolves towards a nonequilibrium steady state (NESS), σ_{NESS} , which breaks detailed balance condition (i.e. $\mathcal{L}^\dagger \sigma_{NESS} = 0$ but \mathcal{L} is non-reversible w.r.t σ_{NESS}) and may sustain currents or exhibit non-thermal properties [LPS22]. Analyzing convergence to NESS is significantly more challenging than standard equilibrium tools, as the standard toolbox often provides insufficient or overly pessimistic estimates, and the dynamics themselves present complex behaviors [SVdPZ25], such as Zeno localization [MBHR21, PPS25], etc.

A common approach to studying such complex dynamics is to separate the fast and slow timescales, known as adiabatic elimination (AE) [GB24, ASR16, TR25]. Given a generator $\mathcal{L}_\gamma = \mathcal{V} + \gamma \mathcal{R}$, where \mathcal{R} induces rapid relaxation (rate $\gamma \gg 1$) towards its kernel (we call it slow subspace or decoherence-free subspace $\mathcal{H}_S = \ker(\mathcal{R})$), AE then derives an effective generator \mathcal{L}_O acting solely on \mathcal{H}_S . This is usually achieved through perturbative expansions and projector operator techniques, effectively “integrating out” the fast variables governed by \mathcal{R} [TR25, ASR16]. AE method, together with other highly relevant techniques in the quantum nonequilibrium dynamical analysis toolbox, including Schrieffer-Wolff transform [MMG22], response theory [ABFJ16], and Zeno dynamics [PEPS18, PP21], etc., paved the way for deriving and investigating master equations that are essential in quantum optics and reservoir engineering where eliminating fast modes yields the desired system [Sel24]. A key observation is that the resulting \mathcal{L}_O frequently describes nonequilibrium dynamics as well, capturing the slow physics induced by the interplay of the perturbation \mathcal{V} and the fast relaxation \mathcal{R} , such as [TR25, LRR23].

While AE simplifies dynamics by focusing on the slow limit, a distinct goal in Monte Carlo is to accelerate inherently slow dynamics, which is called lifting by mathematicians [EL24a, LL25] and theoretical computer scientists [CLP99, ATS17]. Originating from classical Markov chain Monte Carlo (MCMC), lifting involves embedding the original slow state space \mathcal{H}_S into a larger space $\mathcal{H} = \mathcal{H}_S \oplus \mathcal{H}_F$, and designing a new dynamics

\mathcal{L}_γ on \mathcal{H} [EL24a]. The crucial intuition is that \mathcal{L}_γ breaks the detailed balance condition while preserving the target equilibrium state, and thus creates a forward flux for faster relaxation towards steady states.

In order to analyze such rapid convergence with degenerate dissipation, one usually introduces hypocoercivity from kinetic theory [Vil09, IOS17]. The lifted generator often takes the canonical hypocoercive form $\mathcal{L}_\gamma = \mathcal{L}_A + \gamma \mathcal{L}_S$, where the self-adjoint \mathcal{L}_S on \mathcal{H}_F provides strong dissipation off the original slow subspace \mathcal{H}_S , where skew-adjoint \mathcal{L}_A couple the slow dynamics within \mathcal{H}_S to the fast dissipation in \mathcal{H}_F [FLT25]. This engineered interplay allows the lifted system to explore \mathcal{H}_S faster than the original slow process. Most recent hypocoercivity leverages a variational version [BLW25], where space-time/flow Poincaré inequality is derived via abstract divergence lemmas [EGH⁺25, LL24], showcasing that optimally constructed lifts could achieve a diffusive-to-ballistic speedup in L^2 convergence rate, i.e. $\nu(\mathcal{L}_\gamma) = \Theta(\sqrt{\lambda_O})$, where λ_O is the spectral gap of the original slow reversible dynamics.

Comparing AE and lifting reveals a fascinating duality. AE starts with a full (usually hypocoercive) system $\mathcal{L} = \mathcal{V} + \gamma \mathcal{R}$ and derives the slow effective limit \mathcal{L}_O , while lifting drags the slow second-order effective dynamics back to the enlarged space going up the river of overdamped limit. Such duality presents us with the possibility of filling the gaps in each area through tools from the other. Unfortunately, such “inverse AE” relation is currently confined to the equilibrium collapsed generator \mathcal{L}_O due to the presumptions of the lifting paradigm [EL24a], whilst AE itself routinely generates effective non-equilibrium dynamics [LRR23, TR25, MR22]. This highlights the major gap: *Can we apply the constructive “inverse AE” principle to design accelerated dynamics converging towards a desired NESS?* Solving such a problem would provide a systematic methodology for accelerating convergence to NESS, crucial for efficient NESS preparation and simulation, a task that currently lacks a constructive framework.

In this paper, we address this gap under a near-equilibrium regime, where the NESS is generated by an equilibrium perturbed by a non-conservative external field of scale $\eta \ll \min(1, \gamma)$, which is treated as a **fixed small parameter**. Our asymptotic analysis will later (in Sec. 6) require it to be subdominant to the slow dynamics gap. We formally establish that the full, complex generator $\mathcal{L} = \gamma \mathcal{R} + \mathcal{V}$ of a system with timescale separation can be rigorously analyzed as a *lift* of its own effective slow dynamics \mathcal{L}_O , even when \mathcal{L}_O converges to a NESS.

Our main contribution is the formalization of the **Adiabatic Embedding (Ad Embed)** structure, which we introduce in Section 5. This framework is built upon an Approximate Quadratic Form Condition (Proposition 3.2) that precisely quantifies the relationship between \mathcal{L} and the effective generator \mathcal{L}_O , rigorously capturing the non-conservative, non-equilibrium perturbation as an explicitly bounded error proportional to η . We then adapt the variational framework of Flow Poincaré inequalities (Theorem 6.3) to this new structure. This allows us to prove our central theoretical result (Corollary 6.2): under specific structural conditions derived from the AE and the asymptotic regime $\eta \ll s(\mathcal{L}_O)^2$, this non-equilibrium lift achieves the optimal “diffusive-to-ballistic” quadratic speedup, $\nu(\mathcal{L}) = \Theta(\sqrt{s(\mathcal{L}_O)})$, demonstrating that this acceleration is not limited to reversible systems.

The paper is organized as follows. In Section 2, we review the preliminaries for Quantum Markov Semigroups, ergodicity, the KMS inner product, and the concept of hypocoercivity. In Section 3, we employ the Generalized Schrieffer-Wolff formalism to rigorously derive the effective slow generator via adiabatic elimination, which forms the basis for our abstract lift conditions. Section 4 provides the abstract mathematical framework for semigroup convergence. In Section 5, we formally define the Ad Embed Structure. Section 6 contains our main theoretical results, including the derivation of both upper and lower bounds on the convergence rate of the lifted generator, culminating in the proof of optimal quadratic speedup. In Section 7, we validate the entire framework with two canonical non-equilibrium examples—classical Langevin dynamics and a quantum Zeno-limit spin chain—providing both rigorous verification and supporting numerical experiments. Finally, Section 8 concludes with a summary and discussion of future outlook. Detailed proofs are deferred to the Appendices A-E.

2. Preliminaries

In this section, we introduce the foundational concepts and properties required throughout the paper. We provide a concise overview of Quantum Markov Semigroups, ergodicity, and the KMS inner product, with a particular focus on the role of hypocoercivity.

Throughout, we will use the following notations.

Let \mathcal{H} be a finite-dimensional Hilbert space and $\mathcal{B}(\mathcal{H})$ be the associated algebra of linear operators. We denote the identity element by $\mathbf{1} \in \mathcal{B}(\mathcal{H})$ and the identity map by id . The adjoint of an operator $X \in \mathcal{B}(\mathcal{H})$ is X^* . The standard **Hilbert-Schmidt (HS) inner product** on $\mathcal{B}(\mathcal{H})$ is given by $\langle X, Y \rangle = \text{tr}(X^*Y)$, with the induced norm $\|X\| = \sqrt{\langle X, X \rangle}$. A quantum state (or density operator) is an element $\rho \in \mathcal{B}(\mathcal{H})$ satisfying $\rho \succeq 0$ and $\text{tr}(\rho) = 1$. The set of all quantum states is $\mathcal{D}(\mathcal{H})$, and the subset of full-rank states is $\mathcal{D}^+(\mathcal{H})$. The adjoint of a superoperator $\Phi : \mathcal{B}(\mathcal{H}) \rightarrow \mathcal{B}(\mathcal{H})$ with respect to the HS inner product is written as Φ^\dagger . We use standard asymptotic notations $O(\cdot)$, $\Omega(\cdot)$, and $\Theta(\cdot)$.

2.1. Quantum Markov Semigroups and Ergodicity

A **Quantum Markov Semigroup (QMS)** $(\mathcal{P}_t)_{t \geq 0}$ is a semigroup of completely positive and trace-preserving (CPTP) maps on $\mathcal{B}(\mathcal{H})$. Its generator, the **Lindbladian**, is defined by $\mathcal{L} := \lim_{t \downarrow 0} \frac{\mathcal{P}_t(X) - X}{t}$ (in the Heisenberg picture) and has the Gorini-Kossakowski-Sudarshan-Lindblad (GKSL) form:

$$\mathcal{L}(X) = i[H, X] + \sum_{\alpha} \left(L_{\alpha}^* X L_{\alpha} - \frac{1}{2} \{ L_{\alpha}^* L_{\alpha}, X \} \right). \quad (2.1)$$

Here, H is the self-adjoint system Hamiltonian, and $\{L_{\alpha}\}$ are the jump operators describing environmental interaction.

To characterize the long-time behavior of $\mathcal{P}_t = \exp(t\mathcal{L})$, we introduce two key subspaces: the **fixed point space** $\mathcal{F}(\mathcal{L}) = \ker(\mathcal{L})$ and the **decoherence-free subalgebra** $\mathcal{N}(\mathcal{L}) := \{X \in \mathcal{B}(\mathcal{H}) \mid \mathcal{P}_t(X^*X) = \mathcal{P}_t(X)^*\mathcal{P}_t(X), \forall t \geq 0\}$. Since $\mathcal{F}(\mathcal{L})$ is a

von Neumann subalgebra, there exists a unique CPTP projection onto it, denoted by $\mathbb{E}_{\mathcal{F}} : \mathcal{B}(\mathcal{H}) \rightarrow \mathcal{F}(\mathcal{L})$, which is called the **conditional expectation**.

Lemma 2.1 (Ergodicity Criterion). *Let \mathcal{P}_t be a QMS with an invariant state $\sigma \in \mathcal{D}^+(\mathcal{H})$. The semigroup converges to the conditional expectation onto the fixed points, $\lim_{t \rightarrow \infty} \mathcal{P}_t = \mathbb{E}_{\mathcal{F}}$, if and only if the decoherence-free subalgebra coincides with the fixed point space, i.e., $\mathcal{N}(\mathcal{L}) = \mathcal{F}(\mathcal{L})$.*

The proof can be found in [FV82, Theorem 3.3 and 3.4]. A QMS is called **ergodic** if this condition holds and **primitive** if it has a unique invariant state σ . For a primitive semigroup, the limit is $\mathbb{E}_{\mathcal{F}}(X) = \text{tr}(\sigma X)\mathbf{1}$.

Lemma 2.2 (Ergodic Spectrum). *An ergodic QMS is characterized by a generator \mathcal{L} that has no purely imaginary eigenvalues, i.e., every non-zero eigenvalue has a strict negative real part.*

This result, derived from [CSU15, Theorem 29 and Proposition 31], ensures asymptotic stability in the sense that any initial state converges to the steady state subspace.

2.2. Convergence Metrics and KMS Structure

For a primitive QMS with a full-rank invariant state $\sigma \in \mathcal{D}^+(\mathcal{H})$, we define a family of weighted inner products on $\mathcal{B}(\mathcal{H})$ parameterized by $s \in [0, 1]$:

$$\langle X, Y \rangle_{\sigma, s} := \text{tr}(\sigma^s X^* \sigma^{1-s} Y). \quad (2.2)$$

The cases $s = 1$ and $s = 1/2$ are known as the **Gelfand-Naimark-Segal (GNS)** and **Kubo-Martin-Schwinger (KMS)** inner products, respectively. The norm induced by the KMS inner product is central to our analysis and is written as $\|X\|_{2,\sigma} := \sqrt{\langle X, X \rangle_{\sigma, 1/2}}$. We denote the orthogonal complement of the fixed-point space $\mathcal{F}(\mathcal{L})$ with respect to the KMS inner product as $\mathcal{F}(\mathcal{L})^\perp$.

The convergence rate is determined by the “gaps” of the generator \mathcal{L} , as defined below.

Definition 2.1 (Spectral and Singular Value Gaps). Let \mathcal{L} be an ergodic generator with invariant state σ .

1. The **spectral gap** is the smallest real part of non-zero eigenvalues of $-\mathcal{L}$:

$$\lambda(\mathcal{L}) := \inf \{ \text{Re}(\lambda) \mid \lambda \in \text{Spec}(-\mathcal{L}) \setminus \{0\} \}. \quad (2.3)$$

2. The **singular value gap** is the smallest non-zero singular value of \mathcal{L} relative to the KMS inner product:

$$s(\mathcal{L}) := \inf \left\{ \|\mathcal{L}(X)\|_{2,\sigma} \mid X \in \mathcal{F}(\mathcal{L})^\perp, \|X\|_{2,\sigma} = 1 \right\}. \quad (2.4)$$

The spectral gap $\lambda(\mathcal{L})$ determines the sharp *asymptotic* exponential rate of convergence to the steady state. The singular value gap $s(\mathcal{L})$, on the other hand, characterizes the instantaneous rate of dissipation for observables orthogonal to the fixed-point space. For a generator \mathcal{L} that is self-adjoint with respect to the KMS inner product, these two gaps coincide: $\lambda(\mathcal{L}) = s(\mathcal{L})$. However, for non-self-adjoint generators, we only have the inequality $s(\mathcal{L}) \geq \lambda(\mathcal{L})$. The relation between λ and s is also discussed in [Cha25, Section 1.4].

We quantify the convergence speed using the following metrics:

Definition 2.2 (Mixing and Relaxation Time). The **L^1 -mixing time** is defined using the trace norm on states:

$$t_{\text{mix}}(\mathcal{L}) := \inf \left\{ t \geq 0 \mid \sup_{\rho \in \mathcal{D}(\mathcal{H})} \|\mathcal{P}_t^\dagger(\rho) - \sigma\|_{\text{tr}} \leq e^{-1} \right\}, \quad (2.5)$$

and the **L^2 -relaxation time** is defined using the KMS norm on observables:

$$t_{\text{rel}}(\mathcal{L}) := \inf \left\{ t \geq 0 \mid \sup_{X \in \mathcal{F}(\mathcal{L})^\perp} \frac{\|\mathcal{P}_t(X)\|_{2,\sigma}}{\|X\|_{2,\sigma}} \leq e^{-1} \right\}. \quad (2.6)$$

These two times are related by $t_{\text{mix}}(\mathcal{L}) \leq C(\sigma)t_{\text{rel}}(\mathcal{L})$, where $C(\sigma)$ depends weakly on the invariant state σ [LL25, Appendix B]. In this work, we will focus on analyzing the relaxation time t_{rel} .

2.3. Hypocoercivity

For a general ergodic QMS, the convergence to steady state is described by:

$$\|\mathcal{P}_t(X) - \mathbb{E}_{\mathcal{F}}(X)\|_{2,\sigma} \leq Ce^{-\nu t} \|X - \mathbb{E}_{\mathcal{F}}(X)\|_{2,\sigma}, \quad (2.7)$$

where $C \geq 1$ and $\nu > 0$. The sharp asymptotic rate is $\nu = \lambda(\mathcal{L})$ from [EN00].

Definition 2.3 (Coercivity and Hypocoercivity). An ergodic QMS is **coercive** if (2.7) holds with $C = 1$. It is **hypocoercive** if it holds for $C \geq 1$, and **strictly hypocoercive** if $C > 1$ is necessary.

Coercivity implies $\lambda(\mathcal{L}) = s(\mathcal{L})$ and that all modes relax at a uniform exponential rate. Strict hypocoercivity arises when some modes are not directly dissipated ($s(\mathcal{L})$ might be large) but must be mixed by the oscillatory part of the dynamics into dissipative channels, resulting in a slower asymptotic rate $\lambda(\mathcal{L})$.

To characterize this mechanism, we define the adjoint of the Lindbladian \mathcal{L}^\dagger with respect to the KMS inner product:

$$\langle X, \mathcal{L}Y \rangle_{\sigma,1/2} = \langle \mathcal{L}^\dagger X, Y \rangle_{\sigma,1/2}, \quad \forall X, Y \in \mathcal{B}(\mathcal{H}). \quad (2.8)$$

We then decompose \mathcal{L} into its self-adjoint (dissipative) and skew-adjoint (oscillatory) parts relative to this KMS structure:

$$\mathcal{S} = \frac{\mathcal{L} + \mathcal{L}^\dagger}{2}, \quad \mathcal{A} = \frac{\mathcal{L} - \mathcal{L}^\dagger}{2}. \quad (2.9)$$

In a strictly hypocoercive system, there exist observables in $\ker(\mathcal{S})$ that are not steady states (i.e., not in $\mathcal{F}(\mathcal{L})$). The following lemma makes this precise. Recall that we only consider finite dimensional Hilbert space.

Lemma 2.3 (Criterion for Strict Hypocoercivity). *For an ergodic QMS, the fixed-point space is a subspace of the dissipative kernel, $\mathcal{F}(\mathcal{L}) \subset \ker(\mathcal{S})$. The semigroup is strictly hypocoercive if and only if this inclusion is strict:*

$$\dim \ker(\mathcal{S}) > \dim \mathcal{F}(\mathcal{L}). \quad (2.10)$$

Proof. A coercive system satisfies $-\operatorname{Re}\langle X, \mathcal{L}X \rangle_{\sigma,1/2} \geq \nu \|X - \mathbb{E}_\mathcal{F} X\|_{2,\sigma}^2$ for all $X \in \mathcal{F}(\mathcal{L})^\perp$. By definition of \mathcal{S} , this is equivalent to $-\langle X, \mathcal{S}X \rangle_{\sigma,1/2} \geq \nu \|X - \mathbb{E}_\mathcal{F} X\|_{2,\sigma}^2$. This inequality implies that any element in the kernel of \mathcal{S} must also be a fixed point, forcing $\ker(\mathcal{S}) = \mathcal{F}(\mathcal{L})$. Strict hypocoercivity arises precisely when this condition is violated. The full proof is in Appendix A.1. \square

Finally, the relaxation time and decay rate are fundamentally linked to the singular value gap, $s(\mathcal{L})$.

Lemma 2.4 (Singular Value Gap Bounds). *Let $s(\mathcal{L})$ be the singular value gap of an ergodic generator \mathcal{L} . The constants in (2.7) satisfy:*

$$\nu \leq (1 + \log C)s(\mathcal{L}) \quad \text{and} \quad t_{\text{rel}} \geq \frac{1}{2s(\mathcal{L})}. \quad (2.11)$$

A rigorous proof of this relationship is provided in [LL24, Lemma 2.5].

3. Adiabatic Elimination and the Effective Generator

To explicitly construct a lifting for a target slow process, we first need a systematic way to derive such slow dynamics from a larger, more complex system. This is precisely the goal of **Adiabatic Elimination (AE)** [TR25, ASR16]. AE is a general framework for deriving effective dynamics in systems with time-scale separation, encompassing well-known limits such as the overdamped limit in classical Langevin dynamics [IOS17, MR22] and the Zeno limit in open quantum systems as special cases [PEPS18, PP21].

We consider a system described by a Lindbladian exhibiting a clear separation of timescales, characteristic of singular perturbation problems [Tik52, Ver05], and decompose the generator as:

$$\mathcal{L} = \gamma \mathcal{R} + \mathcal{V}, \quad (3.1)$$

where $\gamma \gg 1$ is a large parameter governing the time-scale separation. The “fast” generator \mathcal{R} is assumed to be a self-adjoint dissipative superoperator that is stable, meaning its non-zero eigenvalues have strictly negative real parts (i.e., it has a strictly positive spectral gap $\lambda(\mathcal{R}) > 0$). The “perturbation” generator \mathcal{V} contains the remaining dynamics. We decompose it as $\mathcal{V} = \mathcal{L}_{\text{ham}} + \eta \mathcal{L}_{\text{pert}}$, where \mathcal{L}_{ham} is a skew-adjoint Hamiltonian dynamics and $\mathcal{L}_{\text{pert}}$ is a non-conservative perturbation. The parameter $\eta > 0$ is a fixed, small parameter quantifying the strength of the non-conservative dynamics. Our subsequent analysis will treat η as a fixed parameter, yielding bounds that explicitly depend on it. The specific asymptotic scaling of η required to achieve optimal quadratic speedup will be introduced and analyzed in Section 6.

In the limit $\gamma \rightarrow \infty$, the fast dynamics $e^{t(\gamma\mathcal{R})}$ force the system to rapidly decay onto the kernel of \mathcal{R} , which we will refer to as the **slow subspace** $\mathcal{H}_S := \ker(\mathcal{R})$. The dynamics within this subspace, effectively governed by \mathcal{V} (to second order), are the “slow” dynamics we aim to isolate and subsequently accelerate.

3.1. The Generalized Schrieffer-Wolff Formalism

To rigorously derive the effective dynamics in a singular perturbation limit, such as adiabatic elimination, we employ the **Generalized Schrieffer-Wolff (SW) formalism** for dissipative systems [Kes12]. This method provides a systematic perturbative expansion for an effective generator that acts solely on a “slow” subspace of interest, decoupling it from the “fast” degrees of freedom.

Let $\epsilon = 1/\gamma$. We consider a general Lindbladian generator \mathcal{L} that can be partitioned into an unperturbed part \mathcal{R} and a perturbation \mathcal{V} , scaled by a small dimensionless parameter ϵ :

$$\mathcal{L} = \mathcal{R} + \epsilon \mathcal{V}. \quad (3.2)$$

For the general GSW derivation, the operators \mathcal{R} and \mathcal{V} do not need to be self-adjoint or skew-adjoint, respectively. However, we note that our subsequent convergence analysis in Section 6 will indeed require \mathcal{R} to be self-adjoint.

The unperturbed generator \mathcal{R} defines the “slow” and “fast” subspaces as the kernel of \mathcal{R} and its orthogonal complement, i.e.,

$$\mathcal{H}_S = \ker(\mathcal{R}), \quad \mathcal{H}_F = \ker(\mathcal{R})^\perp. \quad (3.3)$$

We also define the spectral projectors, P_S and P_F , which project onto the slow (\mathcal{H}_S) and fast (\mathcal{H}_F) subspaces, in a constructive way, namely:

$$P_S := \frac{1}{2\pi i} \oint_{\gamma_0} (z - \mathcal{R})^{-1} dz, \quad P_F := \mathbf{1} - P_S, \quad (3.4)$$

where γ_0 is a small contour in the complex plane enclosing only the zero eigenvalue. Any superoperator A can then be decomposed into its block-diagonal part $A^{\text{diag}} = P_S A P_S + P_F A P_F$ and its block-off-diagonal part $A^{\text{offdiag}} = P_S A P_F + P_F A P_S$.

The SW method seeks a non-unitary similarity transformation, $U = e^S$, that “decouples” the slow and fast subspaces. The generator S of this transformation is chosen to be purely block-off-diagonal ($S^{\text{diag}} = 0$). This transformation defines a new generator $L = e^S \mathcal{L} e^{-S}$ that is, by construction, perfectly block-diagonal ($L^{\text{offdiag}} = 0$). The effective generator governing the slow subspace is then precisely the $P_S L P_S$ block of this new, decoupled generator: $\mathcal{L}_{\text{eff}} = P_S L P_S$. This \mathcal{L}_{eff} describes the dynamics within the slow subspace, as it evolves independently of the fast subspace in this transformed frame. The SW formalism provides an exact, non-perturbative expression for L .

Theorem 3.1 (SW Effective Generator Formula). *The block-diagonal transformed generator $L = L^{\text{diag}}$ is given exactly by:*

$$L = \mathcal{L}^{\text{diag}} + \tanh(\widehat{\mathcal{S}}/2) \mathcal{L}^{\text{offdiag}}, \quad (3.5)$$

where $\mathcal{L} = \mathcal{L}^{\text{diag}} + \mathcal{L}^{\text{offdiag}}$ is the decomposition of the full generator, and $\widehat{\mathcal{S}}$ is the adjoint-action superoperator $\widehat{\mathcal{S}}(A) = [\mathcal{S}, A]$. The effective generator for the slow subspace is $\mathcal{L}_{\text{eff}} = P_S L P_S$.

Proof. The proof, based on the derivation in [Kes12], is provided in Appendix B.1. \square

This exact formula’s primary utility is that it can be expanded as a power series in the perturbation parameter ϵ , yielding a systematic expansion for \mathcal{L}_{eff} .

We note that the GSW transformation $U = e^S$ is a similarity transformation, not a unitary one. Consequently, it does not, in general, preserve the Gorini-Kossakowski-Sudarshan-Lindblad (GKSL) form (for situations like [MBHR21, Appendix C], a standard GKSL form for effective dynamics is inaccessible). The resulting effective generator \mathcal{L}_{eff} is not guaranteed to be the generator of a completely positive and trace-preserving (CPTP) semigroup. However, in many physical systems, such as the examples presented in Section 7, the derived effective generator does retain the Lindblad form. For our abstract framework, we will add the assumption that \mathcal{L}_{eff} generates a valid QMS when necessary.

Theorem 3.2 (SW Perturbative Expansion). *The effective generator $\mathcal{L}_{\text{eff}} = P_S L P_S$ has the perturbative expansion $\mathcal{L}_{\text{eff}} = \sum_{n=0}^{\infty} \epsilon^n L_n^{\text{eff}}$. The first three non-trivial orders are given by:*

$$L_1^{\text{eff}} = P_S \mathcal{V} P_S \equiv \mathcal{V}^S \quad (3.6)$$

$$L_2^{\text{eff}} = -P_S \mathcal{V} P_F \mathcal{R}^+ P_F \mathcal{V} P_S \equiv -\mathcal{V}^- \mathcal{R}^+ \mathcal{V}^+ \quad (3.7)$$

$$L_3^{\text{eff}} = \mathcal{V}^- \mathcal{R}^+ \mathcal{V}^F \mathcal{R}^+ \mathcal{V}^+ - \frac{1}{2} \{ \mathcal{V}^S, \mathcal{V}^- (\mathcal{R}^+)^2 \mathcal{V}^+ \}_+ \quad (3.8)$$

where $\mathcal{R}^+ \equiv (P_F \mathcal{R} P_F)^{-1}$ is the inverse of \mathcal{R} on the fast subspace \mathcal{H}_F , and we use the compact notation $\mathcal{V}^- = P_S \mathcal{V} P_F$, $\mathcal{V}^+ = P_F \mathcal{V} P_S$, $\mathcal{V}^S = P_S \mathcal{V} P_S$, and $\mathcal{V}^F = P_F \mathcal{V} P_F$; i.e., in block matrix form

$$\mathcal{V} = \begin{pmatrix} \mathcal{V}^S & \mathcal{V}^- \\ \mathcal{V}^+ & \mathcal{V}^F \end{pmatrix} \quad (3.9)$$

Proof. These formulas are derived by systematically expanding both the generator \mathcal{S} and the effective generator L in powers of ϵ and matching terms. A detailed derivation for the first two orders is provided in Appendix B.2. \square

3.2. The Effective Generator via Adiabatic Elimination

We now apply the Generalized Schrieffer-Wolff (SW) formalism, introduced in Section 3.1, to our specific problem of adiabatic elimination. Our starting point is the full Lindbladian generator $\mathcal{L} = \gamma\mathcal{R} + \mathcal{V}$, where $\gamma \gg 1$ represents the large timescale separation. Here, \mathcal{R} is the self-adjoint fast dissipative part, and \mathcal{V} contains the remaining dynamics. The slow subspace \mathcal{H}_S is the kernel of the fast dynamics, $\mathcal{H}_S = \ker(\mathcal{R})$.

To leverage the standard SW expansion theorems, we first rescale the generator to introduce a small perturbation parameter $\epsilon = 1/\gamma$. This yields a rescaled generator $\mathcal{L}' = \frac{1}{\gamma}\mathcal{L} = \mathcal{R} + \epsilon\mathcal{V}$. Correspondingly, the slow space projector is P_S (the projector onto \mathcal{H}_S), and the fast space projector is $P_F = \mathbf{1} - P_S$. The inverse of the unperturbed generator restricted to the fast subspace, required by the SW formulas, is precisely the pseudo-inverse $\mathcal{R}^+ \equiv (P_F \mathcal{R} P_F)^{-1}$.

The SW formalism provides a perturbative expansion for the effective generator $\mathcal{L}'_{\text{eff}} = P_S L' P_S$ acting on the slow subspace of the rescaled system, where $L' = e^{\mathcal{S}} \mathcal{L}' e^{-\mathcal{S}}$. The effective generator \mathcal{L}_{eff} for the original timescale t is then recovered by reversing the scaling, $\mathcal{L}_{\text{eff}} = \gamma \mathcal{L}'_{\text{eff}}$. Applying the expansion formulas yields the following result:

Theorem 3.3 (Effective Generator via Adiabatic Elimination). *Let $\mathcal{L} = \gamma\mathcal{R} + \mathcal{V}$, and let P_S be the orthogonal projection onto the slow subspace $\mathcal{H}_S := \ker(\mathcal{R})$. The effective generator \mathcal{L}_{eff} governing the dynamics on \mathcal{H}_S has the perturbative expansion:*

$$\mathcal{L}_{\text{eff}} = L^{(1)} + \frac{1}{\gamma} L^{(2)} + O(1/\gamma^2), \quad (3.10)$$

where the first- and second-order terms are explicitly given by:

$$L^{(1)} = P_S \mathcal{V} P_S \quad (3.11)$$

$$L^{(2)} = -P_S \mathcal{V} \mathcal{R}^+ \mathcal{V} P_S. \quad (3.12)$$

Here, $\mathcal{R}^+ = (P_F \mathcal{R} P_F)^{-1}$ is the pseudo-inverse of \mathcal{R} on the fast subspace $\mathcal{H}_F = \mathcal{H}_S^\perp$. The terms $L^{(1)}$ and $L^{(2)}$ correspond precisely to the terms L_1^{eff} and L_2^{eff} derived in Theorem 3.2, respectively.

Proof. The derivation involves applying the general SW expansion formulas stated in Theorem 3.2 to the rescaled generator $\mathcal{L}' = \mathcal{R} + \epsilon\mathcal{V}$, followed by reversing the time scaling. The detailed derivation can be found in Appendix B.3. \square

3.3. Approximation Error

The adiabatic elimination procedure provides a systematic way to approximate the full system dynamics $\mathcal{P}_t = \exp(t\mathcal{L})$ by the dynamics restricted to the slow subspace \mathcal{H}_S . The

full effective generator \mathcal{L}_{eff} , computed to all orders, captures these slow dynamics exactly (up to the similarity transformation), but its computation is generally intractable.

In practice, we often truncate the expansion at a certain order. When the first-order term $L^{(1)} = P_S \mathcal{V} P_S$ vanishes, the dominant slow dynamics are captured by the second-order effective generator $\widehat{\mathcal{L}}_{\text{eff}} := \frac{1}{\gamma} L^{(2)} = -\frac{1}{\gamma} P_S \mathcal{V} \mathcal{R}^+ \mathcal{V} P_S$. The semigroup generated by this approximation is $\mathcal{P}_t^{\text{eff}} = \exp(t \widehat{\mathcal{L}}_{\text{eff}})$.

It is crucial to quantify the error incurred by this approximation. Specifically, we want to bound the difference between the actual state $X(t) = \mathcal{P}_t X(0)$ starting in the slow subspace ($X(0) \in \mathcal{H}_S$) and the state predicted by the second-order approximation $X_{\text{eff}}(t) = \mathcal{P}_t^{\text{eff}} X(0)$.

Theorem 3.4 (Approximation Error of AE Dynamics). *Let $\mathcal{P}_t = \exp(t \mathcal{L})$ be the QMS with generator $\mathcal{L} = \gamma \mathcal{R} + \mathcal{V}$, where \mathcal{R} is self-adjoint with a spectral gap $\lambda_R > 0$ on the fast subspace $\mathcal{H}_F := \ker(\mathcal{R})^\perp$. Assume $L^{(1)} = P_S \mathcal{V} P_S = 0$ and that γ is sufficiently large such that $\gamma \lambda_R > \|\mathcal{V}\|$. Let $X(0) \in \mathcal{H}_S$, $X(t) = \mathcal{P}_t X(0)$, and $X_{\text{eff}}(t) = \exp(t \widehat{\mathcal{L}}_{\text{eff}}) X(0)$ where $\widehat{\mathcal{L}}_{\text{eff}} = \frac{1}{\gamma} L^{(2)}$. Then for any $t \geq 0$, the approximation error is bounded with respect to the KMS norm by:*

$$\|X(t) - X_{\text{eff}}(t)\|_{2,\sigma} \leq \frac{C'_V}{\gamma \lambda_R} \left(1 + t \left(\|\mathcal{V}\| + \frac{\|\mathcal{V}\|^2}{C'_V} \right) \right) \|X(0)\|_{2,\sigma}, \quad (3.13)$$

where $C'_V = \frac{\|\mathcal{V}\|}{1 - \|\mathcal{V}\|/(\gamma \lambda_R)}$ is a constant of order $O(\|\mathcal{V}\|)$.

Proof. The proof involves decomposing the error into components within the slow and fast subspaces. The fast component is bounded uniformly in time using a Grönwall's inequality for Volterra integral equations, which in turn leads to a bound on the slow component that grows only linearly in t . The detailed derivation is provided in Appendix B.4. \square

This theorem establishes that the error between the true dynamics and the second-order adiabatic elimination approximation is of order $O(1/\gamma)$. Such bounds are characteristic of secular approximations on Nakajima–Zwanzig equation [MBHR21, Appendix B], which are expected to be accurate for timescales t such that $t/\gamma \ll 1$, that is, dissipation is far stronger than the correlations. As our main theoretical results on acceleration (Section 6) rely on abstract structural conditions rather than this explicit approximation bound, this result suffices to justify the identification of $\widehat{\mathcal{L}}_{\text{eff}}$ as the correct effective generator, as [LL25, Proposition 2.12] does in the equilibrium case. For more discussions on secular approximation and such an error, please refer to [MBHR21, Sal24].

Remark 3.1 (Origin of the $O(\gamma^{-1})$ Trajectory Error). It is crucial to distinguish between the accuracy of the effective generator and that of the state trajectory. The GSW formalism (Theorem 3.3) provides an expansion for \mathcal{L}_{eff} that is accurate to $O(\gamma^{-2})$ for the generator itself. However, this \mathcal{L}_{eff} describes dynamics on the *exact* invariant slow manifold. This manifold is a perturbation of the uncoupled slow subspace $\mathcal{H}_S = \ker(\mathcal{R})$, related by the similarity transformation $U = e^{\mathcal{S}}$. As shown in the proof of Theorem B.2, the

generator \mathcal{S} is of order $O(\epsilon) = O(\gamma^{-1})$, implying $U = \mathbf{1} + O(\gamma^{-1})$. The dominant $O(\gamma^{-1})$ error in Theorem 3.4 arises directly from this discrepancy: the state $X(t) = \mathcal{P}_t X(0)$ immediately develops an $O(\gamma^{-1})$ component in the fast subspace \mathcal{H}_F , a “leakage” that is not captured by the approximate semigroup $\mathcal{P}_t^{\text{eff}}$, which acts only on \mathcal{H}_S .

3.4. Abstraction of Adiabatic Elimination Structure

The adiabatic elimination procedure reveals a fundamental relationship between the full dynamics \mathcal{L} and the effective slow dynamics \mathcal{L}_{eff} . To formalize this relationship for our convergence analysis, we define the rescaled effective generator $\mathcal{L}_O := \gamma \hat{\mathcal{L}}_{\text{eff}}$. When the first-order term $L^{(1)}$ vanishes, this becomes $\mathcal{L}_O = -P_S \mathcal{V} \mathcal{R}^+ \mathcal{V} P_S$.

The following propositions abstract the essential algebraic structure derived from AE. This structure will form the basis of our *Adiabatic Embedding* framework in Section 4.

For the analysis, we must fix a Hilbert space structure that is independent of the variable γ . We treat $\eta > 0$ as a fixed parameter.

1. Let $\mathcal{H}_S = \ker(\mathcal{R})$ be the slow subspace and $\mathcal{H}_F = \mathcal{H}_S^\perp$ be the fast subspace.
2. Let σ_O be the (fixed, η -dependent) NESS of the effective generator \mathcal{L}_O acting on \mathcal{H}_S . We define the inner product on \mathcal{H}_S as $\langle \cdot, \cdot \rangle_{\mathcal{H}_S} := \langle \cdot, \cdot \rangle_{\sigma_O, 1/2}$.
3. Let $\sigma_{\mathcal{R}}$ be the invariant state of the fast dynamics (e.g., the Maxwell-Boltzmann distribution in the Langevin case).
4. We define the fixed reference inner product on the full space $\mathcal{H} = \mathcal{H}_S \oplus \mathcal{H}_F$ using the limiting product state $\sigma_\infty = \sigma_O \otimes \sigma_{\mathcal{R}}$ as in [CHL24, MR22]. We denote this inner product by $\langle \cdot, \cdot \rangle_{\mathcal{H}} := \langle \cdot, \cdot \rangle_{\sigma_\infty, 1/2}$.

With this definition, the projection P_S is orthogonal, \mathcal{R} is self-adjoint, and for any $A, B \in \mathcal{H}_S$, the inner products are identical: $\langle A, B \rangle_{\mathcal{H}} = \langle A, B \rangle_{\mathcal{H}_S}$. We will use $\|\cdot\|$ for the norm on \mathcal{H} .

We now focus on the common scenario where the first-order term vanishes, $L^{(1)} = P_S \mathcal{V} P_S = 0$.

Proposition 3.1 (Orthogonality Condition). *Assume $L^{(1)} = P_S \mathcal{V} P_S = 0$. Then the perturbation \mathcal{V} maps the slow subspace \mathcal{H}_S to the fast subspace \mathcal{H}_F . Equivalently, for all $X, Y \in \mathcal{H}_S$, the perturbation satisfies:*

$$\langle X, \mathcal{V}Y \rangle_{\mathcal{H}} = 0. \tag{3.14}$$

Proof. This condition is a direct restatement of the vanishing of the first-order effective generator $L^{(1)}$. Since $X, Y \in \mathcal{H}_S$, the orthogonal projection P_S acts as the identity on them. Therefore, $\langle X, \mathcal{V}Y \rangle_{\mathcal{H}} = \langle P_S X, \mathcal{V} P_S Y \rangle_{\mathcal{H}} = \langle X, (P_S \mathcal{V} P_S) Y \rangle_{\mathcal{H}} = \langle X, L^{(1)} Y \rangle_{\mathcal{H}} = 0$. This implies that $\mathcal{V}Y$, for $Y \in \mathcal{H}_S$, must be orthogonal to all $X \in \mathcal{H}_S$, meaning $\mathcal{V}Y \in \mathcal{H}_F$. \square

The following proposition provides the central quantitative estimate. It bridges the two spaces, relating the quadratic form of the full generator's action (on \mathcal{H}) to the magnitude of the effective generator (on \mathcal{H}_S), and explicitly isolates the non-equilibrium perturbation as a bounded error term.

Before start, we establish the stability of the quadratic form associated with the full generator \mathcal{L} by bounding its deviation from the effective dynamics. This bound is expressed explicitly in terms of the spectral gap of the target (perturbed) effective generator, $s(L_O)$, and the dissipation rate λ_R .

Assumption 3.1 (Structural Prerequisites). Let $\mathcal{H} = \mathcal{H}_S \oplus \mathcal{H}_F$ be a finite-dimensional Hilbert space. Let $\mathcal{L} = \gamma\mathcal{R} + \mathcal{V}$ be a generator with $\mathcal{V} = \mathcal{L}_{ham} + \eta\mathcal{L}_{pert}$. We assume:

1. **Dissipativity and Gap:** The operator \mathcal{R} is self-adjoint and non-positive with $\ker(\mathcal{R}) = \mathcal{H}_S$. The restriction $-\mathcal{R}|_{\mathcal{H}_F}$ is strictly positive definite with smallest eigenvalue $\lambda_R > 0$. Consequently, the inverse $S := (-\mathcal{R}|_{\mathcal{H}_F})^{-1}$ satisfies $\|S\| = \lambda_R^{-1}$.
2. **Coupling Structure:** The unperturbed coupling \mathcal{L}_{ham} is skew-adjoint on \mathcal{H} , while the perturbation \mathcal{L}_{pert} is a bounded linear operator.
3. **Effective Spectral Gap:** Let $\mathcal{L}_O(\eta) := -P_S\mathcal{V}S\mathcal{V}P_S$ be the full effective generator. We assume that $\mathcal{L}_O(\eta)$ admits a non-trivial singular value gap $s(L_O) > 0$ on the orthogonal complement of its kernel within \mathcal{H}_S .
4. **Kernel Stability:** The dimension of the kernel $\dim(\ker(\mathcal{L}_O(\eta)))$ is constant for all η in the domain of consideration.

Remark 3.2. This kernel stability condition is physically equivalent to assuming that the non-conservative perturbation does not alter the ergodicity class of the effective dynamics (e.g., by merging previously disconnected subspaces). In standard NESS applications (e.g. examples in Section 7) with unique steady states, this holds trivially.

Such an assumption leads to the following quantitative relationship:

Proposition 3.2 (Approximate Quadratic Form). *Let the operators satisfy Assumption 3.1. Define the dimensionless perturbation constants:*

$$K_{lin} := 2\|\mathcal{L}_{ham}\|\lambda_R^{-1}\|\mathcal{L}_{pert}\|, \quad (3.15)$$

$$K_{quad} := \|\mathcal{L}_{pert}\|^2\lambda_R^{-1}. \quad (3.16)$$

Let $\mathcal{Q}_0 := -P_S\mathcal{L}_{ham}S\mathcal{L}_{ham}P_S$. Define the operator square deviation constant:

$$K_{sq} := 2\|\mathcal{Q}_0\|(K_{lin} + K_{quad}) + (K_{lin} + K_{quad})^2. \quad (3.17)$$

Let the critical perturbation threshold be defined by the target gap: $\eta_{crit} := \min\left(1, \frac{s(L_O)^2}{2K_{sq}}\right)$. Then, for all $\eta \in [0, \eta_{crit}]$ and all vectors $X, Y \in \mathcal{H}_S$, there exists a composite constant C_{AQF} such that:

$$|\langle \mathcal{L}X, S\mathcal{L}Y \rangle_{\mathcal{H}} - \langle X, |\mathcal{L}_O|Y \rangle_{\mathcal{H}_S}| \leq \eta C_{AQF} \|X\|_{\mathcal{H}} \|Y\|_{\mathcal{H}}. \quad (3.18)$$

The constant C_{AQF} is given explicitly by:

$$C_{AQF} := K_{lin} + \eta K_{quad} + \frac{K_{sq}}{\sqrt{2s(L_O)}}. \quad (3.19)$$

Proof. The proof proceeds by bounding the deviation of the bilinear form on the full space and then utilizing the spectral stability of the effective generator to bound the operator square root.

Let $X, Y \in \mathcal{H}_S$. Since $\mathcal{H}_S = \ker(\mathcal{R})$, we have $\mathcal{L}X = \mathcal{V}X$. Expanding the coupling term yields:

$$\langle \mathcal{L}X, S\mathcal{L}Y \rangle_{\mathcal{H}} = \langle (\mathcal{L}_{ham} + \eta\mathcal{L}_{pert})X, S(\mathcal{L}_{ham} + \eta\mathcal{L}_{pert})Y \rangle_{\mathcal{H}}. \quad (3.20)$$

We separate this into the unperturbed term and an error term $E_{\eta}(X, Y)$:

$$\langle \mathcal{L}X, S\mathcal{L}Y \rangle_{\mathcal{H}} = \langle \mathcal{L}_{ham}X, S\mathcal{L}_{ham}Y \rangle_{\mathcal{H}} + E_{\eta}(X, Y), \quad (3.21)$$

where $E_{\eta}(X, Y)$ collects all terms dependent on η . Using the Cauchy-Schwarz inequality and the definition $\|S\| = \lambda_R^{-1}$:

$$|E_{\eta}(X, Y)| \leq \eta (2\|\mathcal{L}_{ham}\|\lambda_R^{-1}\|\mathcal{L}_{pert}\| + \eta\|\mathcal{L}_{pert}\|^2\lambda_R^{-1}) \|X\|_{\mathcal{H}}\|Y\|_{\mathcal{H}} \quad (3.22)$$

$$= \eta(K_{lin} + \eta K_{quad})\|X\|_{\mathcal{H}}\|Y\|_{\mathcal{H}}. \quad (3.23)$$

The unperturbed term corresponds to the quadratic form of \mathcal{Q}_0 . Since \mathcal{L}_{ham} is skew-adjoint and S is self-adjoint positive:

$$\langle \mathcal{L}_{ham}X, S\mathcal{L}_{ham}Y \rangle_{\mathcal{H}} = \langle X, (-P_S\mathcal{L}_{ham}S\mathcal{L}_{ham}P_S)Y \rangle_{\mathcal{H}_S} = \langle X, \mathcal{Q}_0Y \rangle_{\mathcal{H}_S}. \quad (3.24)$$

Since \mathcal{Q}_0 is positive semi-definite, $\mathcal{Q}_0 = |\mathcal{Q}_0|$. Thus:

$$|\langle \mathcal{L}X, S\mathcal{L}Y \rangle_{\mathcal{H}} - \langle X, |\mathcal{Q}_0|Y \rangle_{\mathcal{H}_S}| \leq \eta(K_{lin} + \eta K_{quad})\|X\|_{\mathcal{H}}\|Y\|_{\mathcal{H}}. \quad (3.25)$$

We define the positive operators $A := \mathcal{L}_O(\eta)^\dagger \mathcal{L}_O(\eta)$ and $B := \mathcal{Q}_0^2$. The target operator is $|\mathcal{L}_O| = \sqrt{A}$, and the unperturbed approximation is $|\mathcal{Q}_0| = \sqrt{B}$. The difference in squared operators, $A - B$, arises from the perturbation $\Delta_{\eta} = \mathcal{L}_O(\eta) - (-\mathcal{Q}_0)$. The norm is bounded by:

$$\|A - B\| \leq \eta K_{sq}. \quad (3.26)$$

We now analyze the spectra to apply the Lipschitz continuity of the square root. By Assumption 3.1.3, the non-zero spectrum of A is bounded below by $s(L_O)^2$:

$$\sigma(A) \setminus \{0\} \subseteq [s(L_O)^2, \infty). \quad (3.27)$$

Using Weyl's inequality and the Kernel Stability assumption, the non-zero spectrum of the unperturbed operator B satisfies:

$$\min(\sigma(B) \setminus \{0\}) \geq \min(\sigma(A) \setminus \{0\}) - \|A - B\| \geq s(L_O)^2 - \eta K_{sq}. \quad (3.28)$$

Given the condition $\eta \leq \frac{s(L_O)^2}{2K_{sq}}$, we have $\eta K_{sq} \leq \frac{1}{2}s(L_O)^2$. Therefore:

$$\min(\sigma(B) \setminus \{0\}) \geq \frac{1}{2}s(L_O)^2. \quad (3.29)$$

Both spectra (excluding zero) are contained in the interval $[\mu, \infty)$ with $\mu = \frac{1}{2}s(L_O)^2$. The operator function $f(t) = \sqrt{t}$ is Lipschitz continuous on $[\mu, \infty)$ with constant $L = \frac{1}{2\sqrt{\mu}}$. Substituting μ :

$$L = \frac{1}{2\sqrt{s(L_O)^2/2}} = \frac{1}{\sqrt{2}s(L_O)}. \quad (3.30)$$

Applying this Lipschitz bound to the operator norm difference:

$$\| |\mathcal{L}_O| - |\mathcal{Q}_0| \| = \| \sqrt{A} - \sqrt{B} \| \leq \frac{1}{\sqrt{2}s(L_O)} \| A - B \| \leq \eta \frac{K_{sq}}{\sqrt{2}s(L_O)}. \quad (3.31)$$

We combine the bilinear bound (3.25) and the operator root bound via the triangle inequality:

$$|\langle \mathcal{L}X, S\mathcal{L}Y \rangle_{\mathcal{H}} - \langle X, |\mathcal{L}_O|Y \rangle_{\mathcal{H}_S}| \leq |\langle \mathcal{L}X, S\mathcal{L}Y \rangle_{\mathcal{H}} - \langle X, |\mathcal{Q}_0|Y \rangle_{\mathcal{H}_S}| + |\langle X, (|\mathcal{Q}_0| - |\mathcal{L}_O|)Y \rangle_{\mathcal{H}_S}| \quad (3.32)$$

$$\leq \eta(K_{lin} + \eta K_{quad}) \|X\|_{\mathcal{H}} \|Y\|_{\mathcal{H}} + \eta \frac{K_{sq}}{\sqrt{2}s(L_O)} \|X\|_{\mathcal{H}} \|Y\|_{\mathcal{H}} \quad (3.33)$$

$$= \eta \left(K_{lin} + \eta K_{quad} + \frac{K_{sq}}{\sqrt{2}s(L_O)} \right) \|X\|_{\mathcal{H}} \|Y\|_{\mathcal{H}}. \quad (3.34)$$

Defining the term in parentheses as C_{AQF} completes the proof. \square

These two propositions abstract the core structure resulting from adiabatic elimination (under the $L^{(1)} = 0$ assumption). They establish that the perturbation \mathcal{V} acts as an orthogonal coupling and that the resulting second-order dynamics \mathcal{L}_O can be related back to the action of the full generator \mathcal{L} via a quadratic form that is stable up to an $O(\eta s(L_O)^{-1})$ error. This structure is precisely what the lifting construction leverages.

4. Abstract Framework for Semigroup Convergence

This section details the abstract mathematical framework used to analyze the convergence properties of Markovian dynamics, particularly in the context of lifting. We rely on the theory of strongly continuous semigroups on Hilbert spaces, which provides the necessary tools to handle the operators encountered in open quantum systems.

In this section, we introduce the following notations.

Let \mathcal{H} be a Hilbert space with inner product $\langle \cdot, \cdot \rangle_{\mathcal{H}}$ and induced norm $\|\cdot\|_{\mathcal{H}}$. All operators are assumed to be densely defined and potentially unbounded. For an operator $(T, \text{Dom}(T))$, we often write T when the domain is clear from context. The adjoint of T is T^* , and the operator norm is denoted by $\|T\| := \|T\|_{\mathcal{H} \rightarrow \tilde{\mathcal{H}}}$.

4.1. Abstract Markov Semigroups and Generators

We model the system's evolution using a **contractive strongly continuous semigroup** (or C_0 -semigroup), denoted by $\{P_t\}_{t \geq 0}$, acting on \mathcal{H} . This family of operators satisfies the following standard properties:

1. $P_0 = \text{id}$ (identity operator).
2. $P_s P_t = P_{s+t}$ for all $s, t \geq 0$ (semigroup property).
3. For every $X \in \mathcal{H}$, the map $t \mapsto P_t X$ is continuous (strong continuity).
4. $\|P_t\| \leq 1$ for all $t \geq 0$ (contractivity).

The dynamics generated by such a semigroup are governed by its **generator**, $(L, \text{Dom}(L))$, a closed, densely defined operator. The generator is defined by the limit

$$LX := \lim_{t \downarrow 0} \frac{P_t X - X}{t},$$

for all X in its domain $\text{Dom}(L) \subset \mathcal{H}$ for which this strong limit exists. Key properties relevant to Markovian evolution are summarized below.

Lemma 4.1 (Properties of Contractive C_0 -Semigroups). *Let $\{P_t\}_{t \geq 0}$ be a contractive C_0 -semigroup on \mathcal{H} with generator $(L, \text{Dom}(L))$.*

1. **Well-posedness:** For any initial state $X_0 \in \text{Dom}(L)$, the solution $X_t := P_t X_0$ to the abstract Cauchy problem $\partial_t X_t = LX_t$ exists, is unique, remains in $\text{Dom}(L)$ for all $t \geq 0$, and is continuously differentiable.
2. **Dissipativity:** The generator L is dissipative, meaning $\text{Re}\langle X, LX \rangle \leq 0$ for all $X \in \text{Dom}(L)$. Consequently, its spectrum $\sigma(L)$ is contained in the closed left half of the complex plane, $\{\lambda \in \mathbb{C} \mid \text{Re } \lambda \leq 0\}$.
3. **Steady Subspace:** The set of fixed points, $\mathcal{F} := \ker(L)$, forms a closed subspace of \mathcal{H} . Let $\mathbb{E}_{\mathcal{F}}$ denote the orthogonal projection onto \mathcal{F} . The orthogonal complement \mathcal{F}^\perp is invariant under the semigroup dynamics, i.e., $P_t(\mathcal{F}^\perp) \subseteq \mathcal{F}^\perp$ for all $t \geq 0$.

These are standard results in semigroup theory, detailed for instance in [EN00]. The dissipativity property is fundamental, ensuring that the norm $\|X_t\|$ does not grow over time.

4.2. Convergence to Steady State: Coercivity and Hypocoercivity

We are primarily interested in the rate at which the system approaches its steady state configuration. Assuming the semigroup converges strongly to the steady-state projection, $\lim_{t \rightarrow \infty} P_t = \mathbb{E}_{\mathcal{F}}$, we characterize the speed of this convergence.

Definition 4.1 (Modes of Convergence). A contractive C_0 -semigroup $\{P_t\}_{t \geq 0}$ converging to $\mathbb{E}_{\mathcal{F}}$ is said to exhibit:

1. **Coercivity** if there exists a rate $\nu > 0$ such that for all $X \in \mathcal{H}$:

$$\|P_t X - \mathbb{E}_{\mathcal{F}} X\|_{\mathcal{H}} \leq e^{-\nu t} \|X - \mathbb{E}_{\mathcal{F}} X\|_{\mathcal{H}}. \quad (4.1)$$

2. **Hypocoercivity** if there exist a rate $\nu > 0$ and a constant $C \geq 1$ such that for all $X \in \mathcal{H}$:

$$\|P_t X - \mathbb{E}_{\mathcal{F}} X\|_{\mathcal{H}} \leq C e^{-\nu t} \|X - \mathbb{E}_{\mathcal{F}} X\|_{\mathcal{H}}. \quad (4.2)$$

The system is termed **strictly hypocoercive** if the inequality holds only for some $C > 1$.

The optimal rate ν in these inequalities corresponds to the spectral gap $\lambda(L)$ of the generator.

Coercivity represents the simplest convergence behavior, where all deviations from the steady state decay uniformly at an exponential rate. This is typically linked to a direct dissipativity condition on the generator itself:

$$-\operatorname{Re}\langle X, LX \rangle \geq \nu \|X - \mathbb{E}_{\mathcal{F}} X\|_{\mathcal{H}}^2, \quad \forall X \in \operatorname{Dom}(L). \quad (4.3)$$

Strict hypocoercivity ($C > 1$) arises when this condition fails. This often occurs when the generator L has both dissipative and conservative (skew-adjoint) components, $L = \mathcal{S} + \mathcal{A}$. If the kernel of the dissipative part \mathcal{S} is larger than the kernel of the full generator L ($\ker(\mathcal{S}) \supsetneq \ker(L)$), some modes are not directly damped. Convergence relies on the skew-adjoint part \mathcal{A} mixing these undamped modes into damped ones, leading to the prefactor $C > 1$ [Vil09].

4.3. The Singular Value Gap

A useful quantity for analyzing convergence, particularly in relation to hypocoercivity, is the singular value gap of the generator. It measures the minimum “action” of the generator on states orthogonal to its kernel.

Definition 4.2 (Singular Value Gap). Let L be the generator of a contractive C_0 -semigroup with kernel \mathcal{F} . The **singular value gap** of L , denoted $s(L)$, is defined as:

$$s(L) := \inf \left\{ \|LX\|_{\mathcal{H}} \mid X \in \operatorname{Dom}(L) \cap \mathcal{F}^{\perp}, \|X\|_{\mathcal{H}} = 1 \right\}. \quad (4.4)$$

Equivalently, $s(L)$ is the smallest non-zero singular value of L , or the square root of the smallest non-zero eigenvalue of the positive self-adjoint operator L^*L .

The singular value gap provides a bound on the achievable asymptotic decay rate, especially relevant in hypocoercive scenarios where the exponential convergence rate ν might be much smaller than $s(L)$.

Lemma 4.2 (Decay Rate Bound via Singular Value Gap). *Let $\{P_t\}_{t \geq 0}$ be a hypocoercive semigroup satisfying (4.2) with optimal rate $\nu = \lambda(L)$ and prefactor $C \geq 1$. Then the decay rate is bounded by the singular value gap:*

$$\nu \leq (1 + \log C)s(L). \quad (4.5)$$

Proof. This result relates the asymptotic decay rate ν to the instantaneous action $s(L)$ via the hypocoercivity constant C . A proof, adapted from [LL24, Lemma 2.5], is provided in Appendix C.1. \square

This inequality is fundamental for our analysis. It implies that if we can compute or bound the singular value gap $s(L)$ of a generator and estimate its hypocoercivity constant C , we obtain an upper bound on its exponential convergence rate ν , which determines the relaxation time $t_{\text{rel}} \approx 1/\nu$. This connection will be crucial when comparing the original and lifted dynamics.

5. Abstract Lifting Framework

This section establishes the theoretical framework for analyzing the convergence speed of the full dynamics governed by L , viewing it as a specific type of ‘lift’ of the rescaled effective slow dynamics governed by L_O . We adapt the structure presented in the [EL24a, LL25], refining the definitions to precisely match our adiabatic elimination context and incorporating the necessary modifications, such as the error term arising from the non-skew-adjoint perturbation.

5.1. Base and Lifted Semigroups

We consider the **base semigroup**, $\{P_t^O\}_{t \geq 0} = \{\exp(tL_O)\}_{t \geq 0}$. This represents the rescaled effective slow dynamics identified through adiabatic elimination. This semigroup acts on the Hilbert space $\mathcal{H}_S := \ker(\mathcal{R})$, which is a closed subspace of the full operator space \mathcal{H} . The generator $(L_O, \text{Dom}(L_O))$ is approximated by the rescaled second-order term from the SW expansion, $L_O = -P_S \mathcal{V} \mathcal{R}^+ \mathcal{V} P_S$. We assume these effective dynamics converge towards a steady state, exhibiting hypocoercivity.

Assumption 5.1 (Hypocoercivity of Base Dynamics). *The base semigroup $\{P_t^O\}_{t \geq 0}$ on \mathcal{H}_S is hypocoercive. Specifically, there exist constants $\nu_O > 0$ and $C_O \geq 1$ such that for all $X \in \mathcal{H}_S \cap \ker(L_O)^\perp$:*

$$\|P_t^O X\|_{\mathcal{H}} \leq C_O e^{-\nu_O t} \|X\|_{\mathcal{H}}. \quad (5.1)$$

In addition, we have the **lifted semigroup**, $\{P_t\}_{t \geq 0} = \{\exp(tL)\}_{t \geq 0}$, which corresponds to the full original dynamics. This semigroup acts on the larger Hilbert space \mathcal{H} , and its generator is the full generator $L = \gamma \mathcal{R} + \mathcal{V}$. Our objective is to analyze the convergence rate of $\{P_t\}$ by exploiting its structural connection to $\{P_t^O\}$.

5.2. Ad Embed Structure

We now formalize the connection between the full generator L and the rescaled effective generator L_O using conditions derived directly from our adiabatic elimination analysis. In this context, the perturbation \mathcal{V} within L serves as the operator that couples the slow and fast dynamics.

Definition 5.1 (Adiabatic Embedding Structure). Let $L = \gamma\mathcal{R} + \mathcal{V}$ be a generator on a finite-dimensional Hilbert space \mathcal{H} . We say that L exhibits an **Adiabatic Embedding (Ad Embed) Structure** if it satisfies the following conditions:

1. **Orthogonality Condition:** The perturbation \mathcal{V} maps the slow subspace $\mathcal{H}_S = \ker(\mathcal{R})$ strictly into its orthogonal complement \mathcal{H}_F . Equivalently, for all $X, Y \in \text{Dom}(\mathcal{V}) \cap \mathcal{H}_S$:

$$\langle X, \mathcal{V}Y \rangle_{\mathcal{H}} = 0. \quad (5.2)$$

2. **Approximate Quadratic Form:** Let S be a positive bounded operator restricted to \mathcal{H}_F . Let the coupling admit the decomposition $\mathcal{V} = L_{\text{ham}} + \eta L_{\text{pert}}$. Let $L_O = -P_S \mathcal{V} S V P_S$ be the effective generator, and $Q_O = -P_S L_{\text{ham}} S L_{\text{ham}} P_S$ be the unperturbed effective generator. We assume:

- (a) **Gap Existence:** L_O admits a non-trivial singular value gap $s(L_O) > 0$.
- (b) **Kernel Consistency:** $\dim \ker(L_O)$ equals to $\dim \ker(Q_O)$, a common prerequisite for perturbative arguments.

Under these conditions, there exists a constant $C_{AQF} \geq 0$ such that for all $X, Y \in \text{Dom}(\mathcal{V}) \cap \mathcal{H}_S$, the quadratic form satisfies the bound:

$$|\langle LX, SLY \rangle_{\mathcal{H}} - \langle X, |L_O|Y \rangle_{\mathcal{H}_S}| \leq \eta C_{AQF} \|X\|_{\mathcal{H}} \|Y\|_{\mathcal{H}}, \quad (5.3)$$

where $|L_O| = \sqrt{L_O^\dagger L_O}$.

3. **Generator Decomposition:** The components of L satisfy:

- (a) The coupling $\mathcal{V} = L_{\text{ham}} + \eta L_{\text{pert}}$ contains a dominant skew-adjoint part L_{ham} and a bounded perturbation L_{pert} .
- (b) The dissipation $\gamma\mathcal{R}$ is self-adjoint and annihilates the slow subspace ($\mathcal{H}_S = \ker(\mathcal{R})$). It is strictly coercive on the fast subspace \mathcal{H}_F ; that is, there exists $\lambda_R > 0$ such that $-\mathcal{R} \geq \lambda_R P_F$.
- (c) The steady states coincide: $\ker(L) = \ker(L_O)$, and this subspace \mathcal{F} is strictly contained within the slow subspace, $\mathcal{F} \subset \mathcal{H}_S$.

This definition precisely mirrors the structure derived in Sections 3.2 and 3.4. The Orthogonality condition stems from $L^{(1)} = 0$. The Approximate Quadratic Form condition is abstractly stated here but rigorously justified by Assumption 3.1 and Proposition 3.2, establishing the crucial link between the action of L (filtered by S) and the magnitude of L_O , explicitly accounting for the η -dependent error via C_{AQF} . The Generator Decomposition clarifies the distinct roles of \mathcal{V} and $\gamma\mathcal{R}$. This Ad Embed Structure forms the foundation for applying lifting-based convergence bounds to the full system L .

6. Convergence Bounds for the Lifted Semigroup

Having established the Ad Embed Structure connecting the full generator L to the rescaled effective generator L_O , we now derive bounds on the convergence rate of the full (lifted) semigroup $\{P_t\}$. We leverage the relationships encapsulated in the Orthogonality and Approximate Quadratic Form conditions.

6.1. Upper Bound on the Convergence Rate

The exponential convergence rate $\nu(L)$ governs the asymptotic decay. Lemma 4.2 connects this rate to the singular value gap $s(L)$ via the hypocoercivity constant $C(L)$ as $\nu(L) \leq (1 + \log C(L))s(L)$. We obtain an upper bound on $\nu(L)$ by bounding $s(L)$ in terms of the effective generator L_O and the lifting structure, utilizing the refined Approximate Quadratic Form condition.

Theorem 6.1 (Upper Bound on $\nu(L)$). *Let $\{P_t\}_{t \geq 0}$ be a hypocoercive C_0 -semigroup on \mathcal{H} with generator $L = \gamma\mathcal{R} + \mathcal{V}$ satisfying the Ad Embed Structure (Definition 5.1, using the Approximate Quadratic Form Condition (5.3)) relative to the target effective generator L_O acting on $\mathcal{H}_S = \ker(\mathcal{R})$. Let the decay be characterized by $r(t) = C(L) \exp(-\nu(L)t)$. Let S be the positive definite operator from the Approximate Quadratic Form condition. Define Π_1 as the orthogonal projection onto the subspace $\overline{\text{Ran}(\mathcal{V}|_{\mathcal{H}_S})} \subseteq \mathcal{H}_F$. Then, the exponential convergence rate $\nu(L)$ is bounded by:*

$$\nu(L) \leq (1 + \log C(L)) \sqrt{\frac{s(L_O) + \eta C_{AQF}}{s(\Pi_1 S \Pi_1)}}, \quad (6.1)$$

where $s(L_O)$ is the singular value gap of the effective generator L_O , $s(\Pi_1 S \Pi_1)$ is the smallest eigenvalue (singular value gap) of the positive definite operator $\Pi_1 S \Pi_1$ restricted to the subspace $\text{Ran}(\Pi_1)$, and C_{AQF} is the explicit constant from the Approximate Quadratic Form condition.

Proof. The proof involves bounding the singular value gap $s(L)$ by restricting the infimum defining it to the subspace \mathcal{H}_S . The revised Approximate Quadratic Form condition (5.3) is then used to relate the action of L back to the magnitude of L_O , incorporating the explicit error term bounded by ηC_{AQF} . The detailed derivation is provided in Appendix D.1. \square

This theorem shows that the convergence rate of the full (lifted) system is limited by the singular value gap $s(L_O)$ of the effective dynamics and the “filtering factor” $s(\Pi_1 S \Pi_1)$ related to the operator S . The ηC_{AQF} term indicates that the non-skew-adjoint part of the perturbation \mathcal{V} introduces a small, explicitly bounded correction to this upper limit.

Remark 6.1 (Optimality and the Perturbative Regime). Utilizing the rigorous scaling $C_{AQF} = \Theta(s(L_O)^{-1})$ derived in Proposition 3.2, the effective spectral parameter governing the upper bound behaves as

$$\nu(L) \lesssim \sqrt{s(L_O) + \eta C_{AQF}} \sim \sqrt{s(L_O) + O(\eta s(L_O)^{-1})}. \quad (6.2)$$

We recall that the stability of the effective generator requires the perturbation to satisfy $\eta \leq \eta_{\text{crit}}$, where the critical threshold scales as $\eta_{\text{crit}} = \Theta(s(L_O)^2)$ to prevent the closure of the spectral gap. Consequently, the condition $\eta = O(s(L_O)^2)$ is intrinsic to the validity of the framework. In this regime, the perturbation term $\eta s(L_O)^{-1}$ becomes comparable to the leading order gap $s(L_O)$, preserving the scaling behavior $\sqrt{\Theta(s(L_O))} = \Theta(\sqrt{s(L_O)})$. This square-root dependence represents a transition from the intrinsic *diffusive* relaxation of the effective dynamics ($\tau \sim s(L_O)^{-1}$) to a *ballistic* relaxation in the lifted space ($\tau \sim s(L_O)^{-1/2}$). This saturates the theoretical maximum acceleration for Markovian lifts (often analogous to the Heisenberg limit in quantum metrology), confirming that the non-equilibrium perturbation does not structurally obstruct optimal convergence provided it respects the spectral stability bound.

6.2. Lower Bound of the Convergence Rate

To derive a lower bound on the mixing speed of the full semigroup $\{P_t\}$ generated by L , we adapt the variational framework based on Flow Poincaré inequalities [LL25, LL24, EL24a]. This approach is particularly suited for handling hypocoercivity. Our goal is to relate the convergence rate of L back to the properties of the effective slow dynamics L_O .

6.2.1. Flow Poincaré Inequality Framework

We establish the functional setting for the Flow Poincaré inequality. Let $L^2([0, T]; \mathcal{H})$ be the Bochner space of square-integrable paths $X_t : [0, T] \rightarrow \mathcal{H}$, equipped with the **normalized inner product**:

$$\langle X_t, Y_t \rangle_{T, \mathcal{H}} := \frac{1}{T} \int_0^T \langle X_t, Y_t \rangle_{\mathcal{H}} dt. \quad (6.3)$$

We also consider its closed subspace $L^2([0, T]; \mathcal{H}_S)$ of paths valued in the slow subspace $\mathcal{H}_S = \ker(\mathcal{R})$.

For a closed, densely defined operator A on \mathcal{H} , we define the associated sesquilinear form, often representing a Dirichlet form if $-A$ is dissipative and self-adjoint:

$$\mathcal{E}_A(X, Y) := -\langle X, AY \rangle_{\mathcal{H}}, \quad (6.4)$$

for $X \in \mathcal{H}$ and $Y \in \text{Dom}(A)$. We denote the quadratic form by $\mathcal{E}_A(X) := \mathcal{E}_A(X, X)$. The corresponding time-averaged forms are:

$$\mathcal{E}_{T,A}(X_t, Y_t) := \frac{1}{T} \int_0^T \mathcal{E}_A(X_t, Y_t) dt, \quad \text{and} \quad \mathcal{E}_{T,A}(X_t) := \mathcal{E}_{T,A}(X_t, X_t). \quad (6.5)$$

Crucial to the method is the **Backward Kolmogorov Operator**, which incorporates the time derivative and the “non-dissipative” part of the dynamics. In our Ad Embed structure $L = \gamma\mathcal{R} + \mathcal{V}$, the operator \mathcal{V} acts as the coupling. We define $(\mathcal{A}, \text{Dom}(\mathcal{A}))$ on $L^2([0, T]; \mathcal{H})$ as:

$$\mathcal{A}X_t := -\partial_t X_t + \mathcal{V}X_t, \quad (6.6)$$

with domain:

$$\text{Dom}(\mathcal{A}) := \{X_t \in H^1([0, T]; \mathcal{H}) \mid X_t \in \text{Dom}(\mathcal{V}) \text{ for a.e. } t, \text{ and } \mathcal{V}X_t \in L^2([0, T]; \mathcal{H})\}, \quad (6.7)$$

where H^1 is the standard Sobolev space of paths with square-integrable weak derivatives.

The following lemma connects the action of \mathcal{A} in the full space \mathcal{H} to the rescaled effective dynamics $|L_O|$ in the slow subspace \mathcal{H}_S , incorporating the Approximate Quadratic Form condition. It shows how the structure involving \mathcal{V} and S reduces to the magnitude of the rescaled effective generator L_O when projected appropriately.

Lemma 6.1 (Inner Product Reduction of \mathcal{A}). *Assume the Ad Embed Structure (Definition 5.1) holds, including the Approximate Quadratic Form Condition (5.3) with constant C_{AQF} . Then, for any sufficiently regular paths X_t, Y_t, Z_t taking values in the slow subspace $\mathcal{H}_S = \ker(\mathcal{R})$, the following relation holds:*

$$\langle \mathcal{A}X_t, Z_t + S\mathcal{V}Y_t \rangle_{T, \mathcal{H}} = -\langle \partial_t X_t, Z_t \rangle_{T, \mathcal{H}_S} + \mathcal{E}_{T, -|L_O|}(X_t, Y_t) + R_{T, \eta}(X, Y), \quad (6.8)$$

where the remainder term satisfies $|R_{T, \eta}(X, Y)| \leq \eta C_{AQF} \frac{1}{T} \int_0^T \|X_t\|_{\mathcal{H}} \|Y_t\|_{\mathcal{H}} dt$.

Proof. The identity follows from expanding the inner product on the left-hand side, applying the Orthogonality condition of the Ad Embed Structure to eliminate cross-terms, and using the revised Approximate Quadratic Form condition (5.3) to relate the term $\langle \mathcal{V}X_t, S\mathcal{V}Y_t \rangle$ back to $\langle X_t, |L_O|Y_t \rangle$. The approximation introduces the explicit remainder term $R_{T, \eta}(X, Y)$. A full proof is provided in Appendix E.1. \square

Next, we require the existence of solutions to an abstract divergence equation involving the magnitude of the effective operator $|L_O|$. This technical result enables the construction of auxiliary functions required for the Flow Poincaré inequality.

Assumption 6.1 (Regularity of Effective Operator Magnitude). The operator $|L_O| = \sqrt{L_O^* L_O}$ acting on \mathcal{H}_S has the following properties:

1. **Discrete spectrum:** $|L_O|$ has a discrete spectrum consisting of non-negative eigenvalues.
2. **Non-trivial singular gap:** The smallest non-zero eigenvalue of $|L_O|$ (which is the singular value gap $s(L_O)$) is strictly positive, $s(L_O) > 0$.

Define the subspace $L_{\perp}^2([0, T]; \mathcal{H}_S)$ of paths in $L^2([0, T]; \mathcal{H}_S)$ that are orthogonal to the kernel $\ker(L_O)$ at almost every time t .

$$L_{\perp}^2([0, T]; \mathcal{H}_S) = \{X_t \in L^2([0, T]; \mathcal{H}_S) \mid P_S X_t = 0 \text{ for a.e. } t \in [0, T]\}. \quad (6.9)$$

Theorem 6.2 (Abstract Divergence Lemma). *Under Assumption 6.1, for any $T > 0$ and any path $X_t \in L_{\perp}^2([0, T]; \mathcal{H}_S)$, there exists a pair of paths (Z_t, Y_t) with Z_t, Y_t valued in $\text{Dom}(|L_O|) \subset \mathcal{H}_S$ solving the **abstract divergence equation**:*

$$\partial_t Z_t + |L_O|Y_t = X_t, \quad (6.10)$$

and satisfying the energy estimates:

$$\|L_O|Y_t\|_{T,\mathcal{H}_S} \leq c_1(T)\|X_t\|_{T,\mathcal{H}_S}, \quad \sqrt{\mathcal{E}_{T,-|L_O|}(Z_t)} \leq c_2(T)\|X_t\|_{T,\mathcal{H}_S}, \quad (6.11)$$

$$\sqrt{\mathcal{E}_{T,-|L_O|}(Y_t)} \leq c_3(T)\|X_t\|_{T,\mathcal{H}_S}, \quad \sqrt{\mathcal{E}_{T,-|L_O|}(\partial_t Y_t)} \leq c_4(T)\|X_t\|_{T,\mathcal{H}_S}, \quad (6.12)$$

where $\mathcal{E}_{T,-|L_O|}(W_t) = \langle W_t, |L_O|W_t \rangle_{T,\mathcal{H}_S}$. The constants scale as:

$$c_1 = \Theta(1), \quad c_2 = \Theta(1), \quad c_3 = \Theta\left(T + \frac{1}{\sqrt{s(L_O)}}\right), \quad c_4 = \Theta\left(1 + \frac{1}{T\sqrt{s(L_O)}}\right). \quad (6.13)$$

Proof. The proof adapts the spectral method from [LL25, EGH⁺25], using the eigenbasis of the self-adjoint operator $|L_O|$. The proof structure relies solely on $|L_O|$ and is independent of specific lifting details. A full proof is deferred to Appendix E.1. \square

Before stating the main Flow Poincaré inequality, we need additional regularity assumptions tailored to the Ad Embed structure. These assumptions ensure that the different operator terms behave well with respect to each other and the underlying dissipation.

Assumption 6.2 (Regularity Conditions for the Flow Poincaré Inequality). Let the generator $L = \gamma\mathcal{R} + \mathcal{V}$ satisfy the Ad Embed Structure (Definition 5.1). Let L_O be the target effective generator satisfying Assumption 5.1, and let $|L_O|$ satisfy Assumption 6.1. Let P_S denote the orthogonal projection onto $\mathcal{H}_S = \ker(\mathcal{R})$ and S . We assume:

1. **Existence of a Regular Path Space.** There exists a subspace $\mathcal{C}_0 \subset \mathcal{F}^\perp \cap \text{Dom}(L)$ dense in \mathcal{F}^\perp (where $\mathcal{F} = \ker(L)$). Let $\mathcal{C}_{[0,T]} := \{P_t X_0 \mid X_0 \in \mathcal{F}^\perp, t \in [0, T]\}$ and $\mathcal{C}_{[0,T]}^d := \{P_t X_0 \mid X_0 \in \mathcal{C}_0, t \in [0, T]\}$. We assume that:
 - (a) For any path $X_t \in \mathcal{C}_{[0,T]}^d$, both X_t and its projection $P_S X_t$ belong to the domain required for Theorem 6.2 and the definition of \mathcal{A} .
 - (b) $\mathcal{C}_{[0,T]}^d$ is dense in $\mathcal{C}_{[0,T]}$ with respect to the norm $\|X_t\|_{T,\mathcal{H}} + \sqrt{\mathcal{E}_{T,-|L_O|}(P_S X_t)}$.

2. **Operator Regularity and Bounded Perturbation.** The operators \mathcal{R} , \mathcal{V} and S satisfy standard domain inclusions. We assume the non-skew-adjoint perturbation \mathcal{V} is bounded relative to the (unscaled) fast dissipation \mathcal{R} . Specifically, there exists a constant $K_1 > 0$ such that for all $X \in \text{Dom}(\mathcal{R}) \cap \text{Dom}(\mathcal{V})$ with $X \in \mathcal{H}_F$:

$$\|S^{1/2}\mathcal{V}X\|_{\mathcal{H}} \leq K_1 \sqrt{\mathcal{E}_{\mathcal{R}}(X)}, \quad (6.14)$$

where $\mathcal{E}_{\mathcal{R}}(X) = -\langle X, \mathcal{R}X \rangle$.

3. **Bounded Intertwining Terms.** The terms intertwining the coupling \mathcal{V} and the dissipation \mathcal{R} (via S) are controlled by the effective dynamics. Specifically, there exist constants $K_2, K_3 > 0$ such that for all $Y \in \text{Dom}(L_O)$:

$$\|(\mathbf{1} - P_S)\mathcal{V}^*S\mathcal{V}Y\|_{\mathcal{H}} \leq K_2\|L_O|Y\|_{\mathcal{H}_S} + K_3\sqrt{\mathcal{E}_{-|L_O|}(Y)}. \quad (6.15)$$

These assumptions lead to crucial estimates bounding the coupling between different parts of the generator.

Lemma 6.2 (Coupling Strength Estimates). *Under Assumption 6.2, for sufficiently regular paths $X_t \in \text{Dom}(\mathcal{R})$ and $Y_t \in \text{Dom}(L_O)$, the following bounds hold:*

$$|\langle \mathcal{R}X_t, S\mathcal{V}Y_t \rangle_{\mathcal{H}}| \leq \sqrt{\mathcal{E}_{\mathcal{R}}(X_t)(\mathcal{E}_{-|L_O|}(Y_t) + \eta C_{AQF} \|Y_t\|_{\mathcal{H}}^2)}, \quad (6.16)$$

$$|\langle X_t - P_S X_t, \mathcal{V}Y_t \rangle_{\mathcal{H}}| \leq \sqrt{\mathcal{E}_{\mathcal{R}}(X_t)(\mathcal{E}_{-|L_O|}(Y_t) + \eta C_{AQF} \|Y_t\|_{\mathcal{H}}^2)}, \quad (6.17)$$

$$|\langle \mathcal{V}(X_t - P_S X_t), S\mathcal{V}Y_t \rangle_{\mathcal{H}}| \leq \|X_t - P_S X_t\|_{\mathcal{H}} \left(K_2 \|L_O|Y_t\|_{\mathcal{H}_S} + K_3 \sqrt{\mathcal{E}_{-|L_O|}(Y_t)} \right). \quad (6.18)$$

Proof. These inequalities follow from applying the Cauchy-Schwarz inequality, the properties of S , the Approximate Quadratic Form condition, and the bounds defined in Assumption 6.2. A detailed derivation is in Appendix E.2. \square

With these tools and assumptions, we can now state the Flow Poincaré inequality for our Ad Embed structure. This inequality provides a quantitative link between the average norm of the state trajectory and the average dissipation rate associated with the unscaled fast dynamics \mathcal{R} . A crucial requirement for the following theorem is that the non-conservative perturbation η be small relative to the intrinsic timescales of the effective dynamics (specifically, ensuring $1 - \eta C_{corr} > 0$ as defined below), justifying the perturbative approach for well-behaved target systems.

Theorem 6.3 (Flow Poincaré Inequality for Ad Embed). *Let C_{AQF} be the explicit constant from the Approximate Quadratic Form condition (Definition 5.1). Assume η is sufficiently small such that $1 - \eta C_{corr} > 0$, where $C_{corr} = C_{AQF} s(L_O)^{-1} c_1(T)$ is a structural correction constant. Under Assumption 6.2, for any $T > 0$ and initial state $X_0 \in \mathcal{F}^\perp \cap \text{Dom}(L)$, the trajectory $X_t = P_t X_0$ satisfies the strict Flow Poincaré inequality:*

$$\alpha_T(\eta) \|X_t\|_{T,\mathcal{H}}^2 \leq \mathcal{E}_{T,\mathcal{R}}(X_t), \quad (6.19)$$

with the rate constant

$$\alpha_T(\eta) = \left[\frac{(\gamma \tilde{A}_1(T, \eta) + \tilde{A}_2(T, \eta))^2}{(1 - \eta C_{corr})^2} + \frac{1}{\lambda_R} \right]^{-1}, \quad (6.20)$$

where the η -corrected coefficients are

$$\tilde{A}_1(T, \eta) = c_3(T) + \sqrt{\eta C_{AQF} s(L_O)^{-1}} c_1(T), \quad (6.21)$$

$$\begin{aligned} \tilde{A}_2(T, \eta) = & K_1 c_2(T) + \lambda_R^{-1/2} (\|S\|^{1/2} c_4(T) + K_2 c_1(T) + K_3 c_2(T)) \\ & + \sqrt{\eta C_{AQF}} K_1 s(L_O)^{-1/2} c_2(T). \end{aligned} \quad (6.22)$$

Here, $c_i(T)$, $i = 1, 2, 3, 4$ are the constants from the Abstract Divergence Lemma (Theorem 6.2).

Proof. The proof adapts the variational argument from [LL25]. It involves decomposing the trajectory norm, using the solution (Z_t, Y_t) to the abstract divergence equation to handle the projected part $P_S X_t$, and applying the explicit coupling estimates (Lemma 6.2) derived from the Ad Embed structure. The η -dependent error terms from the Approximate Quadratic Form condition are rigorously tracked and absorbed into the coefficients $\tilde{A}_i(T, \eta)$ and C_{corr} , resulting in a strict inequality without constant error tails. A full, self-contained proof is provided in Appendix E.2. \square

Remark 6.2 (Spectral Stability and the Validity Regime). The condition $1 - \eta C_{corr} > 0$ serves as a rigorous constraint on the perturbation strength relative to the intrinsic timescale of the effective dynamics. Recall that the structural correction constant is defined by $C_{corr} = C_{AQF} s(L_O)^{-1} c_1(T)$. Incorporating the rigorous scaling $C_{AQF} = \Theta(s(L_O)^{-1})$ in Proposition 3.2 and $c_1(T) = \Theta(1)$ in Theorem 6.2, the correction factor scales asymptotically as $C_{corr} = \Theta(s(L_O)^{-2})$. Consequently, the strict positivity of the geometric decay rate $\alpha_T(\eta)$ necessitates that the non-equilibrium perturbation satisfies $\eta = O(s(L_O)^2)$, coinciding with that of Remark 6.1.

6.2.2. Lower Bound Estimation from Flow Poincaré Inequality

The Flow Poincaré inequality established in Theorem 6.3 links the time-averaged state norm to the time-averaged dissipation. This inequality enables the derivation of an explicit lower bound for the convergence rate via a standard Grönwall-type argument applied to a time-averaged energy functional. The resulting bound quantifies the strict exponential decay of this averaged energy.

Theorem 6.4 (T -Average Convergence Lower Bound). *Let the generator $L = \gamma \mathcal{R} + \mathcal{V}$ satisfy the assumptions of Theorem 6.3. Assume η is sufficiently small such that $\alpha_T(\eta) > 0$. For any observation period $T > 0$, provided the effective rate ν_{eff} defined below is positive, any initial state $X_0 \in \mathcal{F}^\perp \cap \text{Dom}(L)$ exhibits time-averaged strict exponential decay bounded by:*

$$\frac{1}{T} \int_t^{t+T} \|P_s X_0\|_{\mathcal{H}}^2 ds \leq e^{-2\nu_{eff} t} \|X_0\|_{\mathcal{H}}^2, \quad (6.23)$$

where the decay rate parameter ν_{eff} depends on γ, η, T as

$$\nu_{eff} = \nu_{eff}(\gamma, \eta, T) := \gamma \alpha_T(\eta) - \eta \|L_{pert}\|. \quad (6.24)$$

Proof. The proof involves defining the time-averaged energy functional

$$E_T(t) = \frac{1}{T} \int_t^{t+T} \|P_s X_0\|_{\mathcal{H}}^2 ds.$$

By differentiating $E_T(t)$ with respect to time and utilizing the properties of the generator $L = \gamma \mathcal{R} + L_{\text{ham}} + \eta L_{\text{pert}}$, we relate $\frac{d}{dt} E_T(t)$ to the dissipation term involving \mathcal{R} and the perturbation term involving L_{pert} . Applying the strict Flow Poincaré inequality

(Theorem 6.3) to bound the dissipation term and using the operator norm to bound the perturbation term leads to the differential inequality

$$\frac{d}{dt} E_T(t) \leq -2\nu_{\text{eff}} E_T(t).$$

Solving this inequality using Grönwall's lemma and bounding the initial condition $E_T(0)$ by $\|X_0\|_{\mathcal{H}}^2$ yields the stated bound. The detailed derivation is provided in Appendix E.3. \square

This theorem provides an explicit lower bound on the time-averaged convergence rate, ν_{eff} . The rate is primarily determined by the Flow Poincaré constant $\alpha_T(\eta)$ scaled by γ , reduced slightly by the contribution from the non-conservative perturbation L_{pert} scaled by η .

The time-averaged decay described in Theorem 6.4 yields an explicit lower bound on the convergence rate. This result can be refined to provide a pointwise exponential decay bound for the trajectory $\|X_t\|_{\mathcal{H}}$, along with an explicit expression for the near-optimal fast dissipation scale γ that maximizes this lower bound for a fixed averaging time T .

Corollary 6.1 (Near-optimal Selection of γ). *Assume η is sufficiently small such that $\alpha_T(\eta) > 0$. Under the assumptions of Theorem 6.4, for any $T > 0$ and initial state $X_0 \in \mathcal{F}^\perp \cap \text{Dom}(L)$, the trajectory $X_t = P_t X_0$ satisfies the pointwise decay bound:*

$$\|X_t\|_{\mathcal{H}} \leq C_T e^{-\nu_{\text{eff}} t} \|X_0\|_{\mathcal{H}}, \quad (6.25)$$

where the decay rate is $\nu_{\text{eff}} = \gamma \alpha_T(\eta) - \eta \|L_{\text{pert}}\|$ and the prefactor is $C_T = e^{\nu_{\text{eff}} T}$.

Furthermore, for a fixed T , the lower bound on the decay rate ν_{eff} is maximized by choosing γ near-optimally as

$$\gamma_{\text{opt}}(T) = \frac{1}{\tilde{A}_1(T, \eta)} \sqrt{\tilde{A}_2(T, \eta)^2 + \frac{(1 - \eta C_{\text{corr}})^2}{2\lambda_R}}, \quad (6.26)$$

where $\tilde{A}_1, \tilde{A}_2, C_{\text{corr}}$ are the η -dependent coefficients defined in Theorem 6.3. This choice yields the corresponding maximal rate lower bound $\nu_{\text{opt}}(T)$ explicitly derived in Appendix E.1.

Proof. The hypocoercive-type estimate follows from the time-averaged bound (Theorem 6.4) using semigroup contractivity. The explicit expressions for $\gamma_{\text{opt}}(T)$ and $\nu_{\text{opt}}(T)$ are obtained by maximizing the rate expression ν_{eff} with respect to γ . The detailed derivation is provided in Appendix E.1. \square

This corollary provides an explicit lower bound $\nu_{\text{opt}}(T)$ on the exponential convergence rate of the full generator L for a given T . It demonstrates how the interplay between the fast dissipation scale γ , the properties of the effective dynamics L_O , and the non-conservative perturbation ηL_{pert} determines the convergence speed. The final step involves analyzing the scaling of $\nu_{\text{opt}}(T)$ by optimizing over the time horizon T .

Finally, by analyzing the dependence of the maximized rate $\nu_{opt}(T)$ on the averaging time T and the singular value gap $s(L_O)$ of the target effective generator, we determine the conditions under which the lifting achieves significant acceleration, specifically the “diffusive-to-ballistic” scaling characteristic of optimal lifts. This involves choosing T optimally to balance contributions that scale differently with $s(L_O)$.

Corollary 6.2 (Optimal Rate Scaling and Quadratic Speedup). *Let $s := s(L_O)$ denote the singular value gap of the target effective generator. Under the assumptions of Theorem 6.3, suppose the structural constants satisfy the scaling conditions $K_1, K_2, \lambda_R, \|S\| = \Theta(1)$ and $K_3 = \Theta(\sqrt{s})$. Assume further that the Approximate Quadratic Form constant scales as $C_{AQF} = \Theta(s^{-1})$ and that the non-conservative perturbation strength η satisfies the strict asymptotic scaling condition:*

$$\eta = o(s^2) \quad \text{as } s \rightarrow 0. \quad (6.27)$$

Then, by choosing the observation time optimally as $T_{opt} = \Theta(s^{-1/2})$, the maximal convergence rate lower bound exhibits quadratic scaling:

$$\nu_{opt}(T_{opt}) = \Theta(\sqrt{s}). \quad (6.28)$$

Moreover, the prefactor $C_{T_{opt}} = e^{\nu_{opt}(T_{opt})T_{opt}}$ associated with the pointwise decay bound remains asymptotically bounded, i.e., $C_{T_{opt}} = \Theta(1)$.

Proof. The proof relies on the asymptotic analysis of the rate expression $\nu_{opt}(T)$ derived in Corollary 6.1. Substituting the scalings of the energy estimate constants $c_i(T)$ with $T = \Theta(s^{-1/2})$ and $K_3 = \Theta(\sqrt{s})$, the dominant behavior of the lifting term is identified as $\Theta(\sqrt{s})$. Crucially, the condition $\eta = o(s^2)$ ensures that the spectral stability correction term ηC_{corr} (which scales as $\Theta(\eta s^{-2})$) vanishes asymptotically, preserving the strict positivity of the Flow Poincaré constant. Furthermore, this subdominance guarantees that the perturbative decay rate reduction $-\eta \|L_{pert}\|$ remains negligible compared to the lifting gain. Finally, the exponent $\nu_{opt}(T_{opt})T_{opt}$ is shown to be $\Theta(1)$, ensuring a bounded prefactor. The detailed rigorous calculation is provided in Appendix E.2. \square

Remark 6.3 (Physicality of Scales and Robustness). We conclude with two observations regarding the physical consistency of the derived scaling laws.

First, the strict subdominance condition $\eta = o(s(L_O)^2)$ imposed in Corollary 6.2 is formally stronger than the spectral stability threshold $\eta = O(s(L_O)^2)$ required for the upper bound (Remark 6.1) and the existence of the Flow Poincaré constant (Remark 6.2). While the stricter $o(s^2)$ condition is necessary to mathematically isolate the pure $\Theta(\sqrt{s})$ asymptotic behavior by suppressing higher-order corrections, the acceleration mechanism itself is robust. The lifting speedup persists in the broader regime $\eta = O(s(L_O)^2)$, provided the perturbation remains below the critical value η_{crit} required to keep the spectral gap open.

Second, the structural scaling assumptions employed in the proof are physically motivated. The conditions $\|S\| = \lambda_R^{-1} = \Theta(1)$ and $C_{AQF} = \Theta(s(L_O)^{-1})$ follow directly from the separation of timescales ($\lambda_R \gg s(L_O)$) and the spectral geometry of the

square root function near zero, as indicated in Proposition 3.2. The intertwining scaling $K_3 = \Theta(\sqrt{s(L_O)})$, which governs the coupling between the dissipative and slow sectors, is not arbitrary; it coincides precisely with the optimal scaling identified for equilibrium lifts in [LL25, Eq. (2.42)], suggesting that the Ad Embed structure successfully generalizes the geometry of optimal reversible lifts to the non-equilibrium setting.

7. Examples

To validate and illustrate the abstract Ad Embed framework, we now apply it to two canonical systems, demonstrating its broad applicability. We first analyze classical nonequilibrium Langevin dynamics [MR22, IOS17], showing how the full underdamped system naturally realizes the Ad Embed Structure as a lift of its overdamped, high-friction limit. We then show how this same mathematical structure emerges in a boundary-driven open quantum system [PEKP20, LPS22], where the full Lindbladian in the Zeno regime acts as a quantum lift of an effective classical Markov process. For both examples, we rigorously verify that the generators satisfy the key Orthogonality and Approximate Quadratic Form conditions. We then present numerical experiments to test our main theoretical predictions: the existence of an optimal, finite dissipation scale (γ_{opt}), and the characteristic quadratic speedup, $\nu_{opt} = \Theta(\sqrt{s(L_O)})$.

7.1. Example: Classical Nonequilibrium Langevin Dynamics

We now illustrate the Adiabatic Embedding (Ad Embed) Structure with a canonical example from classical statistical mechanics: the nonequilibrium Langevin dynamics in the high-friction limit [MR22, IOS17]. This system clearly exhibits the timescale separation required for adiabatic elimination, where the momentum variable equilibrates much faster than the position variable.

7.1.1. Dynamics and Generators

Consider a particle with position $q \in \mathbb{R}^d$ and momentum $p \in \mathbb{R}^d$ evolving according to the underdamped Langevin equations:

$$dq_t = p_t dt, \tag{7.1}$$

$$dp_t = (-\nabla_q U(q_t) + \eta F(q_t))dt - \gamma p_t dt + \sqrt{\frac{2\gamma}{\beta}} dW_t, \tag{7.2}$$

where $U(q)$ is a potential, $\eta F(q)$ is a non-conservative force ($0 \leq \eta \ll \min(1, \gamma)$), where γ is the friction coefficient, $\beta = 1/T$ is the inverse temperature, and W_t is a standard d -dimensional Wiener process. The generator L for this process, acting on suitable test functions $f(q, p)$, is the adjoint of the associated Fokker-Planck operator:

$$Lf(q, p) = p \cdot \nabla_q f + (-\nabla_q U(q) + \eta F(q) - \gamma p) \cdot \nabla_p f + \frac{\gamma}{\beta} \Delta_p f. \tag{7.3}$$

In the high-friction limit $\gamma \rightarrow \infty$, after appropriate time rescaling, the dynamics are expected to converge to the overdamped Langevin equation $dQ_t = (-\nabla_q U(Q_t) + \eta F(Q_t))dt + \sqrt{2/\beta}dW_t$ [MR22]. The generator for this limiting process acts on functions $f(q)$ as:

$$L_O f(q) = (-\nabla_q U(q) + \eta F(q)) \cdot \nabla_q f + \frac{1}{\beta} \Delta_q f. \quad (7.4)$$

This L_O represents the target effective generator whose structure we aim to recover via adiabatic elimination.

7.1.2. Hilbert Space Structure and Decomposition

The natural Hilbert space for the full dynamics is $\mathcal{H} = L^2(\mathbb{R}^{2d}, d\hat{\mu})$, where $\hat{\mu}$ is the invariant measure of the underdamped process (7.3). In the limit $\gamma \rightarrow \infty$, this measure is known to factorize as $d\hat{\mu}(q, p) \rightarrow d\mu(q)g_\beta(p)dp$ in Wasserstein distance [MR22, Theorem 1.1], where μ is the invariant measure for the overdamped dynamics ($L_O^* \mu = 0$) and $g_\beta(p) = (\beta/2\pi)^{d/2} e^{-\beta|p|^2/2}$ is the Maxwell-Boltzmann distribution. We equip \mathcal{H} with the inner product $\langle f, g \rangle_{\mathcal{H}} = \int f^*(q, p)g(q, p)d\hat{\mu}(q, p)$.

We decompose the full generator L according to the AE structure $L = \gamma\mathcal{R} + \mathcal{V}$:

$$\gamma\mathcal{R}f = -\gamma p \cdot \nabla_p f + \frac{\gamma}{\beta} \Delta_p f, \quad (7.5)$$

$$\mathcal{V}f = p \cdot \nabla_q f + (-\nabla_q U(q) + \eta F(q)) \cdot \nabla_p f. \quad (7.6)$$

The operator $\mathcal{R} = -p \cdot \nabla_p + \frac{1}{\beta} \Delta_p$ generates the Ornstein-Uhlenbeck process for the momentum p , which thermalizes to the Maxwell-Boltzmann distribution $g_\beta(p)$. Its kernel consists precisely of functions independent of p . Therefore, the slow subspace is $\mathcal{H}_S = \ker(\mathcal{R}) = \{f \in \mathcal{H} \mid f(q, p) = f(q) \text{ a.e.}\}$, which corresponds to $L^2(\mathbb{R}^d, d\mu)$ in the large γ limit. The orthogonal projection $P_S : \mathcal{H} \rightarrow \mathcal{H}_S$ in this limit is given by averaging over the momentum with the Maxwell-Boltzmann weight: $P_S[f](q) = \int f(q, p)g_\beta(p)dp$. It is known that \mathcal{R} is self-adjoint and negative semi-definite with respect to the inner product weighted by $g_\beta(p)$ (and consequently for $d\hat{\mu}$ in the large γ limit).

7.1.3. Verification of Ad Embed Conditions

We now explicitly verify the key structural conditions required by the AE framework, namely the Orthogonality condition ($P_S \mathcal{V} P_S = 0$) and the second-order formula for L_O .

Proposition 7.1 (Conditions Verification for Langevin). *The Langevin generator $L = \gamma\mathcal{R} + \mathcal{V}$ satisfies:*

- (i) $P_S \mathcal{V} P_S = 0$.
- (ii) $L_O = -P_S \mathcal{V} \mathcal{R}^+ \mathcal{V} P_S$, where L_O is the overdamped generator (7.4).

Proof. (i) *Verification of Orthogonality:* Let $f \in \mathcal{H}$ be an arbitrary function. Its projection onto the slow subspace is $f_q(q) = P_S[f](q)$, which is independent of p . We apply the coupling operator \mathcal{V} to f_q :

$$\mathcal{V}f_q(q) = p \cdot \nabla_q f_q(q) + (-\nabla_q U(q) + \eta F(q)) \cdot \underbrace{\nabla_p f_q(q)}_{=0} = p \cdot \nabla_q f_q(q). \quad (7.7)$$

Now, we project this result back onto the slow subspace using P_S :

$$P_S[\mathcal{V}(P_S f)](q) = \int_{\mathbb{R}^d} (p \cdot \nabla_q f_q(q)) g_\beta(p) dp \quad (7.8)$$

$$= \left(\int_{\mathbb{R}^d} p g_\beta(p) dp \right) \cdot \nabla_q f_q(q). \quad (7.9)$$

The integral $\int p g_\beta(p) dp$ represents the mean momentum under the Maxwell-Boltzmann distribution, which is zero as $g_\beta(p)$ is centered. Consequently, $P_S[\mathcal{V}(P_S f)](q) = 0$ for all f , demonstrating that $P_S \mathcal{V} P_S = 0$.

(ii) *Verification of Second-Order Formula:* We compute the expression $-P_S \mathcal{V} \mathcal{R}^+ \mathcal{V} P_S$ acting on an arbitrary function $f_q(q) \in \mathcal{H}_S$. First, as shown above, $\mathcal{V} P_S[f](q, p) = \mathcal{V} f_q(q) = p \cdot \nabla_q f_q(q)$. Let $h(q, p) = p \cdot \nabla_q f_q(q)$. Next, we determine the action of the pseudo-inverse \mathcal{R}^+ . We need to find $\psi = \mathcal{R}^+ h$, which is the unique solution in \mathcal{H}_F (i.e., $P_S[\psi] = 0$) to the equation $\mathcal{R}\psi = h$:

$$-p \cdot \nabla_p \psi + \frac{1}{\beta} \Delta_p \psi = p \cdot \nabla_q f_q(q). \quad (7.10)$$

By inspection (or using standard results for the Ornstein-Uhlenbeck generator), the solution with mean zero is $\psi(q, p) = -p \cdot \nabla_q f_q(q)$. Indeed, $\nabla_p \psi = -\nabla_q f_q(q)$ and $\Delta_p \psi = 0$, so $\mathcal{R}\psi = -p \cdot (-\nabla_q f_q(q)) + 0 = p \cdot \nabla_q f_q(q) = h$. Thus, $\mathcal{R}^+(p \cdot \nabla_q f_q(q)) = -p \cdot \nabla_q f_q(q)$. Now, we apply \mathcal{V} to ψ :

$$\mathcal{V}\psi = p \cdot \nabla_q \psi + (-\nabla_q U + \eta F) \cdot \nabla_p \psi \quad (7.11)$$

$$= p \cdot \nabla_q (-p \cdot \nabla_q f_q(q)) + (-\nabla_q U + \eta F) \cdot \nabla_p (-p \cdot \nabla_q f_q(q)) \quad (7.12)$$

$$= -(p \otimes p) : \nabla_q^2 f_q(q) + (-\nabla_q U + \eta F) \cdot (-\nabla_q f_q(q)). \quad (7.13)$$

Finally, we apply the projection P_S (momentum averaging with $g_\beta(p)$) and multiply by -1 :

$$-P_S[\mathcal{V} \mathcal{R}^+ \mathcal{V} P_S f] = - \int [-(p \otimes p) : \nabla_q^2 f_q(q) + (\nabla_q U - \eta F) \cdot \nabla_q f_q(q)] g_\beta(p) dp \quad (7.14)$$

$$= \left(\int (p \otimes p) g_\beta(p) dp \right) : \nabla_q^2 f_q(q) - \left(\int g_\beta(p) dp \right) (\nabla_q U - \eta F) \cdot \nabla_q f_q(q). \quad (7.15)$$

Using the standard Gaussian integral results $\int g_\beta(p)dp = 1$ and $\int(p \otimes p)g_\beta(p)dp = \frac{1}{\beta}\mathbf{1}$ (where $\mathbf{1}$ is the identity tensor), we obtain:

$$-P_S[\mathcal{VR}^+\mathcal{VP}_S f] = \frac{1}{\beta}\mathbf{1} : \nabla_q^2 f_q(q) - (\nabla_q U - \eta F) \cdot \nabla_q f_q(q) \quad (7.16)$$

$$= \frac{1}{\beta}\Delta_q f_q(q) + (-\nabla_q U + \eta F) \cdot \nabla_q f_q(q). \quad (7.17)$$

This expression precisely matches the generator $L_O f_q(q)$ of the overdamped Langevin dynamics given in (7.4).

Thus, we have rigorously verified both $P_S \mathcal{VP}_S = 0$ and $L_O = -P_S \mathcal{VR}^+ \mathcal{VP}_S$. This confirms that the classical Langevin system provides a concrete realization of the abstract Ad Embed structure. \square

7.1.4. Numerical Verification

To provide a concrete validation of our theoretical framework, particularly the prediction of an optimal convergence rate and the $\nu = \Theta(\sqrt{s(L_O)})$ scaling (Corollary 6.2), we perform a numerical experiment on the non-reversible Langevin dynamics. This experiment is designed to test two central, non-trivial predictions of the Ad Embed structure: (i) the existence of an optimal, finite dissipation scale γ that maximizes the convergence rate $\nu(L)$, and (ii) a quantitative, super-linear scaling relationship between this accelerated rate and the intrinsic rate $s(L_O)$ of the target effective system.

Numerical Estimate of Convergence Rate. A critical aspect of this numerical validation is the accurate measurement of the exponential convergence rate $\nu(L)$. For a non-reversible NESS, the generator L is non-self-adjoint. Consequently, its spectrum is complex and the autocorrelation function (ACF) of an observable f is not a simple sum of positive decaying exponentials. Instead, it exhibits oscillatory decay.

The dynamics of any observable f (projected onto the subspace orthogonal to the steady state) can be decomposed in the eigenbasis of the generator L with invariant measure π . For t large enough, the dynamics are dominated by the slowest-decaying modes (i.e., the eigenvalues λ_j with the largest real part, $\text{Re}(\lambda_j) = -\nu$). For a non-reversible system, these eigenvalues may be complex, $\lambda_{slow} = -\nu \pm i\omega$. The ACF's asymptotic behavior is thus:

$$\rho_f(t) = \frac{\langle f, e^{tL} f \rangle_\pi}{\|f\|_\pi^2} \approx A e^{-\nu t} \cos(\omega t + \phi), \quad t \rightarrow \infty$$

While $\rho_f(t)$ itself oscillates, the asymptotic convergence rate ν governs the exponential decay of its envelope. We can therefore extract ν by analyzing the logarithm of the envelope's magnitude:

$$\log |\rho_f(t)| \approx \log |A| - \nu t$$

This establishes a linear relationship where the slope is precisely $-\nu$. Our numerical method implements this derivation: we compute the empirical ACF $\hat{\rho}_f(t)$ from a long

simulation, and then perform a linear fit on the slope of its log-envelope, $\log |\widehat{\rho}_f(t)|$, in the asymptotic (linear) tail region to extract $\nu(L)$. For better clarity, we use the median ratio on the control group L_O , which gives it a perfect linear relationship in comparison with L .

Numerical Setup. We model a particle on a two-dimensional torus \mathbb{T}^2 governed by a tilted double-well potential $U(x, y) = h_b/4(x^2 - 1)^2 + \epsilon/2x + 1/2y^2$ and a non-conservative rotational force $F = \alpha(-y, x)^T$. We fix the physical parameters to $\beta = 1.0$ (inverse temperature), $\alpha = 0.5$ (rotational strength, part of L_{pert}), and $\epsilon = 0.1$ (potential tilt). The potential's barrier height, h_b , is varied in the range $[3.0, 5.0]$ to create a set of target systems with progressively slower intrinsic dynamics.

The target effective dynamics are governed by the 2D overdamped generator L_O (analogous to Eq. (7.4)). The baseline convergence rate of this system is given by its singular value gap, $s(L_O)$, which we compute by discretizing the operator on a 50×50 grid and finding its smallest non-zero singular value. The full underdamped Langevin dynamics (generator L in Eq. (7.3)) serves as the Ad Embed system, where the particle's momentum $p = (p_x, p_y)$ is the auxiliary fast variable. The friction coefficient γ corresponds to the fast dissipation scale in our $L = \gamma\mathcal{R} + \mathcal{V}$ decomposition.

We simulate this full system using a BAOAB integrator [KK22]. The convergence rate $\nu(L)$ is quantified by extracting the asymptotic slope from the log-envelope of the ACF of the x -coordinate, as described in our methodology. For each barrier height h_b (i.e., for each $s(L_O)$), we perform a scan over the friction coefficient γ in the range $[0.1, 100]$ to identify the optimal friction γ_{opt} that yields the maximal convergence rate, $\nu_{opt} = \nu(L(\gamma_{opt}))$.

Results and Analysis. The results of our simulations are presented in Figure 1. The non-equilibrium nature of the system is established by its steady-state distribution (Figure 1a), which exhibits persistent probability currents, confirming the absence of detailed balance. This complex non-equilibrium steady state (NESS) is the target distribution for our acceleration analysis.

A key prediction of the theory, encapsulated in Corollary 6.1, is that the acceleration is an optimally tuned effect, not a monotonic limit. We verify this in Figure 1c for the system with the highest barrier ($h_b = 5.0$), where $s(L_O)$ is smallest. We plot the measured convergence rate $\nu(L)$ as a function of the friction coefficient γ . The rate clearly displays a sharp peak at an optimal friction $\gamma_{opt} \approx 34$. This non-trivial result demonstrates that maximal acceleration is achieved at a finite dissipation scale, a regime distinct from both the overdamped ($\gamma \rightarrow \infty$) and Hamiltonian ($\gamma \rightarrow 0$) limits. An explicit comparison of exponential convergence rates (Figure 1b) shows that the optimal lifted generator L consistently mixes faster than the collapsed generator L_O , providing a $1.23 \times$ speedup in median.

The central quantitative test of our framework is the predicted scaling law, $\nu_{opt} \propto \sqrt{s(L_O)}$. In Figure 1d, we plot both the measured optimal lifted rate ν_{opt} (purple) and the baseline collapsed rate $\nu(L_O)$ (blue) against the singular gap $s(L_O)$ on a log-log

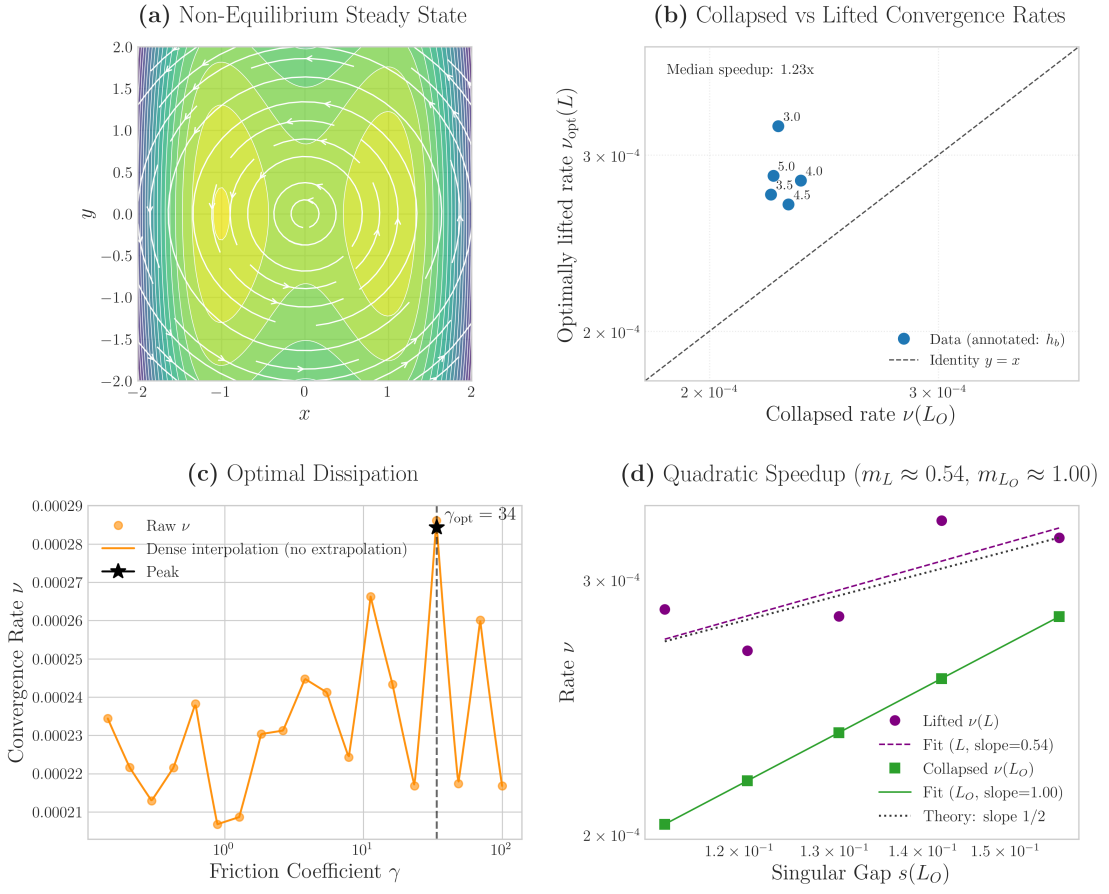


Figure 1: **Numerical Verification for Nonequilibrium Langevin.** (a) The non-equilibrium steady state (NESS) for a particle in a tilted double-well potential ($h_b = 5.0$) with a rotational force. Color map indicates probability density (yellow is high), and white lines show probability currents. (b) Convergence rate comparison between L (optimally lifted) and L_O (collapsed). The lifted dynamics are consistently faster, providing a $1.23\times$ speedup in median. (c) Measured convergence rate ν (from ACF log-envelope slope) as a function of the friction coefficient γ for $h_b = 5.0$. The rate peaks at an optimal value, $\gamma_{\text{opt}} \approx 34$, confirming a key theoretical prediction. (d) Log-log plot of convergence rates versus the singular gap $s(L_O)$. The optimal lifted rate ν_{opt} (purple circles) follows a power-law with slope $m_L \approx 0.54$, indicating a significant speedup towards the theoretical quadratic prediction ($m = 1/2$, dotted line). In contrast, the baseline collapsed rate $\nu(L_O)$ (green squares) scales linearly with slope $m_{L_O} \approx 1.00$ (green dashed line), confirming the perfectly diffusive nature of the unlifted dynamics.

scale. We tune the baseline rate $s(L_O)$ over the range $[0.112, 0.157]$. The baseline rates

follow a linear relationship $\nu(L_O) \propto s(L_O)^{m_{L_O}}$ with a fitted exponent $m_{L_O} \approx 1.00$ (green dashed line), perfectly consistent with standard diffusive dynamics. In stark contrast, the optimally lifted rates follow a power-law $\nu_{opt} \propto s(L_O)^{m_L}$ with a significantly smaller exponent $m_L \approx 0.54$ (black dashed line). This result, while slightly deviating from the ideal asymptotic $1/2$ (likely due to finite η effects), strongly validates our framework by rigorously demonstrating a “diffusive-to-near-ballistic” speedup in a non-equilibrium setting.

In conclusion, this experiment provides compelling numerical evidence for the Ad Embed principle within a classical non-equilibrium system. By coupling the slow dynamics to an auxiliary dissipative channel—specifically, the momentum—we establish a dynamical structure with an optimizable convergence rate. This optimized system effectively circumvents the intrinsic kinetic bottlenecks of the original effective dynamics, offering a novel paradigm for controlling and accelerating convergence in complex non-equilibrium systems.

7.2. Example: Dissipative Zeno-Limit Spin Chain

We now instantiate the Adiabatic Embedding (Ad Embed) Structure with a canonical example from open quantum systems: a boundary-driven quantum spin chain operating in the Zeno regime [PEKP20]. This system is a direct quantum analogue of the classical Langevin case. A strong, fast dissipative process ($\gamma\mathcal{R}$) acts on a small part of the system (the boundaries), forcing the dynamics into a “Zeno” slow subspace. The “slow” coherent Hamiltonian evolution (\mathcal{V}), which contains both a main part and a non-conservative perturbation, acts as the coupling that, in the second order, gives rise to the non-equilibrium effective dynamics L_O .

7.2.1. Dynamics and Generators

We consider a quantum spin chain of length N defined on the system Hilbert space $\mathcal{H}_{sys} = (\mathbb{C}^2)^{\otimes N}$. The dynamics of an observable $X \in \mathcal{B}(\mathcal{H}_{sys})$ are governed by a Lindblad master equation in the Heisenberg picture. The generator \mathcal{L} admits a decomposition based on a separation of timescales:

$$\mathcal{L} = \gamma\mathcal{R} + \mathcal{V}, \quad (7.18)$$

where $\gamma \gg 1$ is a dimensionless parameter quantifying the strength of the dissipation.

The “fast” generator \mathcal{R} describes the interaction with boundary reservoirs, driving the system rapidly toward a specific boundary configuration. It is defined as the sum of two local dissipators:

$$\mathcal{R}(X) = \sum_{k \in \{1, N\}} \left(L_k^\dagger X L_k - \frac{1}{2} \{ L_k^\dagger L_k, X \} \right). \quad (7.19)$$

The jump operators are chosen as $L_1 = \sigma_1^-$ and $L_N = \sigma_N^+$, corresponding to the strong polarization of the first site to the state $|\downarrow\rangle$ and the N -th site to $|\uparrow\rangle$. The kernel of this operator defines the *slow subspace* $\mathcal{H}_S := \ker(\mathcal{R})$. In this setup, \mathcal{H}_S is isomorphic

to the algebra of observables on the inner $N - 2$ spins, embedded in the full space as $X = |\downarrow\rangle\langle\downarrow|_1 \otimes \tilde{X} \otimes |\uparrow\rangle\langle\uparrow|_N$.

The “slow” dynamics are generated by the coupling term $\mathcal{V}(X) = i[H, X]$, which describes coherent evolution. To model a non-equilibrium scenario, we consider a Hamiltonian of the form $H = H_0 + \eta H_1$, where η is a perturbative parameter satisfying $\eta \ll 1$.

(i) H_0 represents a reversible interaction, such as the standard XXZ coupling:

$$H_0 = \sum_{j=1}^{N-1} \left(\sigma_j^x \sigma_{j+1}^x + \sigma_j^y \sigma_{j+1}^y + \Delta \sigma_j^z \sigma_{j+1}^z \right).$$

(ii) ηH_1 introduces a non-conservative perturbation, such as a Dzyaloshinskii-Moriya (DM) interaction [FCTY23] or a symmetry-breaking boundary field [LPS22], which renders the effective dynamics non-reversible.

This structure induces a decomposition of the coupling term $\mathcal{V} = \mathcal{L}_{ham} + \eta \mathcal{L}_{pert}$, with $\mathcal{L}_{ham}(X) = i[H_0, X]$ and $\mathcal{L}_{pert}(X) = i[H_1, X]$.

In the limit $\gamma \rightarrow \infty$, adiabatic elimination yields an effective generator acting on \mathcal{H}_S . Due to the specific parity symmetries of H_0 and the boundary states, the first-order contribution vanishes, i.e., $P_S \mathcal{V} P_S = 0$, where P_S is the orthogonal projection onto \mathcal{H}_S . Consequently, the dominant slow dynamics are governed by the second-order effective generator L_O :

$$L_O = -P_S \mathcal{V} \mathcal{R}^+ \mathcal{V} P_S, \quad (7.20)$$

where \mathcal{R}^+ denotes the Moore-Penrose pseudoinverse of \mathcal{R} restricted to the fast subspace \mathcal{H}_S^\perp . Restricted to the diagonal subalgebra spanned by the effective basis states $\{|\alpha\rangle\}$ of the inner chain, L_O acts as a classical Markov generator. Its action on a diagonal observable $f = \sum_\alpha f_\alpha |\alpha\rangle\langle\alpha| \in \mathcal{H}_S$ is given by

$$(L_O f)_\alpha = \sum_{\beta \neq \alpha} w_{\beta\alpha} (f_\beta - f_\alpha), \quad (7.21)$$

where $w_{\beta\alpha}$ denotes the transition rate from state $|\alpha\rangle$ to $|\beta\rangle$. The expansion $w_{\beta\alpha} = w_{\beta\alpha}^{(0)} + \eta w_{\beta\alpha}^{(1)} + O(\eta^2)$ explicitly captures the non-equilibrium nature of the target dynamics.

7.2.2. Hilbert Space Structure and Decomposition

We analyze the dynamics in the Liouville space of operators $\mathcal{H} = \mathcal{B}(\mathcal{H}_{sys})$, equipped with the Hilbert-Schmidt inner product $\langle A, B \rangle = \text{Tr}(A^\dagger B)$. The generator is decomposed as $\mathcal{L} = \gamma \mathcal{R} + \mathcal{V}$, where the dissipative part $\gamma \mathcal{R}$ and the coupling \mathcal{V} are given by:

$$\gamma \mathcal{R}(X) = \gamma \left(\mathcal{D}^\dagger[\sigma_1^-](X) + \mathcal{D}^\dagger[\sigma_N^+](X) \right), \quad (7.22)$$

$$\mathcal{V}(X) = i[H_0, X] + i[\eta H_1, X]. \quad (7.23)$$

To satisfy the structural assumptions of the Adiabatic Embedding framework (Definition 5.1), we identify the *slow subspace* \mathcal{H}_S with the kernel of the fast dissipation \mathcal{R} .

Physically, this corresponds to the “Zeno subspace” of operators invariant under the boundary dissipation:

$$\mathcal{H}_S := \ker(\mathcal{R}) = \left\{ X \in \mathcal{B}(\mathcal{H}_{sys}) \mid X = P_{bd}XP_{bd} \right\}, \quad (7.24)$$

where $P_{bd} = |\downarrow\rangle\langle\downarrow|_1 \otimes \mathbb{I}_{bulk} \otimes |\uparrow\rangle\langle\uparrow|_N$ is the projection onto the steady state of the boundary spins. The orthogonal projection $P_S : \mathcal{H} \rightarrow \mathcal{H}_S$ acts as the conditional expectation onto this subalgebra.

The *fast subspace* is defined as the orthogonal complement $\mathcal{H}_F := \mathcal{H}_S^\perp$. Since \mathcal{R} consists of local dissipators with unique steady states on the boundaries, it is strictly coercive on \mathcal{H}_F ; that is, there exists $\lambda_R > 0$ such that $-\text{Re}\langle X, \mathcal{R}X \rangle \geq \lambda_R \|X\|_{\mathcal{H}}^2$ for all $X \in \mathcal{H}_F$.

The effective dynamics on \mathcal{H}_S are determined by the perturbative action of \mathcal{V} . We observe that for the specific interaction Hamiltonian H (e.g., XX coupling), the first-order term vanishes:

$$P_S \mathcal{V} P_S = 0. \quad (7.25)$$

This follows because the Hamiltonian terms (e.g., $\sigma_1^x \sigma_2^x$) map states from the boundary-polarized Zeno subspace to states with excitations on the boundaries, which lie entirely in \mathcal{H}_F . Consequently, the effective generator is given by the second-order limit $L_O = -P_S \mathcal{V} \mathcal{R}^+ \mathcal{V} P_S$.

While \mathcal{H}_S generally contains both populations and coherences of the inner spins, the secular approximation (valid when the energy splitting in the effective Hamiltonian is large compared to the linewidth) allows us to decouple the diagonal elements. Restricting L_O to the diagonal subalgebra yields the classical Markov generator described in Eq. (7.21), with transition rates $w_{\beta\alpha}$ derived rigorously via the trace formula on \mathcal{H}_S .

7.2.3. Verification of Ad Embed Conditions

We now verify that the spin chain generator $\mathcal{L} = \gamma \mathcal{R} + \mathcal{V}$ satisfies the structural requirements of the Adiabatic Embedding framework.

Proposition 7.2 (Verification of Structural Conditions). *Let $\mathcal{H}_S = \ker(\mathcal{R})$ be the slow subspace defined above. The generator satisfies:*

- (i) *Orthogonality:* $P_S \mathcal{V} P_S = 0$.
- (ii) *Effective Generator:* The restriction of the second-order effective operator $L_O = -P_S \mathcal{V} \mathcal{R}^+ \mathcal{V} P_S$ to the diagonal subalgebra corresponds to the classical rate generator defined in Eq. (7.21).

Proof. (i) *Verification of Orthogonality.* We show that \mathcal{V} maps the slow subspace \mathcal{H}_S entirely into the fast subspace \mathcal{H}_F . Let $X \in \mathcal{H}_S$. By the characterization of the kernel, X takes the form $X = P_{bd} \otimes \tilde{X}$, where P_{bd} is the boundary steady-state projector. The action of the coupling term is given by $\mathcal{V}(X) = i[H, X]$. The Hamiltonian $H = H_0 + \eta H_1$ contains terms such as $\sigma_1^x \sigma_2^x$ (from the XX interaction) that couple the boundary spins to the bulk. Such operators flip the state of the boundary spins; for instance, σ_1^x maps

the ground state $|\downarrow\rangle_1$ to the excited state $|\uparrow\rangle_1$. Consequently, the operator $[H, X]$ has no support on the boundary steady state configuration; formally, $P_{bd}[H, X]P_{bd} = 0$. Since the projection P_S acts as the conditional expectation onto the boundary steady states, we have

$$P_S \mathcal{V} P_S X = P_S(i[H, X]) = 0. \quad (7.26)$$

Thus, $P_S \mathcal{V} P_S = 0$.

(ii) *Derivation of the Effective Generator.* We compute the matrix elements of the effective generator $L_O = -P_S \mathcal{V} \mathcal{R}^+ \mathcal{V} P_S$ in the basis of the slow subspace. We focus on the diagonal subalgebra spanned by the projections $X_\alpha = |\alpha\rangle\langle\alpha|$ corresponding to the computational basis states of the inner spins. The transition rate from state $|\alpha\rangle$ to $|\beta\rangle$ is given by the matrix element $F_{\beta\alpha}$ of the generator. Using the Hilbert-Schmidt inner product $\langle A, B \rangle = \text{Tr}(A^\dagger B)$, we have:

$$F_{\beta\alpha} = \text{Tr}(X_\beta L_O(X_\alpha)) = -\text{Tr}(X_\beta \mathcal{V} \mathcal{R}^+ \mathcal{V}(X_\alpha)). \quad (7.27)$$

Substituting the decomposition $\mathcal{V}(\cdot) = i[H_0 + \eta H_1, \cdot]$ and expanding to first order in η , we obtain:

$$F_{\beta\alpha} = w_{\beta\alpha}^{(0)} + \eta w_{\beta\alpha}^{(1)} + O(\eta^2). \quad (7.28)$$

The zeroth-order term corresponds to the reversible dynamics:

$$w_{\beta\alpha}^{(0)} = -\text{Tr}(X_\beta i[H_0, \mathcal{R}^+(i[H_0, X_\alpha])]). \quad (7.29)$$

Due to the Hermiticity of H_0 and the preservation of detailed balance by the boundary dissipators in the absence of the perturbation, this term is symmetric, i.e., $w_{\beta\alpha}^{(0)} = w_{\alpha\beta}^{(0)}$. The first-order correction arises from the cross terms:

$$w_{\beta\alpha}^{(1)} = -\text{Tr}(X_\beta (i[H_0, \mathcal{R}^+(i[H_1, X_\alpha])] + i[H_1, \mathcal{R}^+(i[H_0, X_\alpha])])). \quad (7.30)$$

The interaction H_1 (e.g., Dzyaloshinskii-Moriya) breaks the parity symmetry of the Hamiltonian. Consequently, $w_{\beta\alpha}^{(1)} \neq w_{\alpha\beta}^{(1)}$, introducing non-reciprocity into the transition rates.

Finally, the action of L_O on an observable $f = \sum_\alpha f_\alpha X_\alpha$ is recovered by linearity:

$$L_O(f) = \sum_\alpha f_\alpha \sum_\beta F_{\beta\alpha} X_\beta = \sum_\beta X_\beta \left(\sum_\alpha F_{\beta\alpha} f_\alpha \right). \quad (7.31)$$

Probability conservation implies $\sum_\beta F_{\beta\alpha} = 0$ (trace preservation of the pre-dual). This enforces the diagonal constraint $F_{\alpha\alpha} = -\sum_{\beta \neq \alpha} F_{\beta\alpha}$. Denoting the off-diagonal rates by $w_{\beta\alpha} := F_{\beta\alpha}$ for $\beta \neq \alpha$, we obtain the standard Master equation form:

$$(L_O f)_\beta = \sum_{\alpha \neq \beta} w_{\beta\alpha} f_\alpha - \left(\sum_{\gamma \neq \beta} w_{\gamma\beta} \right) f_\beta = \sum_{\alpha \neq \beta} w_{\beta\alpha} (f_\alpha - f_\beta). \quad (7.32)$$

This matches Eq. (7.21), confirming that the effective dynamics correspond to a classical Markov chain with non-equilibrium rates induced by ηH_1 . \square

7.2.4. Numerical Verification

To provide a concrete validation of our theoretical framework, particularly the prediction of an optimal convergence rate and the $\nu = \Theta(\sqrt{s(L_O)})$ scaling (Corollary 6.2), we perform a numerical experiment on the non-reversible Zeno-limit spin chain. This experiment is designed to test two central, non-trivial predictions of the Ad Embed structure: (i) the existence of an optimal, finite dissipation scale γ that maximizes the convergence rate $\nu(L)$, and (ii) a quantitative, super-linear scaling relationship between this accelerated rate and the intrinsic rate $s(L_O)$ of the target effective system.

Numerical Estimate of Convergence Rate. A critical aspect of this numerical validation is the accurate measurement of the asymptotic convergence rate $\nu(L)$. For a non-reversible NESS, the generator L is non-self-adjoint. Consequently, its spectrum is complex, and the autocorrelation function (ACF) of an observable f is not a simple sum of positive decaying exponentials. Instead, it exhibits oscillatory decay.

The dynamics of any observable f (projected onto the subspace orthogonal to the steady state) can be decomposed in the eigenbasis of the generator L with invariant measure π . For t large enough, the dynamics are dominated by the slowest-decaying modes (i.e., the eigenvalues λ_j with the largest real part, $\text{Re}(\lambda_j) = -\nu$). For a non-reversible system, these eigenvalues may be complex, $\lambda_{slow} = -\nu \pm i\omega$. The ACF's asymptotic behavior is thus:

$$\rho_f(t) = \frac{\langle f, e^{tL} f \rangle_\pi}{\|f\|_\pi^2} \approx A e^{-\nu t} \cos(\omega t + \phi), \quad t \rightarrow \infty$$

While $\rho_f(t)$ itself oscillates, the asymptotic convergence rate ν governs the exponential decay of its envelope. We can therefore extract ν by analyzing the logarithm of the envelope's magnitude:

$$\log |\rho_f(t)| \approx \log |A| - \nu t$$

This establishes a linear relationship where the slope is precisely $-\nu$. Our numerical method implements this derivation: we compute the empirical ACF $\hat{\rho}_f(t)$ from a long Quantum Jump Monte Carlo (QJMC) trajectory, and then perform a linear fit on the slope of its log-envelope, $\log |\hat{\rho}_f(t)|$, in the asymptotic (linear) tail region to extract $\nu(L)$. For better clarity, we use the median ratio on the control group L_O , which gives it a perfect linear relationship in comparison with L .

Numerical Setup. We model a 3-spin chain ($N = 3$) governed by the Lindbladian in Eq. (7.18). The Hamiltonian is $H = JH_0 + DH_1$, where $H_0 = \sum_{j=1,2} (\sigma_j^x \sigma_{j+1}^x + \sigma_j^y \sigma_{j+1}^y)$ is the XX coupling and $H_1 = \sigma_1^y \sigma_2^z - \sigma_2^z \sigma_1^y$ is a non-conservative DM-like interaction. We fix the non-conservative strength $D = 0.5$ (our η) and vary the main coupling strength, J , in the range $[0.2, 1.2]$ to create a set of target systems with progressively slower intrinsic dynamics.

The target effective dynamics are governed by the 2-state classical generator L_O (Eq. (7.21)) acting on the $M = N - 2 = 1$ inner spin. We compute this singular gap of

L_O by first numerically constructing the full 64×64 superoperator $L_O = -P_S \mathcal{VR}^+ \mathcal{V} P_S$ using the matrix pseudoinverse, and then extracting the 2×2 classical rate matrix F and computing its smallest non-zero singular value.

The full 3-spin Lindblad dynamics (generator L in Eq. (7.18)) serves as the Ad Embed system. The states of the boundary spins (sites 1 and 3) serve as the auxiliary fast variables. The dissipation strength γ corresponds to the fast dissipation scale γ in our $L = \gamma \mathcal{R} + \mathcal{V}$ decomposition.

We simulate this full system using a Quantum Jump Monte Carlo (QJMC) trajectory [LGM⁺26]. The convergence rate $\nu(L)$ is quantified by extracting the asymptotic slope from the log-envelope of the ACF of the “slow” observable $O = \sigma_2^z$ (the magnetization of the inner spin), as described in our methodology. For a direct comparison, the convergence rate of the collapsed system, $\nu(L_O)$, is also computed via the same ACF log-envelope method, but applied to a separate QJMC simulation of the 2×2 classical dynamics. For each coupling J (i.e., for each $s(L_O)$), we perform a scan over the dissipation γ in the range $[10^{-1.5}, 10^{2.0}]$ to identify the optimal dissipation γ_{opt} that yields the maximal convergence rate, $\nu_{opt} = \nu(L(\gamma_{opt}))$.

Results and Analysis. The results of our simulations are presented in Figure 2. The non-equilibrium nature of the system is established by its steady-state density matrix for the inner spin (Figure 2a), which exhibits non-zero coherences. Furthermore, we compute a non-zero classical probability current within the slow subspace, obtaining $\approx -7.8 \times 10^{-13}$, confirming the absence of detailed balance. This complex non-equilibrium steady state (NESS) is the target distribution for our acceleration analysis.

A key prediction of the theory, encapsulated in Corollary 6.1, is that the acceleration is an optimally tuned effect, not a monotonic limit. We verify this in Figure 2c for the system with $J = 1.2$. We plot the measured convergence rate $\nu(L)$ (via ACF log-envelope slope) as a function of the dissipation strength γ . The rate clearly displays a sharp peak at an optimal dissipation $\gamma_{opt} \approx 1.4$. This non-trivial result demonstrates that maximal acceleration is achieved at a finite dissipation scale, a regime distinct from both the slow ($\gamma \rightarrow \infty$) and fast ($\gamma \rightarrow 0$) coherent limits. An explicit comparison of the practical convergence rates between L and L_O is provided in Figure 2b, indicating that L consistently mixes faster than L_O , providing a $\approx 1.40 \times$ speedup in median (max $2.30 \times$).

The central quantitative test of our framework is the predicted scaling law, $\nu_{opt} \propto \sqrt{s(L_O)}$. In Figure 2d, we plot both the measured optimal lifted rate ν_{opt} (purple) and the baseline collapsed rate $\nu(L_O)$ (blue) against the singular gap $s(L_O)$ for each coupling J on a log-log scale. We tune the baseline singular gap $s(L_O)$ over the range $[\approx 9.5 \times 10^{-12}, \approx 3.2 \times 10^{-11}]$. The baseline rates follow a linear relationship $\nu(L_O) \propto s(L_O)^{m_{L_O}}$ with a fitted exponent $m_{L_O} \approx 1.00$ (green dashed line), perfectly consistent with standard diffusive dynamics. In contrast, the optimally lifted rates follow a power-law $\nu_{opt} \propto s(L_O)^{m_L}$ with a significantly smaller exponent $m_L \approx 0.43$ (black dashed line). This result is in strong agreement with the ideal asymptotic prediction of $m_L = 1/2$ (dotted line), rigorously confirming the “diffusive-to-ballistic” speedup in a complex quantum setting.

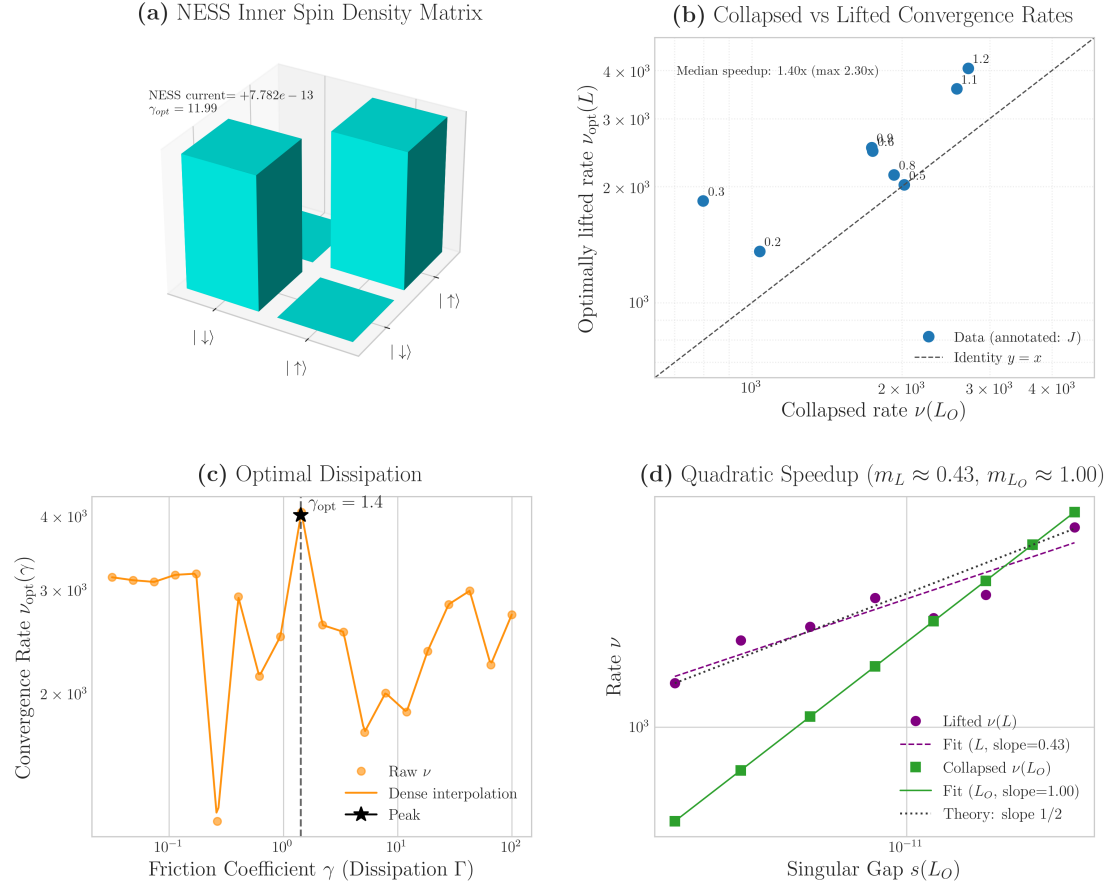


Figure 2: **Numerical Verification for Nonequilibrium Spin Chain.** (a) The non-equilibrium steady state (NESS) of the inner spin ($N = 2$) for a system with $J \approx 0.9$ (matching $\gamma_{opt} \approx 11.99$ from the label). The non-zero off-diagonal elements and the non-zero classical current ($\approx -7.8 \times 10^{-13}$) confirm the non-equilibrium nature. (b) Convergence rate comparison (ν vs. ν) between L and L_O . The lifted dynamics are consistently faster, providing a $\approx 1.40 \times$ speedup in median (max $2.30 \times$). (c) Measured convergence rate ν (from ACF log-envelope slope) as a function of the dissipation strength γ for $J = 1.2$. The rate peaks at an optimal value, $\gamma_{opt} \approx 1.4$, confirming a key theoretical prediction. (d) Log-log plot of convergence rates versus the singular gap $s(L_O)$. The optimal lifted rate ν_{opt} (purple circles) follows a power-law with slope $m_L \approx 0.43$ (black dashed line), indicating a significant speedup towards the theoretical quadratic prediction ($m = 1/2$, dotted line). In contrast, the baseline collapsed rate $\nu(L_O)$ (green squares) scales linearly with slope $m_{L_O} \approx 1.00$ (green dashed line), confirming the diffusive nature of the unlifted dynamics.

In conclusion, this experiment provides compelling numerical evidence for the Ad Embed principle in a quantum, non-equilibrium system. By coupling the slow (inner) spin

dynamics to an auxiliary dissipative channel (the boundary spins), we create a dynamical structure whose convergence rate can be optimized. This optimal system circumvents the intrinsic kinetic bottlenecks of the original effective dynamics, offering a new paradigm for controlling and accelerating convergence in complex quantum systems out of equilibrium.

8. Conclusion

In this work, we have established a rigorous connection between the physical theory of adiabatic elimination (AE) and the mathematical theory of lifting for accelerating Markov processes, extending the framework in [EL24a, LL25] to non-equilibrium systems. We show that the full generator $\mathcal{L} = \gamma\mathcal{R} + \mathcal{V}$ of a system with timescale separation can be formally analyzed as a *lift* of the effective slow dynamics \mathcal{L}_O . We show that this “inverse AE” perspective provides a systematic framework for analyzing convergence to *Non-Equilibrium Steady States* (NESS), a domain where traditional lifting techniques for equilibrium processes do not apply.

The theoretical core of our approach is the “Adiabatic Embedding (Ad Embed) Structure” (Definition 5.1). This structure, built upon the Orthogonality and Approximate Quadratic Form conditions derived from AE, rigorously incorporates the non-conservative, non-equilibrium-inducing perturbation (via $\eta\mathcal{L}_{\text{pert}}$) as an explicitly bounded error term proportional to η . By adapting the variational framework of Flow Poincaré inequalities [BLW25, LL25] to this novel structure, we derived explicit lower bounds on the convergence rate of the full (lifted) generator \mathcal{L} . Our main theoretical result, Corollary 6.2, demonstrates that under the asymptotic regime where the non-equilibrium perturbation is subdominant to the slow dynamics gap ($\eta \ll s(\mathcal{L}_O)^2$), this non-equilibrium lift achieves the optimal “diffusive-to-ballistic” quadratic speedup, $\nu_{\text{opt}} = \Theta(\sqrt{s(\mathcal{L}_O)})$, a characteristic acceleration previously established only for reversible systems. This was validated by two canonical, non-equilibrium examples—classical Langevin dynamics in Section 7.1 and a quantum Zeno-limit spin chain in Section 7.2—where we confirmed both the existence of an optimal, finite dissipation scale γ_{opt} and the predicted quadratic speedup.

Limitations. Despite these advances, our framework has notable limitations that define clear avenues for future research. The current analysis is fundamentally perturbative; it requires the non-equilibrium perturbation η to be small relative to the intrinsic slow timescales to guarantee the strict positivity of the Flow Poincaré constant. How to extend this hypocoercive analysis to strongly non-equilibrium systems, where the non-conservative part is not small, remains a significant open challenge. Furthermore, our “inverse AE” approach is analytical rather than constructive. It provides a powerful tool for analyzing the convergence of a *given* full physical system \mathcal{L} , but it does not yet offer a general, constructive algorithm to design an optimal lift \mathcal{L} for an *arbitrary*, pre-defined slow NESS generator \mathcal{L}_O .

Future Works. Looking forward, this work opens several promising research directions. A natural extension is to explore the possibility of iterative lifting. One can envision

applying this lifting principle recursively—identifying new fast degrees of freedom to “lift a lift”—potentially creating a hierarchy of generators that forms a scalable algorithm for achieving arbitrarily fast dynamics. Addressing the limitations of the current work, a primary goal will be to develop non-perturbative bounds for strongly non-equilibrium lifts, perhaps by integrating techniques from linear response theory [BKAS17, ABFJ16], dilation theory [HJLZ23, LLY⁺25], Floquet engineering [PYW⁺20] and projector framework [GB24], or developing new variational principles. Finally, a significant theoretical challenge is to invert the paradigm: to find a general constructive method for NESS lifting, and to identify the precise physical properties of the coupling \mathcal{V} and dissipator \mathcal{R} that guarantee the structural scaling assumptions (e.g., $K_3 = \Theta(\sqrt{s(\mathcal{L}_O)})$) required for optimal acceleration. In bridging reservoir engineering [Nas25, Sel24, JBP25] with hypocoercivity [Vil09, LL24, FLT25], this framework offers a new paradigm for the analysis and, ultimately, the design of rapid, non-equilibrium quantum processes.

References

- [ABFJ16] Victor V. Albert, Barry Bradlyn, Martin Fraas, and Liang Jiang. Geometry and response of Lindbladians. *Phys. Rev. X*, 6:041031, 2016.
- [APS22] Radosław Adamczak, Bartłomiej Polaczyk, and Michał Strzelecki. Modified log-sobolev inequalities, beckner inequalities and moment estimates. *Journal of Functional Analysis*, 282(7):109349, 2022.
- [ASR16] Remi Azouit, Alain Sarlette, and Pierre Rouchon. Adiabatic elimination for open quantum systems with effective Lindblad master equations. arXiv preprint arXiv:1603.04630, 2016.
- [ATS17] Simon Apers, Francesco Ticozzi, and Alain Sarlette. Lifting Markov chains to mix faster: Limits and opportunities. arXiv preprint arXiv:1705.08253, 2017.
- [BKAS17] Masashi Ban, Sachiko Kitajima, Toshihico Arimitsu, and Fumiaki Shibata. Linear response theory for open systems: Quantum master equation approach. *Phys. Rev. A*, 95(2):022126, Feb 2017.
- [BLW25] Giovanni Brigati, Francis Lörler, and Lihan Wang. Hypocoercivity meets lifts. arXiv preprint arXiv:2412.10890, 2025.
- [Cha25] Sourav Chatterjee. Spectral gap of nonreversible markov chains. arXiv preprint arXiv:2310.10876, 2025.
- [CHL24] Eric A. Carlen, David A. Huse, and Joel L. Lebowitz. Stationary states of boundary driven quantum systems: some exact results. arXiv preprint arXiv:2408.06887, 2024.

[CLP99] Fang Chen, László Lovász, and Igor Pak. Lifting Markov chains to speed up mixing. In *Proceedings of the Thirty-First Annual ACM Symposium on Theory of Computing*, STOC '99, pages 275–281, New York, 1999. ACM.

[CSU15] Raffaella Carbone, Emanuela Sasso, and Veronica Umanit  . Environment induced decoherence for Markovian evolutions. *J. Math. Phys.*, 56(9):092704, 2015.

[DOvdH25] Rocco Duvenhage, Kyle Oerder, and Keagan van den Heuvel. Quantum detailed balance via elementary transitions. *Quantum*, 9:1743, 2025.

[EGH⁺25] Andreas Eberle, Arnaud Guillin, Leo Hahn, Francis L  rler, and Manon Michel. Convergence of non-reversible markov processes via lifting and flow poincar   inequality. arXiv preprint arXiv:2503.04238, 2025.

[EL24a] Andreas Eberle and Francis L  rler. Non-reversible lifts of reversible diffusion processes and relaxation times. arXiv preprint arXiv:2402.05041, 2024.

[EL24b] Andreas Eberle and Francis L  rler. Space-time divergence lemmas and optimal non-reversible lifts of diffusions on riemannian manifolds with boundary. arXiv preprint arXiv:2412.16710, 2024.

[EN00] Klaus-Jochen Engel and Rainer Nagel. *One-Parameter Semigroups for Linear Evolution Equations*, volume 194 of *Graduate Texts in Mathematics*. Springer-Verlag, New York, 2000.

[Eva10] Lawrence C. Evans. *Partial Differential Equations*, volume 19 of *Graduate Studies in Mathematics*. American Mathematical Society, Providence, RI, second edition, 2010.

[FCTY23] Albert Fert, Mairbek Chshiev, Andr   Thiaville, and Hongxin Yang. From early theories of dzyaloshinskii-moriya interactions in metallic systems to today's novel roads. *Journal of the Physical Society of Japan*, 92(8), Aug 2023.

[FLT25] Di Fang, Jianfeng Lu, and Yu Tong. Mixing time of open quantum systems via hypocoercivity. *Phys. Rev. Lett.*, 134:140405, 2025.

[FPSU24] Franco Fagnola, Damiano Poletti, Emanuela Sasso, and Veronica Umanit  . The spectral gap of a gaussian quantum markovian generator. arXiv preprint arXiv:2405.04947, 2024.

[FV82] Alberto Frigerio and Maurizio Verri. Long-time asymptotic properties of dynamical semigroups on W^* -algebras. *Math. Z.*, 180(2):275–286, 1982.

[GB24] C. Gonzalez-Ballester. Tutorial: projector approach to master equations for open quantum systems. *Quantum*, 8:1454, Aug 2024.

[GHC⁺25] Jinkang Guo, Oliver Hart, Chi-Fang Chen, Aaron J. Friedman, and Andrew Lucas. Designing open quantum systems with known steady states: Davies generators and beyond. *Quantum*, 9:1612, 2025.

[GKS76] Vittorio Gorini, Andrzej Kossakowski, and E. C. G. Sudarshan. Completely positive dynamical semigroups of N-level systems. *J. Math. Phys.*, 17(5):821–825, 1976.

[HJLZ23] Junpeng Hu, Shi Jin, Nana Liu, and Lei Zhang. Dilation theorem via schrödingerisation, with applications to the quantum simulation of differential equations. arXiv preprint arXiv:2309.16262, 2023.

[IOS17] Alessandra Iacobucci, Stefano Olla, and Gabriel Stoltz. Convergence rates for nonequilibrium langevin dynamics. arXiv preprint arXiv:1702.03685, 2017.

[JBP25] Marcelo Janovitch, Matteo Brunelli, and Patrick P. Potts. Active quantum reservoir engineering: Using a qubit to manipulate its environment. arXiv preprint arXiv:2505.16898, 2025.

[Kes12] E. M. Kessler. Generalized schrieffer-wolff formalism for dissipative systems. *Physical Review A*, 86(1), Jul 2012.

[KK22] Stefanie Kieninger and Bettina G. Keller. Gromacs stochastic dynamics and baoab are equivalent configurational sampling algorithms. *Journal of Chemical Theory and Computation*, 18(10):5792–5798, Sep 2022.

[LB15] Nicolai Lang and Hans Peter Büchler. Exploring quantum phases by driven dissipation. *Physical Review A*, 92(1), Jul 2015.

[LGM⁺26] Neill Lambert, Eric Giguère, Paul Menczel, Boxi Li, Patrick Hopf, Gerardo Suárez, Marc Gali, Jake Lishman, Rushiraj Gadhvi, Rochisha Agarwal, Asier Galicia, Nathan Shammah, Paul Nation, J. R. Johansson, Shahnawaz Ahmed, Simon Cross, Alexander Pitchford, and Franco Nori. Qutip 5: The quantum toolbox in Python. *Physics Reports*, 1153:1–62, 2026.

[LL24] Bowen Li and Jianfeng Lu. Quantum space-time Poincaré inequality for Lindblad dynamics. arXiv preprint arXiv:2406.09115, 2024.

[LL25] Bowen Li and Jianfeng Lu. Speeding up quantum Markov processes through lifting. arXiv preprint arXiv:2505.12187, 2025.

[LLY⁺25] S. X. Li, Keren Li, J. B. You, Y.-H. Chen, Clemens Gneiting, Franco Nori, and X. Q. Shao. Variational quantum algorithm for unitary dilation. arXiv preprint arXiv:2510.19157, 2025.

[LPS22] Gabriel T. Landi, Dario Poletti, and Gernot Schaller. Nonequilibrium boundary-driven quantum systems: Models, methods, and properties. *Rev. Mod. Phys.*, 94:045006, 2022.

[LRR23] François-Marie Le Régent and Pierre Rouchon. Adiabatic elimination for composite open quantum systems: reduced model formulation and numerical simulations. arXiv preprint arXiv:2303.05089, 2023.

[MBHR21] Thibaud Maimbourg, Denis M. Basko, Markus Holzmann, and Alberto Rosso. Bath-induced Zeno localization in driven many-body quantum systems. *Phys. Rev. Lett.*, 126:120603, 2021.

[MMG22] Moein Malekakhlagh, Easwar Magesan, and Luke C. G. Govia. Time-dependent schrieffer-wolff-lindblad perturbation theory: Measurement-induced dephasing and second-order stark shift in dispersive readout. *Physical Review A*, 106(5), Nov 2022.

[MR22] Pierre Monmarché and Mouad Ramil. Overdamped limit at stationarity for non-equilibrium langevin diffusions. arXiv preprint arXiv:2110.01238, 2022.

[Nas25] M. Tahir Naseem. Reservoir-engineered mechanical cat states with a driven qubit. arXiv preprint arXiv:2508.10500, 2025.

[Pav14] Grigorios A. Pavliotis. *Stochastic Processes and Applications: Diffusion Processes, the Fokker-Planck and Langevin Equations*, volume 60 of *Texts in Applied Mathematics*. Springer, New York, 2014.

[PEKP20] Vladislav Popkov, Simon Essink, Corinna Kollath, and Carlo Presilla. Dissipative generation of pure steady states and a gambler’s ruin problem. *Physical Review A*, 102(3), Sep 2020.

[PEPS18] Vladislav Popkov, Simon Essink, Carlo Presilla, and Gunter Schütz. Effective quantum zeno dynamics in dissipative quantum systems. *Physical Review A*, 98(5), Nov 2018.

[PP21] Vladislav Popkov and Carlo Presilla. Full spectrum of the Liouvillian of open dissipative quantum systems in the Zeno limit. *Phys. Rev. Lett.*, 126:190402, 2021.

[PPS25] Vladislav Popkov, Carlo Presilla, and Mario Salerno. Manifolds of exceptional points and effective zeno limit of an open two-qubit system. arXiv preprint arXiv:2412.13674, 2025.

[PYW⁺20] Yiming Pan, Ye Yu, Huaiqiang Wang, Tao Chen, Xiaopeng Shen, and Qingqing Cheng. Beyond adiabatic elimination in topological floquet engineering. arXiv preprint arXiv:1810.00054, 2020.

[RLC21] David Roberts, Andrew Lingenfelter, and A. A. Clerk. Hidden time-reversal symmetry, quantum detailed balance and exact solutions of driven-dissipative quantum systems. *PRX Quantum*, 2:020336, 2021.

- [RRS24] Rémi Robin, Pierre Rouchon, and Lev-Arcady Sellem. Convergence of bipartite open quantum systems stabilized by reservoir engineering. *Annales Henri Poincaré*, 26(5):1769–1819, Nov 2024.
- [Sal24] Robert Salzmann. Quantitative quantum zeno and strong damping limits in strong topology. arXiv preprint arXiv:2409.06469, 2024.
- [Sel24] Lev-Arcady Sellem. *Bosonic qubits and quantum reservoirs: taming the environment*. PhD thesis, Université Paris sciences et lettres, Paris, France, 2024.
- [SS21] Holger Sambale and Arthur Sinulis. Modified log-sobolev inequalities and two-level concentration. *Latin American Journal of Probability and Mathematical Statistics*, 18(1):855, 2021.
- [SVdPZ25] Kilian Seibold, Greta Villa, Javier del Pino, and Oded Zilberberg. Manifestations of flow topology in a quantum driven-dissipative system. arXiv preprint arXiv:2508.16486, 2025.
- [Tik52] A. N. Tikhonov. Systems of differential equations containing small parameters in the derivatives. *Mat. Sb. (N.S.)*, 31(73):575–586, 1952. (in Russian).
- [TR25] Masaaki Tokieda and Angela Riva. Time-convolutionless master equation applied to adiabatic elimination. *Physical Review A*, 111(5), May 2025.
- [Ver05] Ferdinand Verhulst. *Methods and Applications of Singular Perturbations: Boundary Layers and Multiple Timescale Dynamics*, volume 50 of *Texts in Applied Mathematics*. Springer-Verlag, New York, 2005.
- [Vil09] Cédric Villani. *Hypocoercivity*, volume 202 of *Mem. Amer. Math. Soc.* American Mathematical Society, Providence, RI, 2009.

A. Proof for Preliminary

Lemma A.1 (Criterion for Strict Hypocoercivity, cf. Lemma 2.3). *For an ergodic QMS, the fixed-point space is a subspace of the dissipative kernel, $\mathcal{F}(\mathcal{L}) \subset \ker(\mathcal{S})$. The semi-group is strictly hypocoercive if and only if this inclusion is strict:*

$$\dim \ker(\mathcal{S}) > \dim \mathcal{F}(\mathcal{L}). \quad (\text{A.1})$$

Proof. When $X \in \mathcal{F}(\mathcal{L})$, we have $\mathcal{L}(X) = 0$, thus:

$$\langle X, \mathcal{S}(X) \rangle_{\sigma,1/2} = \text{Re} \langle X, \mathcal{L}(X) \rangle_{\sigma,1/2} = 0. \quad (\text{A.2})$$

From \mathcal{P}_t is ergodic, from Lemma 2.1, we know \mathcal{S} must be negative, combined with (A.2), we have $\mathcal{S}(X) = 0$, namely $X \in \ker(\mathcal{S})$. Thus, $\mathcal{F}(\mathcal{L}) \subset \ker(\mathcal{S})$.

When \mathcal{P}_t is ergodic with invariant measure σ , we have (2.3) holds with $C \geq 1$. It suffices to show $\dim \ker(\mathcal{S}) = \dim \mathcal{F}(\mathcal{L})$ is equivalent to $C = 1$.

Assuming \mathcal{P}_t is coercive, we take time derivative and apply Grönwall's inequality to the following inequality:

$$\|\mathcal{P}_t(X) - \mathbb{E}_{\mathcal{F}}(X)\|_{2,\sigma} \leq e^{-2\nu t} \|X - \mathbb{E}_{\mathcal{F}}(X)\|_{2,\sigma}, \quad (\text{A.3})$$

which indicates that when $C = 1$ we have

$$\nu \|X - \mathbb{E}_{\mathcal{F}}(X)\|_{2,\sigma}^2 \leq -\langle X, \mathcal{S}(X) \rangle_{\sigma,1/2}. \quad (\text{A.4})$$

Apparently, (A.4) implies $\ker(\mathcal{S}) \subset \mathcal{F}(\mathcal{L})$, and hence $\dim \ker(\mathcal{S}) = \dim \mathcal{F}(\mathcal{L})$ follows.

On the other hand, assuming $\dim \ker(\mathcal{S}) = \dim \mathcal{F}(\mathcal{L})$, since \mathcal{H} is finite dimensional, we have $\ker(\mathcal{S}) = \mathcal{F}(\mathcal{L})$. Thus, $\mathbb{E}_{\mathcal{F}}$ coincides with $\mathbb{E}_{\ker(\mathcal{S})}$, and $\mathcal{F}(\mathcal{L})^\perp = \ker(\mathcal{S})^\perp$. Moreover, from the $\mathcal{S} \leq 0$, there exists $\nu > 0$ such that: $\nu \|X - \mathbb{E}_{\ker(\mathcal{S})}(X)\|_{2,\sigma}^2 \leq -\langle X, \mathcal{S}(X) \rangle_{\sigma,1/2}$, for all $X \in \ker(\mathcal{S})^\perp$. Thus, for all $X \in \mathcal{F}(\mathcal{L})^\perp$, we also have:

$$\nu \|X - \mathbb{E}_{\mathcal{F}}(X)\|_{2,\sigma}^2 \leq -\langle X, \mathcal{S}(X) \rangle_{\sigma,1/2}. \quad (\text{A.5})$$

Note that (A.4) holds trivially on $\mathcal{F}(\mathcal{L})$, combined with equivalence established above, we deduce $C = 1$. \square

B. Proofs for Adiabatic Elimination

Theorem B.1 (SW Effective Generator Formula, cf. Theorem 3.1). *The block-diagonal transformed generator L is given by:*

$$L = \mathcal{L}^{\text{diag}} + \tanh(\widehat{\mathcal{S}}/2) \mathcal{L}^{\text{offdiag}}, \quad (\text{B.1})$$

where $\mathcal{L} = \mathcal{L}^{\text{diag}} + \mathcal{L}^{\text{offdiag}}$ is the decomposition of the full generator, and $\widehat{\mathcal{S}}$ is the adjoint-action superoperator $\widehat{\mathcal{S}}(A) = [\mathcal{S}, A]$. The effective generator for the slow subspace is $\mathcal{L}_{\text{eff}} = P_S L P_S$.

Proof. We define the similarity transformation via the adjoint action $\widehat{\mathcal{S}}(A) = [\mathcal{S}, A]$. The transformed generator is $L = e^{\widehat{\mathcal{S}}}(\mathcal{L})$. We decompose the superoperator $e^{\widehat{\mathcal{S}}}$ into its even and odd parts, $e^{\widehat{\mathcal{S}}} = \cosh(\widehat{\mathcal{S}}) + \sinh(\widehat{\mathcal{S}})$.

The generator \mathcal{S} is purely block-off-diagonal ($\mathcal{S}^{\text{diag}} = 0$). The adjoint action $\widehat{\mathcal{S}}$ thus maps block-diagonal operators to block-off-diagonal ones, and vice-versa. Consequently, $\cosh(\widehat{\mathcal{S}})$ (containing only even powers of $\widehat{\mathcal{S}}$) maps diagonal-to-diagonal ($\text{diag} \rightarrow \text{diag}$) and off-diagonal-to-off-diagonal ($\text{offdiag} \rightarrow \text{offdiag}$), while $\sinh(\widehat{\mathcal{S}})$ (containing only odd powers) maps $\text{diag} \rightarrow \text{offdiag}$ and $\text{offdiag} \rightarrow \text{diag}$.

We apply this to the full generator $L = (\cosh(\widehat{\mathcal{S}}) + \sinh(\widehat{\mathcal{S}}))(\mathcal{L}^{\text{diag}} + \mathcal{L}^{\text{offdiag}})$. Separating the resulting block-diagonal and block-off-diagonal parts gives:

$$L^{\text{diag}} = \cosh(\widehat{\mathcal{S}})\mathcal{L}^{\text{diag}} + \sinh(\widehat{\mathcal{S}})\mathcal{L}^{\text{offdiag}} \quad (\text{B.2})$$

$$L^{\text{offdiag}} = \sinh(\widehat{\mathcal{S}})\mathcal{L}^{\text{diag}} + \cosh(\widehat{\mathcal{S}})\mathcal{L}^{\text{offdiag}} \quad (\text{B.3})$$

The SW formalism requires that \mathcal{S} be chosen to satisfy the **decoupling condition** $L^{\text{offdiag}} = 0$. From (B.3), this gives the fundamental identity:

$$\sinh(\widehat{\mathcal{S}})\mathcal{L}^{\text{diag}} = -\cosh(\widehat{\mathcal{S}})\mathcal{L}^{\text{offdiag}}. \quad (\text{B.4})$$

We now derive the final form of L^{diag} . We start from (B.2) and add and subtract $\mathcal{L}^{\text{diag}}$:

$$L^{\text{diag}} = \mathcal{L}^{\text{diag}} + (\cosh(\widehat{\mathcal{S}}) - \mathbf{1})\mathcal{L}^{\text{diag}} + \sinh(\widehat{\mathcal{S}})\mathcal{L}^{\text{offdiag}}. \quad (\text{B.5})$$

We use the identity (B.4) to replace $\mathcal{L}^{\text{diag}}$:

$$L^{\text{diag}} = \mathcal{L}^{\text{diag}} + (\cosh(\widehat{\mathcal{S}}) - \mathbf{1}) \left(-\sinh(\widehat{\mathcal{S}})^{-1} \cosh(\widehat{\mathcal{S}})\mathcal{L}^{\text{offdiag}} \right) + \sinh(\widehat{\mathcal{S}})\mathcal{L}^{\text{offdiag}}. \quad (\text{B.6})$$

Factoring out $\mathcal{L}^{\text{offdiag}}$ gives:

$$L^{\text{diag}} = \mathcal{L}^{\text{diag}} + \left(\frac{-(\cosh(\widehat{\mathcal{S}}) - \mathbf{1}) \cosh(\widehat{\mathcal{S}}) + \sinh^2(\widehat{\mathcal{S}})}{\sinh(\widehat{\mathcal{S}})} \right) \mathcal{L}^{\text{offdiag}}. \quad (\text{B.7})$$

We simplify the numerator:

$$-\cosh^2(\widehat{\mathcal{S}}) + \cosh(\widehat{\mathcal{S}}) + \sinh^2(\widehat{\mathcal{S}}) = \cosh(\widehat{\mathcal{S}}) - (\cosh^2(\widehat{\mathcal{S}}) - \sinh^2(\widehat{\mathcal{S}})) = \cosh(\widehat{\mathcal{S}}) - \mathbf{1}. \quad (\text{B.8})$$

Substituting this back, we find:

$$L^{\text{diag}} = \mathcal{L}^{\text{diag}} + \left(\frac{\cosh(\widehat{\mathcal{S}}) - \mathbf{1}}{\sinh(\widehat{\mathcal{S}})} \right) \mathcal{L}^{\text{offdiag}}. \quad (\text{B.9})$$

Finally, using the hyperbolic identity $\tanh(x/2) = \frac{\cosh(x)-1}{\sinh(x)}$, we arrive at the exact expression:

$$L^{\text{diag}} = \mathcal{L}^{\text{diag}} + \tanh(\widehat{\mathcal{S}}/2)\mathcal{L}^{\text{offdiag}}, \quad (\text{B.10})$$

which is the result stated in [Kes12]. \square

Theorem B.2 (SW Perturbative Expansion, cf. Theorem 3.2). . The effective generator $\mathcal{L}_{\text{eff}} = P_S L P_S$ has the perturbative expansion $\mathcal{L}_{\text{eff}} = \sum_{n=0}^{\infty} \epsilon^n L_n^{\text{eff}}$. The first three non-trivial orders are given by:

$$L_1^{\text{eff}} = P_S \mathcal{V} P_S \equiv \mathcal{V}^S \quad (\text{B.11})$$

$$L_2^{\text{eff}} = -P_S \mathcal{V} P_F \mathcal{R}^+ P_F \mathcal{V} P_S \equiv -\mathcal{V}^- \mathcal{R}^+ \mathcal{V}^+ \quad (\text{B.12})$$

$$L_3^{\text{eff}} = \mathcal{V}^- \mathcal{R}^+ \mathcal{V}^F \mathcal{R}^+ \mathcal{V}^+ - \frac{1}{2} \{ \mathcal{V}^S, \mathcal{V}^- (\mathcal{R}^+)^2 \mathcal{V}^+ \}_+ \quad (\text{B.13})$$

where $\mathcal{R}^+ \equiv (P_F \mathcal{R} P_F)^{-1}$ is the inverse of \mathcal{R} on the fast subspace \mathcal{H}_F , and we use the compact notation $\mathcal{V}^- = P_S \mathcal{V} P_F$, $\mathcal{V}^+ = P_F \mathcal{V} P_S$, $\mathcal{V}^S = P_S \mathcal{V} P_S$, and $\mathcal{V}^F = P_F \mathcal{V} P_F$.

Proof. We derive the expansion using a 2×2 block matrix representation for operators on the decomposed space $\mathcal{H} = \mathcal{H}_S \oplus \mathcal{H}_F$. An operator A is written as $A = \begin{pmatrix} P_S A P_S & P_S A P_F \\ P_F A P_S & P_F A P_F \end{pmatrix}$.

The setup is $\mathcal{L} = \mathcal{R} + \epsilon \mathcal{V}$. Since $\mathcal{H}_S = \ker(\mathcal{R})$, the unperturbed operator \mathcal{R} is block-diagonal. Let $\mathcal{R}_F := P_F \mathcal{R} P_F$. The perturbation \mathcal{V} has all four blocks.

$$\mathcal{R} = \begin{pmatrix} 0 & 0 \\ 0 & \mathcal{R}_F \end{pmatrix}, \quad \mathcal{V} = \begin{pmatrix} \mathcal{V}^S & \mathcal{V}^- \\ \mathcal{V}^+ & \mathcal{V}^F \end{pmatrix}. \quad (\text{B.14})$$

The full generator is $\mathcal{L} = \begin{pmatrix} \epsilon \mathcal{V}^S & \epsilon \mathcal{V}^- \\ \epsilon \mathcal{V}^+ & \mathcal{R}_F + \epsilon \mathcal{V}^F \end{pmatrix}$. This gives the block-diagonal and block-off-diagonal parts:

$$\mathcal{L}^{\text{diag}} = \begin{pmatrix} \epsilon \mathcal{V}^S & 0 \\ 0 & \mathcal{R}_F + \epsilon \mathcal{V}^F \end{pmatrix}, \quad \mathcal{L}^{\text{offdiag}} = \begin{pmatrix} 0 & \epsilon \mathcal{V}^- \\ \epsilon \mathcal{V}^+ & 0 \end{pmatrix}. \quad (\text{B.15})$$

The generator \mathcal{S} is expanded as $\mathcal{S} = \sum_{n=1}^{\infty} \epsilon^n \mathcal{S}_n$, where each \mathcal{S}_n is purely block-off-diagonal:

$$\mathcal{S}_n = \begin{pmatrix} 0 & \mathcal{S}_n^- \\ \mathcal{S}_n^+ & 0 \end{pmatrix}. \quad (\text{B.16})$$

Step 1: Determine \mathcal{S}_1 . We expand the decoupling condition $\sinh(\widehat{\mathcal{S}}) \mathcal{L}^{\text{diag}} + \cosh(\widehat{\mathcal{S}}) \mathcal{L}^{\text{offdiag}} = 0$. We use $\sinh(\widehat{\mathcal{S}}) = \epsilon \widehat{\mathcal{S}}_1 + O(\epsilon^3)$, $\cosh(\widehat{\mathcal{S}}) = \mathbf{1} + O(\epsilon^2)$, $\mathcal{L}^{\text{diag}} = \mathcal{R} + O(\epsilon)$, and $\mathcal{L}^{\text{offdiag}} = \epsilon \mathcal{V}^{\text{offdiag}}$. Matching terms of order $O(\epsilon)$ yields:

$$(\epsilon \widehat{\mathcal{S}}_1)(\mathcal{R}) + (\mathbf{1})(\epsilon \mathcal{V}^{\text{offdiag}}) = 0 \implies [\mathcal{S}_1, \mathcal{R}] = -\mathcal{V}^{\text{offdiag}}. \quad (\text{B.17})$$

We solve this commutator equation in block matrix form:

$$\begin{pmatrix} 0 & \mathcal{S}_1^- \\ \mathcal{S}_1^+ & 0 \end{pmatrix} \begin{pmatrix} 0 & 0 \\ 0 & \mathcal{R}_F \end{pmatrix} - \begin{pmatrix} 0 & 0 \\ 0 & \mathcal{R}_F \end{pmatrix} \begin{pmatrix} 0 & \mathcal{S}_1^- \\ \mathcal{S}_1^+ & 0 \end{pmatrix} = - \begin{pmatrix} 0 & \mathcal{V}^- \\ \mathcal{V}^+ & 0 \end{pmatrix} \quad (\text{B.18})$$

$$\begin{pmatrix} 0 & \mathcal{S}_1^- \mathcal{R}_F \\ 0 & 0 \end{pmatrix} - \begin{pmatrix} 0 & 0 \\ \mathcal{R}_F \mathcal{S}_1^+ & 0 \end{pmatrix} = \begin{pmatrix} 0 & -\mathcal{V}^- \\ -\mathcal{V}^+ & 0 \end{pmatrix} \quad (\text{B.19})$$

$$\begin{pmatrix} 0 & \mathcal{S}_1^- \mathcal{R}_F \\ -\mathcal{R}_F \mathcal{S}_1^+ & 0 \end{pmatrix} = \begin{pmatrix} 0 & -\mathcal{V}^- \\ -\mathcal{V}^+ & 0 \end{pmatrix}. \quad (\text{B.20})$$

Equating the blocks and using the invertibility of \mathcal{R}_F on \mathcal{H}_F (with inverse \mathcal{R}^+):

1. (1,2) block: $\mathcal{S}_1^- \mathcal{R}_F = -\mathcal{V}^- \implies \mathcal{S}_1^- = -\mathcal{V}^- \mathcal{R}^+$.
2. (2,1) block: $-\mathcal{R}_F \mathcal{S}_1^+ = -\mathcal{V}^+ \implies \mathcal{S}_1^+ = \mathcal{R}^+ \mathcal{V}^+$.

Step 2: Determine L_n^{eff} . The transformed generator is $L^{\text{diag}} = \mathcal{L}^{\text{diag}} + \tanh(\hat{\mathcal{S}}/2) \mathcal{L}^{\text{offdiag}}$. The effective generator $\mathcal{L}_{\text{eff}} = \sum \epsilon^n L_n^{\text{eff}}$ is the $P_S L^{\text{diag}} P_S$ block (the (1,1) block) of L^{diag} . We expand $L^{\text{diag}} = \sum \epsilon^n L^{(n)}$ in powers of ϵ :

$$L^{\text{diag}} = (\mathcal{R} + \epsilon \mathcal{V}^{\text{diag}}) + \left(\frac{1}{2} \hat{\mathcal{S}} + O(\hat{\mathcal{S}}^3) \right) \mathcal{L}^{\text{offdiag}}. \quad (\text{B.21})$$

Substituting $\hat{\mathcal{S}} = \epsilon \hat{\mathcal{S}}_1 + O(\epsilon^2)$ and $\mathcal{L}^{\text{offdiag}} = \epsilon \mathcal{V}^{\text{offdiag}}$:

$$L^{\text{diag}} = (\mathcal{R} + \epsilon \mathcal{V}^{\text{diag}}) + \left(\frac{\epsilon}{2} \hat{\mathcal{S}}_1 + O(\epsilon^3) \right) (\epsilon \mathcal{V}^{\text{offdiag}}) \quad (\text{B.22})$$

We collect terms by order:

1. $O(\epsilon^0)$: $L^{(0)} = \mathcal{R} = \begin{pmatrix} 0 & 0 \\ 0 & \mathcal{R}_F \end{pmatrix} \implies L_0^{\text{eff}} = P_S L^{(0)} P_S = 0$.
2. $O(\epsilon^1)$: $\epsilon L^{(1)} = \epsilon \mathcal{V}^{\text{diag}} = \epsilon \begin{pmatrix} \mathcal{V}^S & 0 \\ 0 & \mathcal{V}^F \end{pmatrix} \implies L_1^{\text{eff}} = P_S L^{(1)} P_S = \mathcal{V}^S$.
3. $O(\epsilon^2)$: $\epsilon^2 L^{(2)} = \frac{\epsilon}{2} \hat{\mathcal{S}}_1 (\epsilon \mathcal{V}^{\text{offdiag}}) = \frac{\epsilon^2}{2} [\mathcal{S}_1, \mathcal{V}^{\text{offdiag}}]$.

We compute the $O(\epsilon^2)$ term $L^{(2)} = \frac{1}{2} [\mathcal{S}_1, \mathcal{V}^{\text{offdiag}}]$ using block matrices:

$$[\mathcal{S}_1, \mathcal{V}^{\text{offdiag}}] = \begin{pmatrix} 0 & \mathcal{S}_1^- \\ \mathcal{S}_1^+ & 0 \end{pmatrix} \begin{pmatrix} 0 & \mathcal{V}^- \\ \mathcal{V}^+ & 0 \end{pmatrix} - \begin{pmatrix} 0 & \mathcal{V}^- \\ \mathcal{V}^+ & 0 \end{pmatrix} \begin{pmatrix} 0 & \mathcal{S}_1^- \\ \mathcal{S}_1^+ & 0 \end{pmatrix} \quad (\text{B.23})$$

$$= \begin{pmatrix} \mathcal{S}_1^- \mathcal{V}^+ & 0 \\ 0 & \mathcal{S}_1^+ \mathcal{V}^- \end{pmatrix} - \begin{pmatrix} \mathcal{V}^- \mathcal{S}_1^+ & 0 \\ 0 & \mathcal{V}^+ \mathcal{S}_1^- \end{pmatrix} \quad (\text{B.24})$$

$$= \begin{pmatrix} \mathcal{S}_1^- \mathcal{V}^+ - \mathcal{V}^- \mathcal{S}_1^+ & 0 \\ 0 & \mathcal{S}_1^+ \mathcal{V}^- - \mathcal{V}^+ \mathcal{S}_1^- \end{pmatrix}. \quad (\text{B.25})$$

The effective generator L_2^{eff} is the (1,1) block of $L^{(2)} = \frac{1}{2} [\mathcal{S}_1, \mathcal{V}^{\text{offdiag}}]$:

$$L_2^{\text{eff}} = \frac{1}{2} (\mathcal{S}_1^- \mathcal{V}^+ - \mathcal{V}^- \mathcal{S}_1^+). \quad (\text{B.26})$$

Finally, we substitute the expressions for \mathcal{S}_1^- and \mathcal{S}_1^+ from Step 1:

$$L_2^{\text{eff}} = \frac{1}{2} ((-\mathcal{V}^- \mathcal{R}^+) \mathcal{V}^+ - \mathcal{V}^- (\mathcal{R}^+ \mathcal{V}^+)) \quad (\text{B.27})$$

$$= \frac{1}{2} (-\mathcal{V}^- \mathcal{R}^+ \mathcal{V}^+ - \mathcal{V}^- \mathcal{R}^+ \mathcal{V}^+) \quad (\text{B.28})$$

$$= -\mathcal{V}^- \mathcal{R}^+ \mathcal{V}^+. \quad (\text{B.29})$$

This rigorously derives the first- and second-order terms. The third-order term L_3^{eff} follows from this same procedure by matching terms at $O(\epsilon^3)$, which involves finding \mathcal{S}_2 and including the $O(\hat{\mathcal{S}}^3)$ term from $\tanh(\hat{\mathcal{S}}/2)$. The full derivation is found in [Kes12]. \square

Theorem B.3 (Effective Generator via Adiabatic Elimination, cf. Theorem 3.3). *Let $\mathcal{L} = \gamma\mathcal{R} + \mathcal{V}$ be a generator, where $\gamma \gg 1$, \mathcal{R} is self-adjoint with $\ker(\mathcal{R}) \neq \{0\}$, and P_S is the orthogonal projection onto the slow subspace $\mathcal{H}_S := \ker(\mathcal{R})$. Let \mathcal{R}^+ be the pseudo-inverse of \mathcal{R} on the fast subspace $\mathcal{H}_F = \mathcal{H}_F$. The effective generator \mathcal{L}_{eff} acting on \mathcal{H}_S is given by the expansion:*

$$\mathcal{L}_{\text{eff}} = L^{(1)} + \frac{1}{\gamma} L^{(2)} + O(1/\gamma^2), \quad (\text{B.30})$$

where the first- and second-order terms are:

$$L^{(1)} = P_S \mathcal{V} P_S \quad (\text{B.31})$$

$$L^{(2)} = -P_S \mathcal{V} \mathcal{R}^+ \mathcal{V} P_S. \quad (\text{B.32})$$

Proof. The derivation proceeds by first rescaling the generator to cast the problem into the standard perturbation form required by the SW formalism, then applying the established SW expansion formulas, and finally reversing the rescaling to obtain the generator for the original timescale.

We begin by defining the small parameter $\epsilon = 1/\gamma$ and the rescaled generator $\mathcal{L}' = \frac{1}{\gamma} \mathcal{L} = \mathcal{R} + \epsilon \mathcal{V}$. This allows us to identify the components needed for the SW expansion (Theorem 3.2). The projection onto the slow subspace $\ker(\mathcal{R})$ is P_S , and the projection onto the fast subspace is $P_F = \mathbf{1} - P_S$.

The SW formalism provides the perturbative expansion for the effective generator $\mathcal{L}'_{\text{eff}} = P_S L' P_S$ of the rescaled system, where $L' = e^{\mathcal{S}} \mathcal{L}' e^{-\mathcal{S}}$. According to Theorem 3.2, the expansion is $\mathcal{L}'_{\text{eff}} = L_0^{\text{eff}} + \epsilon L_1^{\text{eff}} + \epsilon^2 L_2^{\text{eff}} + O(\epsilon^3)$. We compute the first few terms explicitly.

The zeroth-order term is $L_0^{\text{eff}} = P_S \mathcal{R} P_S$. Since P_S projects onto the kernel of \mathcal{R} , this term vanishes: $L_0^{\text{eff}} = 0$.

The first-order term is $L_1^{\text{eff}} = P_S \mathcal{V} P_S$ from Theorem 3.2.

The second-order term, from Theorem 3.2, is $L_2^{\text{eff}} = -P_S \mathcal{V} P_F \mathcal{R}^+ P_F \mathcal{V} P_S$. Since $\mathcal{R}^+ \equiv (P_F \mathcal{R} P_F)^{-1}$ is the pseudo-inverse on the fast subspace, it maps $\mathcal{H}_F \rightarrow \mathcal{H}_F$, implying $\mathcal{R}^+ = P_F \mathcal{R}^+ P_F$. Thus, the expression simplifies to $L_2^{\text{eff}} = -P_S \mathcal{V} \mathcal{R}^+ \mathcal{V} P_S$.

Combining these terms yields the expansion for the rescaled effective generator:

$$\mathcal{L}'_{\text{eff}} = 0 + \epsilon(P_S \mathcal{V} P_S) + \epsilon^2(-P_S \mathcal{V} \mathcal{R}^+ \mathcal{V} P_S) + O(\epsilon^3). \quad (\text{B.33})$$

To find the effective generator \mathcal{L}_{eff} for the original timescale t , we reverse the rescaling by multiplying $\mathcal{L}'_{\text{eff}}$ by $\gamma = 1/\epsilon$:

$$\mathcal{L}_{\text{eff}} = \gamma \mathcal{L}'_{\text{eff}} = \frac{1}{\epsilon} [\epsilon(P_S \mathcal{V} P_S) + \epsilon^2(-P_S \mathcal{V} \mathcal{R}^+ \mathcal{V} P_S) + O(\epsilon^3)] \quad (\text{B.34})$$

$$= (1)(P_S \mathcal{V} P_S) + \epsilon(-P_S \mathcal{V} \mathcal{R}^+ \mathcal{V} P_S) + O(\epsilon^2) \quad (\text{B.35})$$

$$= P_S \mathcal{V} P_S + \frac{1}{\gamma} (-P_S \mathcal{V} \mathcal{R}^+ \mathcal{V} P_S) + O(1/\gamma^2). \quad (\text{B.36})$$

This result precisely identifies the first-order term $L^{(1)} = P_S \mathcal{V} P_S$ and the second-order term $L^{(2)} = -P_S \mathcal{V} \mathcal{R}^+ \mathcal{V} P_S$, matching Theorem 3.3. \square

Lemma B.1 (Iterative Dyson Expansion). *Let $\mathcal{L}' = \mathcal{A} + \mathcal{B}$ be a generator and $\mathcal{P}'_t = \exp(t\mathcal{L}')$. The semigroup satisfies the identity:*

$$\mathcal{P}'_t = \exp(t\mathcal{A}) \left(\mathbf{1} + \int_0^t dt_1 \exp(-t_1\mathcal{A}) \mathcal{B} \mathcal{P}'_{t_1} \right). \quad (\text{B.37})$$

Proof. We use the ansatz $\mathcal{P}'_t = \exp(t\mathcal{A})\mathcal{U}(t)$ for some superoperator $\mathcal{U}(t)$. Taking the time derivative, we have:

$$\frac{d}{dt} \mathcal{P}'_t = \mathcal{L}' \mathcal{P}'_t = (\mathcal{A} + \mathcal{B}) \exp(t\mathcal{A}) \mathcal{U}(t). \quad (\text{B.38})$$

Using the product rule on the ansatz, we also have:

$$\frac{d}{dt} \mathcal{P}'_t = \mathcal{A} \exp(t\mathcal{A}) \mathcal{U}(t) + \exp(t\mathcal{A}) \frac{d}{dt} \mathcal{U}(t). \quad (\text{B.39})$$

Equating the two expressions for the derivative yields:

$$(\mathcal{A} + \mathcal{B}) \exp(t\mathcal{A}) \mathcal{U}(t) = \mathcal{A} \exp(t\mathcal{A}) \mathcal{U}(t) + \exp(t\mathcal{A}) \frac{d}{dt} \mathcal{U}(t) \quad (\text{B.40})$$

$$\mathcal{B} \exp(t\mathcal{A}) \mathcal{U}(t) = \exp(t\mathcal{A}) \frac{d}{dt} \mathcal{U}(t) \quad (\text{B.41})$$

$$\implies \frac{d}{dt} \mathcal{U}(t) = \exp(-t\mathcal{A}) \mathcal{B} \mathcal{P}'_t. \quad (\text{B.42})$$

We integrate this differential equation from 0 to t , using the initial condition $\mathcal{U}(0) = \mathbf{1}$ (since $\mathcal{P}'_0 = \mathbf{1}$):

$$\mathcal{U}(t) = \mathbf{1} + \int_0^t dt_1 \exp(-t_1\mathcal{A}) \mathcal{B} \mathcal{P}'_{t_1}. \quad (\text{B.43})$$

Substituting this expression for $\mathcal{U}(t)$ back into the ansatz $\mathcal{P}'_t = \exp(t\mathcal{A})\mathcal{U}(t)$ gives the desired result. \square

Lemma B.2 (Grönwall's Inequality for Volterra's Equations). *Let $f(t)$ be a non-negative, locally integrable function on $[0, \infty)$ satisfying the integral inequality:*

$$f(t) \leq A + C \int_0^t e^{-\lambda(t-s)} f(s) ds \quad (\text{B.44})$$

for constants $A \geq 0$, $C \geq 0$, and $\lambda > 0$. If $C < \lambda$, then $f(t)$ is uniformly bounded for all $t \geq 0$ by:

$$f(t) \leq \frac{A\lambda}{\lambda - C}. \quad (\text{B.45})$$

Proof. Let $g(t) = e^{\lambda t} f(t)$. Multiplying the inequality by $e^{\lambda t}$, we obtain

$$g(t) \leq A e^{\lambda t} + C \int_0^t e^{\lambda s} f(s) ds = A e^{\lambda t} + C \int_0^t g(s) ds. \quad (\text{B.46})$$

Let $G(t) = \int_0^t g(s)ds$. Then $G'(t) = g(t)$, and the inequality is $G'(t) \leq Ae^{\lambda t} + CG(t)$. This is a first-order linear differential inequality $G'(t) - CG(t) \leq Ae^{\lambda t}$. We multiply by the integrating factor e^{-Ct} :

$$\frac{d}{dt}(G(t)e^{-Ct}) \leq Ae^{(\lambda-C)t}. \quad (\text{B.47})$$

Integrating from 0 to t , and using $G(0) = 0$, we find (assuming $\lambda \neq C$):

$$G(t)e^{-Ct} \leq \int_0^t Ae^{(\lambda-C)s}ds = \frac{A}{\lambda-C}(e^{(\lambda-C)t} - 1). \quad (\text{B.48})$$

Thus, $G(t) \leq \frac{A}{\lambda-C}(e^{\lambda t} - e^{Ct})$. Substituting this back into the inequality for $g(t)$:

$$g(t) \leq Ae^{\lambda t} + CG(t) \leq Ae^{\lambda t} + \frac{AC}{\lambda-C}(e^{\lambda t} - e^{Ct}) = \frac{A\lambda}{\lambda-C}e^{\lambda t} - \frac{AC}{\lambda-C}e^{Ct}. \quad (\text{B.49})$$

Finally, we recover $f(t) = g(t)e^{-\lambda t}$:

$$f(t) \leq \frac{A\lambda}{\lambda-C} - \frac{AC}{\lambda-C}e^{(C-\lambda)t}. \quad (\text{B.50})$$

Since $C < \lambda$ by hypothesis, the exponent $(C - \lambda)$ is strictly negative. The second term is thus non-positive and decays to zero, which gives the uniform bound $f(t) \leq \frac{A\lambda}{\lambda-C}$. \square

Theorem B.4 (Approximation Error of AE Dynamics, cf. Theorem 3.4). *Let $\mathcal{P}_t = \exp(t\mathcal{L})$ be the QMS with generator $\mathcal{L} = \gamma\mathcal{R} + \mathcal{V}$, where \mathcal{R} is self-adjoint with a spectral gap $\lambda_R > 0$ on the fast subspace $\mathcal{H}_F := \ker(\mathcal{R})^\perp$. Assume $L^{(1)} = P_S\mathcal{V}P_S = 0$ and that γ is sufficiently large such that $\gamma\lambda_R > \|\mathcal{V}\|$. Let $X(0) \in \mathcal{H}_S$, $X(t) = \mathcal{P}_t X(0)$, and $X_{\text{eff}}(t) = \exp(t\hat{\mathcal{L}}_{\text{eff}})X(0)$ where $\hat{\mathcal{L}}_{\text{eff}} = \frac{1}{\gamma}L^{(2)}$. Then for any $t \geq 0$, the approximation error is bounded with respect to the KMS norm by:*

$$\|X(t) - X_{\text{eff}}(t)\|_{2,\sigma} \leq \frac{C'_V}{\gamma\lambda_R} \left(1 + t \left(\|\mathcal{V}\| + \frac{\|\mathcal{V}\|^2}{C'_V} \right) \right) \|X(0)\|_{2,\sigma}, \quad (\text{B.51})$$

where $C'_V = \frac{\|\mathcal{V}\|}{1 - \|\mathcal{V}\|/(\gamma\lambda_R)}$ is a constant of order $O(\|\mathcal{V}\|)$.

Proof. We decompose the error $X(t) - X_{\text{eff}}(t)$ into its orthogonal components in the slow subspace \mathcal{H}_S and the fast subspace \mathcal{H}_F :

$$X(t) - X_{\text{eff}}(t) = \underbrace{P_F \mathcal{P}_t X(0)}_{X_F(t)} + \underbrace{(P_S \mathcal{P}_t - \exp(t\hat{\mathcal{L}}_{\text{eff}}))X(0)}_{Z(t)}. \quad (\text{B.52})$$

By the Pythagorean theorem, $\|X(t) - X_{\text{eff}}(t)\|_{2,\sigma}^2 = \|X_F(t)\|_{2,\sigma}^2 + \|Z(t)\|_{2,\sigma}^2$. We can bound the total error by the sum of the norms: $\|X(t) - X_{\text{eff}}(t)\|_{2,\sigma} \leq \|X_F(t)\|_{2,\sigma} + \|Z(t)\|_{2,\sigma}$. We now bound each term:

1. Bound on Leakage $X_F(t)$: We analyze the rescaled dynamics $t' = \gamma t$, $\mathcal{L}' = \mathcal{R} + \epsilon \mathcal{V}$ with $\epsilon = 1/\gamma$. Let $\mathcal{P}'_{t'} = \mathcal{P}_{t'/\gamma}$. The leakage is $X_F(t') = P_F \mathcal{P}'_{t'} X(0)$. Using the iterative Dyson expansion (Lemma B.1) with $\mathcal{A} = \mathcal{R}$ and $\mathcal{B} = \epsilon \mathcal{V}$, and $X(0) \in \ker(\mathcal{R}) = \mathcal{H}_S$:

$$X_F(t') = P_F \int_0^{t'} dt_1 e^{(t'-t_1)\mathcal{R}} (\epsilon \mathcal{V}) \mathcal{P}'_{t_1} X(0). \quad (\text{B.53})$$

Let $X_S(t_1) = P_S \mathcal{P}'_{t_1} X(0)$ and $X_F(t_1) = P_F \mathcal{P}'_{t_1} X(0)$. The assumption $P_S \mathcal{V} P_S = 0$ implies $P_F \mathcal{V} P_S = \mathcal{V} P_S$.

$$X_F(t') = \epsilon P_F \int_0^{t'} dt_1 e^{(t'-t_1)\mathcal{R}} \mathcal{V} (X_S(t_1) + X_F(t_1)) \quad (\text{B.54})$$

$$= \epsilon \int_0^{t'} dt_1 e^{(t'-t_1)\mathcal{R}} \mathcal{V} X_S(t_1) + \epsilon \int_0^{t'} dt_1 e^{(t'-t_1)\mathcal{R}} P_F \mathcal{V} X_F(t_1). \quad (\text{B.55})$$

Let $f(t') = \|X_F(t')\|_{2,\sigma}$. We take the norm of the inequality, using $\|e^{s\mathcal{R}} P_F\| \leq e^{-s\lambda_R}$ and the contractivity $\|X_S(t_1)\|_{2,\sigma} \leq \|X(0)\|_{2,\sigma}$:

$$f(t') \leq \epsilon \int_0^{t'} e^{-(t'-t_1)\lambda_R} \|\mathcal{V}\| \|X_S(t_1)\|_{2,\sigma} dt_1 + \epsilon \int_0^{t'} e^{-(t'-t_1)\lambda_R} \|\mathcal{V}\| f(t_1) dt_1 \quad (\text{B.56})$$

$$\leq \left(\epsilon \|\mathcal{V}\| \|X(0)\|_{2,\sigma} \int_0^{t'} e^{-(t'-s)\lambda_R} ds \right) + \epsilon \|\mathcal{V}\| \int_0^{t'} e^{-(t'-t_1)\lambda_R} f(t_1) dt_1. \quad (\text{B.57})$$

Bounding the integral $\int_0^{t'} e^{-u\lambda_R} du \leq \int_0^\infty e^{-u\lambda_R} du = 1/\lambda_R$, we obtain:

$$f(t') \leq \left(\epsilon \frac{\|\mathcal{V}\|}{\lambda_R} \|X(0)\|_{2,\sigma} \right) + \epsilon \|\mathcal{V}\| \int_0^{t'} e^{-(t'-t_1)\lambda_R} f(t_1) dt_1. \quad (\text{B.58})$$

This is precisely the form of Lemma B.2 with $A = \epsilon \frac{\|\mathcal{V}\|}{\lambda_R} \|X(0)\|_{2,\sigma}$, $C = \epsilon \|\mathcal{V}\|$, and $\lambda = \lambda_R$. The condition $C < \lambda$ is $\epsilon \|\mathcal{V}\| < \lambda_R$, or $\gamma \lambda_R > \|\mathcal{V}\|$, which is assumed. Applying Lemma B.2 yields the uniform-in-time bound:

$$f(t') \leq \frac{A \lambda_R}{\lambda_R - C} = \frac{(\epsilon \|\mathcal{V}\| \|X(0)\|_{2,\sigma} / \lambda_R) \cdot \lambda_R}{\lambda_R - \epsilon \|\mathcal{V}\|} = \frac{\epsilon \|\mathcal{V}\|}{\lambda_R - \epsilon \|\mathcal{V}\|} \|X(0)\|_{2,\sigma}. \quad (\text{B.59})$$

Substituting back $\epsilon = 1/\gamma$ and $t' = \gamma t$, we have for all $t \geq 0$:

$$\|X_F(t)\|_{2,\sigma} \leq \frac{\|\mathcal{V}\|/\gamma}{\lambda_R - \|\mathcal{V}\|/\gamma} \|X(0)\|_{2,\sigma} = \frac{\|\mathcal{V}\|}{\gamma \lambda_R - \|\mathcal{V}\|} \|X(0)\|_{2,\sigma}. \quad (\text{B.60})$$

2. Bound on Intrinsic Error $Z(t)$: Let $X_S(t) = P_S \mathcal{P}_t X(0)$. The derivative of the slow component is $\frac{d}{dt} X_S(t) = P_S \mathcal{L} \mathcal{P}_t X(0) = P_S (\gamma \mathcal{R} + \mathcal{V})(X_S(t) + X_F(t))$. Since $P_S \mathcal{R} = 0$ and $P_S \mathcal{V} P_S = 0$, this simplifies to $\frac{d}{dt} X_S(t) = P_S \mathcal{V} X_F(t)$. The error $Z(t) = X_S(t) - X_{\text{eff}}(t)$ satisfies $\frac{d}{dt} Z(t) = (P_S \mathcal{V} X_F(t)) - (\hat{\mathcal{L}}_{\text{eff}} X_{\text{eff}}(t))$.

$$\frac{d}{dt} Z(t) = \hat{\mathcal{L}}_{\text{eff}} Z(t) + \left(P_S \mathcal{V} X_F(t) - \hat{\mathcal{L}}_{\text{eff}} X_{\text{eff}}(t) \right). \quad (\text{B.61})$$

Let $\mathcal{E}(t) = P_S \mathcal{V} X_F(t) - \widehat{\mathcal{L}}_{\text{eff}} X_S(t)$. By Duhamel's principle [Eva10], $Z(t) = \int_0^t e^{(t-s)\widehat{\mathcal{L}}_{\text{eff}}} \mathcal{E}(s) ds$. Since $\widehat{\mathcal{L}}_{\text{eff}}$ generates a contractive semigroup, $\|e^{(t-s)\widehat{\mathcal{L}}_{\text{eff}}}\| \leq 1$, and we have

$$\|Z(t)\|_{2,\sigma} \leq \int_0^t \|\mathcal{E}(s)\|_{2,\sigma} ds \leq \int_0^t \left(\|P_S \mathcal{V}\| \|X_F(s)\|_{2,\sigma} + \|\widehat{\mathcal{L}}_{\text{eff}}\| \|X_S(s)\|_{2,\sigma} \right) ds. \quad (\text{B.62})$$

We use the bound $\|L^{(2)}\| = \|P_S \mathcal{V} \mathcal{R}^+ \mathcal{V} P_S\| \leq \|\mathcal{V}\| \|\mathcal{R}^+\| \|\mathcal{V}\| \leq \|\mathcal{V}\|^2 / \lambda_R$. Thus, $\|\widehat{\mathcal{L}}_{\text{eff}}\| = \frac{1}{\gamma} \|L^{(2)}\| \leq \frac{\|\mathcal{V}\|^2}{\gamma \lambda_R}$. Using contractivity $\|X_S(s)\|_{2,\sigma} \leq \|X(0)\|_{2,\sigma}$ and the bound (B.60):

$$\|\mathcal{E}(s)\|_{2,\sigma} \leq \|\mathcal{V}\| \left(\frac{\|\mathcal{V}\|}{\gamma \lambda_R - \|\mathcal{V}\|} \|X(0)\|_{2,\sigma} \right) + \left(\frac{\|\mathcal{V}\|^2}{\gamma \lambda_R} \right) \|X(0)\|_{2,\sigma} \quad (\text{B.63})$$

$$= \left(\frac{\|\mathcal{V}\|^2}{\gamma \lambda_R - \|\mathcal{V}\|} + \frac{\|\mathcal{V}\|^2}{\gamma \lambda_R} \right) \|X(0)\|_{2,\sigma}. \quad (\text{B.64})$$

This bound is uniform in s . Integrating from 0 to t :

$$\|Z(t)\|_{2,\sigma} \leq t \cdot \left(\frac{\|\mathcal{V}\|^2}{\gamma \lambda_R - \|\mathcal{V}\|} + \frac{\|\mathcal{V}\|^2}{\gamma \lambda_R} \right) \|X(0)\|_{2,\sigma}. \quad (\text{B.65})$$

3. Total Error Bound: We define the constant $C'_{\mathcal{V}} = \frac{\|\mathcal{V}\|}{1 - \|\mathcal{V}\|/(\gamma \lambda_R)}$, which is $O(\|\mathcal{V}\|)$. Combine (B.60) and (B.65) directly:

$$\|X(t) - X_{\text{eff}}(t)\|_{2,\sigma} \leq \|X_F(t)\|_{2,\sigma} + \|Z(t)\|_{2,\sigma} \quad (\text{B.66})$$

$$\leq \left[\frac{\|\mathcal{V}\|}{\gamma \lambda_R - \|\mathcal{V}\|} + t \left(\frac{\|\mathcal{V}\|^2}{\gamma \lambda_R - \|\mathcal{V}\|} + \frac{\|\mathcal{V}\|^2}{\gamma \lambda_R} \right) \right] \|X(0)\|_{2,\sigma} \quad (\text{B.67})$$

$$= \left[\frac{C'_{\mathcal{V}}}{\gamma \lambda_R} + t \left(\frac{\|\mathcal{V}\| C'_{\mathcal{V}}}{\gamma \lambda_R} + \frac{\|\mathcal{V}\|^2}{\gamma \lambda_R} \right) \right] \|X(0)\|_{2,\sigma} \quad (\text{B.68})$$

$$= \frac{C'_{\mathcal{V}}}{\gamma \lambda_R} \left[1 + t \left(\|\mathcal{V}\| + \frac{\|\mathcal{V}\|^2}{C'_{\mathcal{V}}} \right) \right] \|X(0)\|_{2,\sigma}. \quad (\text{B.69})$$

This provides a rigorous bound that is $O(1/\gamma)$ at $t = 0$ and grows only linearly in t . \square

C. Proof for Abstract framework

Lemma C.1 (Decay Rate Bound via Singular Value Gap, cf. Lemma 4.2). *Let $\{P_t\}_{t \geq 0}$ be a hypocoercive semigroup satisfying (4.2) with optimal rate $\nu = \lambda(L)$ and prefactor $C \geq 1$. Then the decay rate is bounded by the singular value gap:*

$$\nu \leq (1 + \log C) s(L). \quad (\text{C.1})$$

Proof. Note that the exponential decay

$$\|P_t x - P_\infty x\|_{\mathcal{H}} \leq C e^{-\nu t} \|x - P_\infty x\|_{\mathcal{H}} \quad (\text{C.2})$$

is equivalent (for some $\nu > 0$ and $T = (\log C)/\nu$ with $C \geq 1$) to

$$\|P_t x - P_\infty x\|_{\mathcal{H}} \leq e^{-\nu(t-T)} \|x - P_\infty x\|_{\mathcal{H}} \quad \text{for all } t \geq 0. \quad (\text{C.3})$$

Fix $T, \nu > 0$ as in (C.3) and let $x \in \mathcal{F}^\perp$ (so $P_\infty x = 0$). Then

$$\int_0^\infty \|P_t x\|_{\mathcal{H}} dt = \int_0^T \|P_t x\|_{\mathcal{H}} dt + \int_T^\infty \|P_t x\|_{\mathcal{H}} dt \leq \int_0^T \|x\|_{\mathcal{H}} dt + \int_T^\infty e^{-\nu(t-T)} \|x\|_{\mathcal{H}} dt. \quad (\text{C.4})$$

Evaluating the integrals gives

$$\int_0^\infty \|P_t x\|_{\mathcal{H}} dt \leq (T + \frac{1}{\nu}) \|x\|_{\mathcal{H}}. \quad (\text{C.5})$$

Hence the operator defined by

$$x \mapsto \int_0^\infty P_t x dt, x \in \mathcal{F}^\perp, \quad (\text{C.6})$$

is well-defined and bounded on \mathcal{F}^\perp . It follows that 0 belongs to the resolvent set of the generator of the restricted contraction semigroup $P_t : \mathcal{F}^\perp \rightarrow \mathcal{F}^\perp$, so the inverse $(-L|_{\mathcal{F}^\perp})^{-1}$ is a bounded operator on \mathcal{F}^\perp . Moreover,

$$\|(-L|_{\mathcal{F}^\perp})^{-1} x\|_{\mathcal{H}} \leq \int_0^\infty \|P_t x\|_{\mathcal{H}} dt \leq (T + \frac{1}{\nu}) \|x\|_{\mathcal{H}}. \quad (\text{C.7})$$

Using $T = (\log C)/\nu$ from above and (C.3) (or the equivalent estimate for C), we obtain the spectral bound estimate

$$\frac{1}{s(L)} = \sup_{y \in \text{Dom}(L|_{\mathcal{F}^\perp}) \setminus \{0\}} \frac{\|y\|_{\mathcal{H}}}{\|L|_{\mathcal{F}^\perp} y\|_{\mathcal{H}}} = \sup_{x \in \mathcal{F}^\perp \setminus \{0\}} \frac{\|(-L|_{\mathcal{F}^\perp})^{-1} x\|_{\mathcal{H}}}{\|x\|_{\mathcal{H}}} \leq \frac{1}{\nu} (1 + \log C), \quad (\text{C.8})$$

as desired. \square

D. Proof for Upper bound

Theorem D.1 (Upper Bound on $\nu(L)$, cf. Theorem 6.1). *Under the assumptions stated in Theorem 6.1, the exponential convergence rate $\nu(L)$ satisfies:*

$$\nu(L) \leq (1 + \log C(L)) \sqrt{\frac{s(L_O) + \eta C_{AQF}}{s(\Pi_1 S \Pi_1)}}, \quad (\text{D.1})$$

where C_{AQF} is the constant from the Approximate Quadratic Form Condition.

Proof. From Lemma 4.2, we know that the exponential convergence rate $\nu(L)$ is bounded by $\nu(L) \leq (1 + \log C(L))s(L)$, where $s(L)$ is the singular value gap of the full generator L . Our goal is to derive an upper bound for $s(L)$.

The singular value gap is defined as $s(L) = \inf\{\|LX\|_{\mathcal{H}} \mid X \in \text{Dom}(L) \cap \mathcal{F}^\perp, \|X\|_{\mathcal{H}} = 1\}$, where $\mathcal{F} = \ker(L) = \ker(L_O)$. Since the target effective generator L_O acts on \mathcal{H}_S and $\ker(L_O) \subset \mathcal{H}_S$, the subspace $\text{Dom}(L_O) \cap \mathcal{F}^\perp \cap \mathcal{H}_S$ is a subset of $\text{Dom}(L) \cap \mathcal{F}^\perp$ (assuming $\text{Dom}(L_O) \subset \text{Dom}(\mathcal{V})$). Restricting the infimum to this smaller subspace provides an upper bound for $s(L)$:

$$s(L) \leq \inf\{\|LX\|_{\mathcal{H}} \mid X \in \text{Dom}(L_O) \cap \mathcal{F}^\perp, \|X\|_{\mathcal{H}} = 1\}. \quad (\text{D.2})$$

Note that for $X \in \mathcal{H}_S$, we have $LX = (\gamma\mathcal{R} + \mathcal{V})X = \mathcal{V}X$. So, $\|LX\| = \|\mathcal{V}X\|$.

Let $Y = LX = \mathcal{V}X$. By the Orthogonality condition, $Y \in \mathcal{H}_F$. Let Π_1 be the orthogonal projection onto $\overline{\text{Ran}(\mathcal{V}|_{\mathcal{H}_S})} \subseteq \mathcal{H}_F$. Since Y belongs to this range space, $\Pi_1 Y = Y$. Let $\bar{S} = \Pi_1 S \Pi_1$. The operator S is strictly positive definite and bounded on \mathcal{H}_F . When restricted to the subspace $\text{Ran}(\Pi_1)$, \bar{S} remains strictly positive definite. Let $s(\bar{S}) > 0$ be its smallest eigenvalue (singular value gap) on this subspace.

We relate $\|Y\|_{\mathcal{H}}$ to the quadratic form involving S :

$$\langle Y, SY \rangle_{\mathcal{H}} = \langle \Pi_1 Y, S \Pi_1 Y \rangle_{\mathcal{H}} = \langle Y, \bar{S}Y \rangle_{\mathcal{H}}. \quad (\text{D.3})$$

Since \bar{S} is positive definite on $\text{Ran}(\Pi_1)$, we have $\langle Y, \bar{S}Y \rangle_{\mathcal{H}} \geq s(\bar{S})\|Y\|_{\mathcal{H}}^2$. Therefore,

$$\|Y\|_{\mathcal{H}}^2 \leq s(\bar{S})^{-1} \langle Y, \bar{S}Y \rangle_{\mathcal{H}} = s(\bar{S})^{-1} \langle Y, SY \rangle_{\mathcal{H}}. \quad (\text{D.4})$$

Taking the square root and substituting $Y = LX$:

$$\|LX\|_{\mathcal{H}} \leq s(\bar{S})^{-1/2} \langle LX, SLX \rangle_{\mathcal{H}}^{1/2}. \quad (\text{D.5})$$

Now we apply the explicit Approximate Quadratic Form condition (5.3): $\langle LX, SLX \rangle_{\mathcal{H}} \leq \langle X, |L_O|X \rangle_{\mathcal{H}_S} + \eta C_{AQF} \|X\|_{\mathcal{H}}^2$ for $X \in \mathcal{H}_S$. Substituting this into (D.5) for X with $\|X\|_{\mathcal{H}} = 1$:

$$\|LX\|_{\mathcal{H}} \leq s(\bar{S})^{-1/2} (\langle X, |L_O|X \rangle_{\mathcal{H}_S} + \eta C_{AQF})^{1/2}. \quad (\text{D.6})$$

We insert this bound back into the inequality for $s(L)$ from (D.2):

$$s(L) \leq \inf \left\{ s(\bar{S})^{-1/2} (\langle X, |L_O|X \rangle_{\mathcal{H}_S} + \eta C_{AQF})^{1/2} \mid X \in \text{Dom}(L_O) \cap \mathcal{F}^\perp, \|X\|_{\mathcal{H}} = 1 \right\} \quad (\text{D.7})$$

$$\leq s(\bar{S})^{-1/2} \left(\inf \left\{ \langle X, |L_O|X \rangle_{\mathcal{H}_S} \mid X \in \text{Dom}(L_O) \cap \mathcal{F}^\perp, \|X\|_{\mathcal{H}} = 1 \right\} + \eta C_{AQF} \right)^{1/2}. \quad (\text{D.8})$$

The operator $|L_O|$ is positive semi-definite and self-adjoint. The infimum of the Rayleigh quotient $\langle X, |L_O|X \rangle / \|X\|_{\mathcal{H}}^2$ over the subspace $\mathcal{F}^\perp = \ker(L_O)^\perp$ is the smallest non-zero eigenvalue of $|L_O|$, which is exactly the singular value gap $s(L_O)$. Therefore,

$$s(L) \leq \sqrt{\frac{s(L_O) + \eta C_{AQF}}{s(\Pi_1 S \Pi_1)}}. \quad (\text{D.9})$$

Finally, using the relationship $\nu(L) \leq (1 + \log C(L))s(L)$, we obtain the desired upper bound:

$$\nu(L) \leq (1 + \log C(L)) \sqrt{\frac{s(L_O) + \eta C_{AQF}}{s(\Pi_1 S \Pi_1)}}. \quad (\text{D.10})$$

□

E. Proof for Lower bound

Lemma E.1 (Inner Product Reduction of \mathcal{A} , cf. Lemma 6.1). *Assume the Ad Embed Structure (Definition 5.1) holds, including the Approximate Quadratic Form Condition (5.3) with constant C_{AQF} . Then, for any sufficiently regular paths X_t, Y_t, Z_t taking values in the slow subspace $\mathcal{H}_S = \ker(\mathcal{R})$, the following relation holds:*

$$\langle \mathcal{A}X_t, Z_t + S\mathcal{V}Y_t \rangle_{T, \mathcal{H}} = -\langle \partial_t X_t, Z_t \rangle_{T, \mathcal{H}_S} + \mathcal{E}_{T, -|L_O|}(X_t, Y_t) + R_{T, \eta}(X, Y), \quad (\text{E.1})$$

where the remainder term satisfies $|R_{T, \eta}(X, Y)| \leq \eta C_{AQF} \frac{1}{T} \int_0^T \|X_t\|_{\mathcal{H}} \|Y_t\|_{\mathcal{H}} dt$.

Proof. The proof involves a direct calculation starting from the left-hand side (LHS). We substitute the definition of the operator $\mathcal{A}X_t = -\partial_t X_t + \mathcal{V}X_t$:

$$\text{LHS} = \langle -\partial_t X_t + \mathcal{V}X_t, Z_t + S\mathcal{V}Y_t \rangle_{T, \mathcal{H}} \quad (\text{E.2})$$

$$= \frac{1}{T} \int_0^T \langle -\partial_t X_t + \mathcal{V}X_t, Z_t + S\mathcal{V}Y_t \rangle_{\mathcal{H}} dt. \quad (\text{E.3})$$

We expand the inner product inside the integral into four terms:

$$\text{LHS} = \frac{1}{T} \int_0^T \left(\underbrace{-\langle \partial_t X_t, Z_t \rangle_{\mathcal{H}}}_{\text{(i)}} - \underbrace{\langle \partial_t X_t, S\mathcal{V}Y_t \rangle_{\mathcal{H}}}_{\text{(ii)}} + \underbrace{\langle \mathcal{V}X_t, Z_t \rangle_{\mathcal{H}}}_{\text{(iii)}} + \underbrace{\langle \mathcal{V}X_t, S\mathcal{V}Y_t \rangle_{\mathcal{H}}}_{\text{(iv)}} \right) dt. \quad (\text{E.4})$$

We analyze each term individually:

Term (i): Yields $-\langle \partial_t X_t, Z_t \rangle_{T, \mathcal{H}_S}$, as $X_t, Z_t \in \mathcal{H}_S$.

Term (ii): Vanishes because $\partial_t X_t \in \mathcal{H}_S$ and $S\mathcal{V}Y_t \in \mathcal{H}_F$ (using Orthogonality).

Term (iii): Vanishes because $\mathcal{V}X_t \in \mathcal{H}_F$ (using Orthogonality) and $Z_t \in \mathcal{H}_S$.

Term (iv): This term involves the quadratic form. For $X_t, Y_t \in \mathcal{H}_S$, we have $LX_t = \mathcal{V}X_t$ and $LY_t = \mathcal{V}Y_t$. Thus, $\langle \mathcal{V}X_t, S\mathcal{V}Y_t \rangle_{\mathcal{H}} = \langle LX_t, SLY_t \rangle_{\mathcal{H}}$. We now apply the explicit Approximate Quadratic Form Condition (5.3): Define the error term for a fixed t as $E(X_t, Y_t) = \langle LX_t, SLY_t \rangle_{\mathcal{H}} - \langle X_t, |L_O|Y_t \rangle_{\mathcal{H}_S}$. The condition states $|E(X_t, Y_t)| \leq \eta C_{AQF} \|X_t\|_{\mathcal{H}} \|Y_t\|_{\mathcal{H}}$. So, $\langle \mathcal{V}X_t, S\mathcal{V}Y_t \rangle_{\mathcal{H}} = \langle X_t, |L_O|Y_t \rangle_{\mathcal{H}_S} + E(X_t, Y_t)$. By definition, $\mathcal{E}_{-|L_O|}(X_t, Y_t) = -\langle X_t, (-|L_O|)Y_t \rangle_{\mathcal{H}_S} = \langle X_t, |L_O|Y_t \rangle_{\mathcal{H}_S}$. Integrating term (iv) over time gives:

$$\frac{1}{T} \int_0^T \langle \mathcal{V}X_t, S\mathcal{V}Y_t \rangle_{\mathcal{H}} dt = \frac{1}{T} \int_0^T (\mathcal{E}_{-|L_O|}(X_t, Y_t) + E(X_t, Y_t)) dt \quad (\text{E.5})$$

$$= \mathcal{E}_{T, -|L_O|}(X_t, Y_t) + \frac{1}{T} \int_0^T E(X_t, Y_t) dt. \quad (\text{E.6})$$

Let $R_{T,\eta}(X, Y) = \frac{1}{T} \int_0^T E(X_t, Y_t) dt$. Then:

$$|R_{T,\eta}(X, Y)| = \left| \frac{1}{T} \int_0^T E(X_t, Y_t) dt \right| \leq \frac{1}{T} \int_0^T |E(X_t, Y_t)| dt \leq \eta C_{AQF} \frac{1}{T} \int_0^T \|X_t\|_{\mathcal{H}} \|Y_t\|_{\mathcal{H}} dt. \quad (\text{E.7})$$

Combining the results for the four terms, we find:

$$\text{LHS} = -\langle \partial_t X_t, Z_t \rangle_{T,\mathcal{H}_S} + 0 + 0 + (\mathcal{E}_{T,-|L_O|}(X_t, Y_t) + R_{T,\eta}(X, Y)). \quad (\text{E.8})$$

This yields the desired identity with the explicitly bounded error term. \square

Theorem E.1 (Abstract Divergence Lemma, cf. Theorem 6.2). *Under Assumption 6.1, for any $T > 0$ and any path $X_t \in L^2_{\perp}([0, T]; \mathcal{H}_S)$, there exists a pair of paths (Z_t, Y_t) with Z_t, Y_t valued in $\text{Dom}(|L_O|) \subset \mathcal{H}_S$ solving the **abstract divergence equation**:*

$$\partial_t Z_t + |L_O| Y_t = X_t, \quad (\text{E.9})$$

and satisfying the energy estimates:

$$\| |L_O| Y_t \|_{T,\mathcal{H}_S} \leq c_1(T) \| X_t \|_{T,\mathcal{H}_S}, \quad \sqrt{\mathcal{E}_{T,-|L_O|}(Z_t)} \leq c_2(T) \| X_t \|_{T,\mathcal{H}_S}, \quad (\text{E.10})$$

$$\sqrt{\mathcal{E}_{T,-|L_O|}(Y_t)} \leq c_3(T) \| X_t \|_{T,\mathcal{H}_S}, \quad \sqrt{\mathcal{E}_{T,-|L_O|}(\partial_t Y_t)} \leq c_4(T) \| X_t \|_{T,\mathcal{H}_S}, \quad (\text{E.11})$$

where $\mathcal{E}_{T,-|L_O|}(W_t) = \langle W_t, |L_O| W_t \rangle_{T,\mathcal{H}_S}$. The constants scale as:

$$c_1 = \Theta(1), \quad c_2 = \Theta(1), \quad c_3 = \Theta\left(T + \frac{1}{\sqrt{s(L_O)}}\right), \quad c_4 = \Theta\left(1 + \frac{1}{T\sqrt{s(L_O)}}\right). \quad (\text{E.12})$$

Proof. The entire proof mirrors the version in [LL25, Lemma 3.12]. We include the proof here for self-containedness and to make sure the component extraction on L_O does not inherently affect the conclusion.

By Assumption 6.1 and 5.1, we know $-|L_O|$ is a semi-negative-definite operator with discrete spectrum. Thus, there exists an orthonormal basis $\{e_k\}_{k \geq 0}$ of \mathcal{H}_S , such that $-|L_O|e_k = -\mu_k^2 e_k$ with $0 = \mu_0^2 \leq \mu_1^2 \leq \dots$. Since $\dim \ker(-|L_O|) < \infty$, we assume e_0, e_1, \dots, e_{K_0} spans the kernel space of $-|L_O|$ for some $K_0 > 0$ with $\mu_0 = \mu_1 = \dots = \mu_{K_0} = 0$. The singular value gap $s(L_O)$ can be characterized by $s(L_O) = \inf_{k > K_0} \{\mu_k^2\} > 0$, by 6.1.

Now we define the time-augmented basis:

$$H_k^a = (t - (T - t)) e_k, \quad 0 \leq k \leq K_0, \quad (\text{E.13})$$

$$H_k^a = \left(e^{-\mu_k t} - e^{-\mu_k(T-t)} \right) e_k, \quad k > K_0, \quad (\text{E.14})$$

$$H_k^s = \left(e^{-\mu_k t} + e^{-\mu_k(T-t)} \right) e_k, \quad k > K_0, \quad (\text{E.15})$$

which constitutes an orthogonal basis of the subspace:

$$\mathbb{H} = \{X_t \in L^2_{\perp}([0, T]; \mathcal{H}_S); X_t \in H^2([0, T]; \mathcal{H}_S), \quad (\text{E.16})$$

$$X_t \in \text{Dom}(L_O) \text{ for a.e. } t, \partial_{tt}X_t - (-|L_O|)X_t = 0\}. \quad (\text{E.17})$$

It allows us to further decompose $L^2_{\perp}([0, T]; \mathcal{H}_S)$ into symmetric and antisymmetric modes with low and high energies:

$$L^2_{\perp}([0, T]; \mathcal{H}_S) = \underbrace{\mathbb{H}_{l,a} \oplus \mathbb{H}_{l,s} \oplus \mathbb{H}_{h,a} \oplus \mathbb{H}_{h,s}}_{=\mathbb{H}} \oplus \mathbb{H}^{\perp}, \quad (\text{E.18})$$

where:

$$\mathbb{H}_{l,a} = \text{Span} \left\{ H_k^a; \mu_k^2 \leq \frac{4}{T^2} \right\}, \quad \mathbb{H}_{l,s} = \text{Span} \left\{ H_k^s; \mu_k^2 \leq \frac{4}{T^2} \right\}, \quad (\text{E.19})$$

$$\mathbb{H}_{h,a} = \overline{\text{Span} \left\{ H_k^a; \mu_k^2 > \frac{4}{T^2} \right\}}, \quad \mathbb{H}_{h,s} = \overline{\text{Span} \left\{ H_k^s; \mu_k^2 > \frac{4}{T^2} \right\}}. \quad (\text{E.20})$$

Now we leverage the decomposition (E.18), and construct a coupled solution (Z_t, Y_t) in each subspace with Dirichlet form estimations.

Case 1: $X_t \in \mathbb{H}^{\perp}$. Define $\tilde{L}_O := \partial_{tt} - |L_O|$ on $L^2([0, T]; \mathcal{H}_S)$ with Neumann boundary condition in t and the domain given by

$$\text{Dom}(\tilde{L}_O) = \left\{ X_t \in L^2([0, T]; \mathcal{H}_O); X_t \in H^2([0, T]; \mathcal{H}_O), X_t \in \text{Dom}(L_O) \text{ for a.e. } t, \right. \quad (\text{E.21})$$

$$\left. \partial_t X_t|_{t=0,T} = 0, \tilde{L}_O(X_t) \in L^2([0, T]; \mathcal{H}_O) \right\}. \quad (\text{E.22})$$

Also note that:

$$\ker(\tilde{L}_O) = \{X_t \in L^2([0, T]; \mathcal{H}_S); X_t = X_0 \text{ for a.e. } t, X_0 \in \ker(L_O)\}. \quad (\text{E.23})$$

We denote P and \tilde{P} the projections to $\ker(L_O)$ and $\ker(\tilde{L}_O)$ respectively, which satisfies:

$$\tilde{P}X_t = \frac{1}{T} \int_0^T P X_t dt. \quad (\text{E.24})$$

Then by tensorization technique in [LL24, Lemma 4.5], we have the Poincaré inequality for \tilde{L}_O :

$$\|X_t - \tilde{P}X_t\|_{T, \mathcal{H}_O}^2 = \|X_t - \tilde{P}X_t\|_{T, \mathcal{H}_O}^2 + \|PX_t - \tilde{P}X_t\|_{T, \mathcal{H}_O}^2 \quad (\text{E.25})$$

$$\leq \frac{1}{s(L_O)} \mathcal{E}_{T, -|L_O|}(X_t) + \frac{T^2}{\pi^2} \|\partial_t PX_t\|_{T, \mathcal{H}_O}^2 \quad (\text{E.26})$$

$$\leq \max \left\{ \frac{1}{s(L_O)}, \frac{T^2}{\pi^2} \right\} \langle X_t, -\tilde{L}_O X_t \rangle_{T, \mathcal{H}_O}. \quad (\text{E.27})$$

It follows that $-\tilde{L}_O : \text{Dom}(\tilde{L}_O) \cap L^2_\perp([0, T]; \mathcal{H}_O) \rightarrow L^2_\perp([0, T]; \mathcal{H}_O)$ admits a bounded inverse:

$$\tilde{G} : L^2_\perp([0, T]; \mathcal{H}_O) \rightarrow \text{Dom}(\tilde{L}_O) \cap L^2_\perp([0, T]; \mathcal{H}_O), \quad (\text{E.28})$$

with operator norm bound:

$$\|\tilde{G}\|_{L^2_\perp([0, T]; \mathcal{H}_O) \rightarrow L^2_\perp([0, T]; \mathcal{H}_O)} \leq \max \left\{ \frac{1}{s(L_O)}, \frac{T^2}{\pi^2} \right\}. \quad (\text{E.29})$$

We define $Y_t = \tilde{G}X_t$ and $Z_t = -\partial_t Y_t$ that solves the divergence equation with $Z_t|_{t=0, T} = 0$ since $Y_t = \tilde{G}X_t$ satisfies Neumann boundary condition in t . To illustrate that Y_t satisfies the Dirichlet boundary condition, we take $W_t \in \mathbb{H}$, then the integration by parts gives:

$$0 = \langle W_t, X_t \rangle_{T, \mathcal{H}_O} = \langle W_t, -\tilde{L}_O Y_t \rangle_{T, \mathcal{H}_O} = \langle -\tilde{L}_O W_t, Y_t \rangle_{T, \mathcal{H}_O} + \langle \partial_t W_t, Y_t \rangle_{\mathcal{H}_O}|_{t=0}^{t=T}, \quad (\text{E.30})$$

which implies $Y_0 = Y_T = 0$ since $\tilde{L}_O W_t = 0$ and (E.30) holds for all $W_t|_{t=0, T} = 0$.

Now we estimate the energy. Firstly, we note that the operators ∂_{tt} and $-|L_O|$ on $L^2_\perp([0, T]; \mathcal{H}_O) \rightarrow \text{Dom}(\tilde{L}_O)$ commute and admit discrete spectrum, as demonstrated in [EGH⁺25]. Also, it holds that both the operator norms of $-|L_O|\tilde{G}$ and $\partial_{tt}\tilde{G}$ are bounded by 1. This allows us to conclude that in the case $X_t \in \mathbb{H}^\perp$, we have:

$$\| |L_O| Y_t \|_{T, \mathcal{H}_O} \leq \| |L_O| \tilde{G} X_t \|_{T, \mathcal{H}_O} \leq \| X_t \|_{T, \mathcal{H}_O}, \quad (\text{E.31})$$

$$\mathcal{E}_{T, -|L_O|}(Z_t) = \mathcal{E}_{T, -|L_O|}(\partial_t Y_t) = \langle \partial_{tt} \tilde{G} X_t, (-|L_O|) \tilde{G} X_t \rangle_{T, \mathcal{H}_O} \leq \| X_t \|_{T, \mathcal{H}_O}^2, \quad (\text{E.32})$$

$$\mathcal{E}_{T, -|L_O|}(Y_t) = -\langle \tilde{G} X_t, (-|L_O|) \tilde{G} X_t \rangle_{T, \mathcal{H}_O} \leq \max \left\{ \frac{1}{s(L_O)}, \frac{T^2}{\pi^2} \right\} \| X_t \|_{T, \mathcal{H}_O}^2, \quad (\text{E.33})$$

that is, the estimates hold with:

$$c_1 = c_2 = c_4 = 1, \quad c_3 = \max \left\{ \frac{1}{\sqrt{s(L_O)}}, \frac{T}{\pi} \right\}. \quad (\text{E.34})$$

Case 2: $X_t \in \mathbb{H}_{l,a}$. In this case, we set $Z_t = \int_0^t X_s ds$ and $y = 0$, which solves the equation with $Z_t|_{t=0, T} = Y_t|_{t=0, T}$. We estimate:

$$\| Z_t \|_{T, \mathcal{H}_S}^2 = \frac{1}{T} \int_0^T \left\langle \int_0^t X_s ds, \int_0^t X_s ds \right\rangle_{\mathcal{H}_S} dt \quad (\text{E.35})$$

$$\leq \frac{1}{T} \int_0^T t \int_0^t \langle X_s, X_s \rangle_{\mathcal{H}_S} ds dt \quad (\text{E.36})$$

$$\leq \int_0^T t dt \| X_t \|_{T, \mathcal{H}_S}^2 \quad (\text{E.37})$$

$$= \frac{T^2}{2} \| X_t \|_{T, \mathcal{H}_S}^2, \quad (\text{E.38})$$

where the second line comes from the convexity of $\|\cdot\|_{\mathcal{H}_S}^2$. Likewise, we have:

$$\|L_O|Z_t\|_{T,\mathcal{H}_S}^2 \leq \frac{1}{T} \int_0^T t dt \int_0^t \|L_O|X_s\|_{\mathcal{H}_S}^2 ds. \quad (\text{E.39})$$

From the definition of $\mathbb{H}_{l,a}$, we have:

$$\|L_O|Z_t\|_{T,\mathcal{H}_S}^2 \leq \frac{1}{T} \int_0^T t dt \int_0^t \|L_O|X_s\|_{\mathcal{H}_S}^2 ds \quad (\text{E.40})$$

$$\leq \frac{1}{T} \int_0^T t dt \int_0^t \frac{16}{T^4} \|X_s\|_{\mathcal{H}_S}^2 ds \quad (\text{E.41})$$

$$\leq \frac{8}{T^2} \|X_t\|_{T,\mathcal{H}_S}^2. \quad (\text{E.42})$$

Thus, it follows that by the Cauchy inequality that:

$$\mathcal{E}_{T,-|L_O|}(Z_t) \leq 2\|X_t\|_{T,\mathcal{H}_S}^2. \quad (\text{E.43})$$

Thus, we conclude that for $X_t \in \mathbb{H}_{l,a}$, we have:

$$c_1 = c_3 = c_4 = 0, \quad c_2 = \sqrt{2}. \quad (\text{E.44})$$

Case 3: $X_t \in \mathbb{H}_{l,s}$. Following [EL24b, Theorem 15], we consider decomposition $X_t = \overline{X_t^{(0)} + X_t^{(1)}}$, where $X_t^{(0)} = X_0 \cos(\frac{2\pi t}{T})$. By definition, there holds:

$$\int_0^T X_t^{(0)} dt = 0, \quad X_t^{(1)}|_{t=0,T} = 0. \quad (\text{E.45})$$

We then set $Z_t = \int_0^t X_s^{(0)} ds$ that satisfies the Dirichlet boundary condition on $[0, T]$, and $Y_t = GX_t^{(1)}$, where G is defined as the inverse of $|L_O|$ on finite-dimensional space $\text{Span}(\{e_k; 0 < \mu_k^2 \leq \frac{2}{T}\})$. Apparently, we have:

$$\partial_t Z_t - (-|L_O|)Y_t = X_t^{(0)} + X_t^{(1)} = X_t. \quad (\text{E.46})$$

It suffices to estimate the energy. Note that:

$$\|X_t^{(0)}\|_{T,\mathcal{H}_O}^2 = \frac{T}{2} \|x_0\|_{\mathcal{H}_O}^2 \quad (\text{E.47})$$

$$= \frac{T}{2} \sum_{0 < \mu_k \leq \frac{2}{T}} b_k^2 (1 + e^{-\mu_k T})^2 \quad (\text{E.48})$$

$$\leq 2T \sum_{0 < \mu_k \leq \frac{2}{T}} b_k^2 \quad (\text{E.49})$$

$$\leq \frac{e^2}{2} \|X_t\|_{T,\mathcal{H}_O}^2, \quad (\text{E.50})$$

and that under expansion $X_t = \sum_{0 < \mu_k \leq \frac{2}{T}} b_k H_A^s$:

$$\|X_t\|_{T, \mathcal{H}_S}^2 = \sum_{0 < \mu_k \leq \frac{2}{T}} b_k^2 \int_0^T \left(e^{-\mu_k t} + e^{-\mu_k(T-t)} \right)^2 dt \quad (\text{E.51})$$

$$\geq \sum_{0 < \mu_k \leq \frac{2}{T}} T b_k^2 \min_{t \in [0, T]} \left(e^{-\mu_k t} + e^{-\mu_k(T-t)} \right)^2 \quad (\text{E.52})$$

$$= \sum_{0 < \mu_k \leq \frac{2}{T}} 4e^{-\mu_k T} T b_k^2 \quad (\text{E.53})$$

$$\geq 4e^{-2T} \sum_{0 < \mu_k \leq \frac{2}{T}} b_k^2. \quad (\text{E.54})$$

Combining (E.50) and (E.54), we observe:

$$\|L_O|Y_t\|_{T, \mathcal{H}_O}^2 = \|X_t^{(1)}\|_{T, \mathcal{H}_O}^2 \leq (1 + e/\sqrt{2})^2 \|X_t\|_{T, \mathcal{H}_O}^2. \quad (\text{E.55})$$

Arguing by the same procedure as (E.43), we obtain:

$$\mathcal{E}_{T, -|L_O|}(Z_t) \leq 2\|X_t^{(0)}\|_{T, \mathcal{H}_O}^2 \leq e^2 \|X_t\|_{T, \mathcal{H}_O}^2. \quad (\text{E.56})$$

Applying the Poincaré inequality of $-|L_O|$ to (E.56) and combing the estimate of (E.55), we have:

$$\mathcal{E}_{T, -|L_O|}(Y_t) \leq \frac{1}{s(L_O)} \|L_O|Y_t\|_{T, \mathcal{H}_O}^2 \leq \frac{1}{s(L_O)} (1 + e/\sqrt{2})^2 \|X_t\|_{T, \mathcal{H}_O}^2, \quad (\text{E.57})$$

$$\mathcal{E}_{T, -|L_O|}(\partial_t Y_t) \leq \frac{1}{s(L_O)} \|\partial_t X_t^{(1)}\|_{T, \mathcal{H}_O}^2. \quad (\text{E.58})$$

Moreover, by the same argument as (E.50), we have:

$$\|\partial_t X_t^{(1)}\|_{T, \mathcal{H}_O} \leq \|\partial_t X_t^{(0)}\|_{T, \mathcal{H}_S} + \|\partial_t X_t\|_{T, \mathcal{H}_S} \quad (\text{E.59})$$

$$\leq \frac{\sqrt{2}\pi e + 2}{T} \|X_t\|_{T, \mathcal{H}_O}. \quad (\text{E.60})$$

Plugging (E.60) in (E.58), we derive:

$$\mathcal{E}_{T, -|L_O|}(\partial_t Y_t) \leq \frac{1}{s(L_O)} \|\partial_t X_t^{(1)}\|_{T, \mathcal{H}_O}^2 \quad (\text{E.61})$$

$$\leq \frac{(\sqrt{2}\pi e + 2)^2}{T^2 s(L_O)} \|X_t\|_{T, \mathcal{H}_O}^2. \quad (\text{E.62})$$

Thus, for $X_t \in \mathbb{H}_{l,s}$ we have:

$$c_1 = 1 + \frac{e}{\sqrt{2}}, c_2 = e, c_3 = \frac{1 + e/\sqrt{2}}{\sqrt{s(L_O)}}, c_4 = \frac{\sqrt{2}\pi e + 2}{\sqrt{s(L_O)}T}. \quad (\text{E.63})$$

Case 4: $X_t \in \mathbb{H}_{h,a}$. By completeness and linearity, it suffices to construct (Z_t, Y_t) for each basis $X_t = H_k^a = (e^{-\mu_k t} - e^{-\mu_k(T-t)}) e_k$ for $\mu_k \geq \frac{2}{T}$. We set $u_k(t) = e^{-\mu_k t} - e^{-\mu_k(T-t)}$, and consider the following ansatz:

$$Z_t = v_k(t) e_k, \quad Y_t = \frac{1}{\mu_k^2} w_k(t) e_k, \quad (\text{E.64})$$

with $v_k|_{t=0,T} = 0, w_k|_{t=0,T} = 0$. It follows from the construction that:

$$\partial_t Z_t - (-|L_O|) Y_t = (v'_k(t) + w_k(t)) e_k = u_k(t) e_k, \quad (\text{E.65})$$

or equivalently, $u_k(t) = v'_k(t) + w_k(t)$. Now we construct the functions v_k and w_k satisfying this condition as provided in [EL24b]. Firstly, we let:

$$\varphi_k(t) = (\mu_k t - 1)^2 \chi_{[0, \mu_k^{-1}]}(t) \in C^1([0, 1]), \quad (\text{E.66})$$

satisfying $\varphi_k(\frac{T}{2}) = 0$. Then, for $t \in [0, \frac{T}{2}]$, we define:

$$v_k(t) = \varphi_k(t) \int_0^t u_k(s) ds, \quad w_k(t) = u_k(t) - \dot{v}_k(t) = (1 - \varphi_k(t)) u_k(t) - \dot{\varphi}_k(t) \int_0^t u_k(s) ds, \quad (\text{E.67})$$

and for $t \in [\frac{T}{2}, T]$, we set:

$$v_k(t) = -\varphi_k(T-t) \int_t^T u_k(s) ds, \quad w_k(t) = u_k(t) - \dot{v}_k(t). \quad (\text{E.68})$$

Apparently, v_k and w_k constructed above are continuous and piecewise C^1 with $v_k|_{t=0} = v_k|_{t=T} = 0$. Also, we observe that:

$$w_k(0) = u_k(0) - \dot{v}_k(0) = 0, \quad w_k(T) = u_k(T) - \dot{v}_k(T) = 0. \quad (\text{E.69})$$

Furthermore, we have:

$$v_k\left(\frac{T}{2}\right) = \dot{v}_k\left(\frac{T}{2}\right) = 0, \quad \dot{v}_k(0) = u_k(0), \quad \dot{v}_k(T) = u_k(T). \quad (\text{E.70})$$

Hence, it suffices to attain energy estimation. We compute:

$$\|L_O|Y_t\|_{T, \mathcal{H}_O}^2 = \frac{1}{T} \int_0^T w_k^2(t) dt, \quad \mathcal{E}_{T, -|L_O|}(Z_t) = \frac{\mu_k^2}{T} \int_0^T v_k^2(t) dt, \quad (\text{E.71})$$

$$\mathcal{E}_{T, -|L_O|}(Y_t) = \frac{1}{\mu_k^2 T} \int_0^T w_k^2(t) dt, \quad \mathcal{E}_{T, -|L_O|}(\partial_t Y_t) = \frac{1}{\mu_k^2 T} \int_0^T \dot{w}_k^2(t) dt, \quad (\text{E.72})$$

and that $\|X_t\|_{T, \mathcal{H}_S}^2 = \frac{1}{T} \int_0^T u_k^2(t) dt$. Estimating such integrals as [EL24b] yields constants:

$$c_1 = 1 + \frac{1}{\sqrt{3}}, \quad c_2 = \frac{1}{\sqrt{30}}, \quad c_3 = \frac{T}{2} \left(1 + \frac{1}{\sqrt{3}}\right), \quad c_4 = 8. \quad (\text{E.73})$$

Case 5: $X_t \in \mathbb{H}_{h,s}$. This case can be obtained similarly as Case 4. We consider $X_t = \underline{H_k^s} = u_k(t)e_k$ for $\mu_k \geq \frac{2}{T}$, where $u_k = e^{-\mu_k t} + e^{-\mu_k(T-t)}$ and (Z_t, Y_t) has same ansatz as in (E.64). The constructions of v_k and w_k are identical to those of Case 4. The only difference occurs when we bound $\|X_t\|_{T,\mathcal{H}_S}^2 = \frac{1}{T} \int_0^T u_k^2(t) dt$ due to different u_k . By computations in [EL24b], we conclude that:

$$c_1 = 1 + \frac{1}{\sqrt{3}}, \quad c_2 = \frac{1}{\sqrt{30}}, \quad c_3 = \frac{T}{2} \left(1 + \frac{1}{\sqrt{3}} \right), \quad c_4 = 5 + \sqrt{2}. \quad (\text{E.74})$$

Combining (E.34), (E.44), (E.63), (E.73), and (E.74), the conclusion follows by rescaling. \square

Lemma E.2 (Coupling Strength Estimates, cf. Lemma 6.2). *Under Assumption 6.2, for sufficiently regular paths $X_t \in \text{Dom}(\mathcal{R})$ and $Y_t \in \text{Dom}(L_O)$, the following bounds hold:*

$$|\langle \mathcal{R}X_t, S\mathcal{V}Y_t \rangle_{\mathcal{H}}| \leq \sqrt{\mathcal{E}_{\mathcal{R}}(X_t)(\mathcal{E}_{-|L_O|}(Y_t) + \eta C_{AQF} \|Y_t\|_{\mathcal{H}}^2)}, \quad (\text{E.75})$$

$$|\langle X_t - P_S X_t, \mathcal{V}Y_t \rangle_{\mathcal{H}}| \leq \sqrt{\mathcal{E}_{\mathcal{R}}(X_t)(\mathcal{E}_{-|L_O|}(Y_t) + \eta C_{AQF} \|Y_t\|_{\mathcal{H}}^2)}, \quad (\text{E.76})$$

$$|\langle \mathcal{V}(X_t - P_S X_t), S\mathcal{V}Y_t \rangle_{\mathcal{H}}| \leq \|X_t - P_S X_t\|_{\mathcal{H}} \left(K_2 \|L_O|Y_t\|_{\mathcal{H}_S} + K_3 \sqrt{\mathcal{E}_{-|L_O|}(Y_t)} \right). \quad (\text{E.77})$$

Proof. We establish each inequality in turn, using the Cauchy-Schwarz inequality, the Ad Embed structure (Definition 5.1), and Assumption 6.2. Let $X_t^F = X_t - P_S X_t$. Note that $\mathcal{E}_{\mathcal{R}}(X_t) = -\langle X_t, \mathcal{R}X_t \rangle = -\langle X_t^F, \mathcal{R}X_t^F \rangle = \mathcal{E}_{\mathcal{R}}(X_t^F)$.

Proof of first inequality: We manipulate the inner product using $S^{1/2}$.

$$\langle \mathcal{R}X_t, S\mathcal{V}Y_t \rangle = \langle S^{1/2}\mathcal{R}X_t, S^{1/2}\mathcal{V}Y_t \rangle \quad (\text{E.78})$$

$$\leq \|S^{1/2}\mathcal{R}X_t\| \|S^{1/2}\mathcal{V}Y_t\| \quad (\text{by C-S}). \quad (\text{E.79})$$

We evaluate the norms. First, $\|S^{1/2}\mathcal{R}X_t\|^2 = \langle \mathcal{R}X_t, S\mathcal{R}X_t \rangle = \langle X_t, \mathcal{R}S\mathcal{R}X_t \rangle$. Since $\mathcal{R}S\mathcal{R} = \mathcal{R}(-\mathcal{R}^+)\mathcal{R} = -\mathcal{R}$ on \mathcal{H}_F , this becomes $\langle X_t^F, -\mathcal{R}X_t^F \rangle = \mathcal{E}_{\mathcal{R}}(X_t^F) = \mathcal{E}_{\mathcal{R}}(X_t)$. Thus, $\|S^{1/2}\mathcal{R}X_t\| = \sqrt{\mathcal{E}_{\mathcal{R}}(X_t)}$. Second, from the explicit Approximate Quadratic Form condition (5.3) with $X = Y = Y_t$: $\|S^{1/2}\mathcal{V}Y_t\|^2 = \langle \mathcal{V}Y_t, S\mathcal{V}Y_t \rangle \leq \langle Y_t, |L_O|Y_t \rangle + \eta C_{AQF} \|Y_t\|_{\mathcal{H}}^2 = \mathcal{E}_{-|L_O|}(Y_t) + \eta C_{AQF} \|Y_t\|_{\mathcal{H}}^2$. Combining these gives:

$$|\langle \mathcal{R}X_t, S\mathcal{V}Y_t \rangle| \leq \sqrt{\mathcal{E}_{\mathcal{R}}(X_t)(\mathcal{E}_{-|L_O|}(Y_t) + \eta C_{AQF} \|Y_t\|_{\mathcal{H}}^2)}. \quad (\text{E.80})$$

Proof of second inequality: We use $S^{1/2}$ and $S^{-1/2} = \sqrt{-\mathcal{R}|_{\mathcal{H}_F}}$ on \mathcal{H}_F .

$$\langle X_t^F, \mathcal{V}Y_t \rangle = \langle S^{-1/2}X_t^F, S^{1/2}\mathcal{V}Y_t \rangle \quad (\text{E.81})$$

$$\leq \|S^{-1/2}X_t^F\| \|S^{1/2}\mathcal{V}Y_t\| \quad (\text{by C-S}). \quad (\text{E.82})$$

We evaluate $\|S^{-1/2}X_t^F\|^2 = \langle X_t^F, S^{-1}X_t^F \rangle = \langle X_t^F, (-\mathcal{R})X_t^F \rangle = \mathcal{E}_{\mathcal{R}}(X_t^F) = \mathcal{E}_{\mathcal{R}}(X_t)$. Thus, $\|S^{-1/2}X_t^F\| = \sqrt{\mathcal{E}_{\mathcal{R}}(X_t)}$. Using the result for $\|S^{1/2}\mathcal{V}Y_t\|$ from the previous step:

$$|\langle X_t^F, \mathcal{V}Y_t \rangle| \leq \sqrt{\mathcal{E}_{\mathcal{R}}(X_t)(\mathcal{E}_{-|L_O|}(Y_t) + \eta C_{AQF}\|Y_t\|_{\mathcal{H}}^2)}. \quad (\text{E.83})$$

Proof of third inequality: We move the operator \mathcal{V} using the adjoint.

$$\langle \mathcal{V}X_t^F, S\mathcal{V}Y_t \rangle = \langle X_t^F, \mathcal{V}^*S\mathcal{V}Y_t \rangle \quad (\text{E.84})$$

$$= \langle X_t^F, (\mathbf{1} - P_S)\mathcal{V}^*S\mathcal{V}Y_t \rangle \quad (\text{since } X_t^F \in \mathcal{H}_F). \quad (\text{E.85})$$

Applying Cauchy-Schwarz:

$$|\langle \mathcal{V}X_t^F, S\mathcal{V}Y_t \rangle| \leq \|X_t^F\| \|(\mathbf{1} - P_S)\mathcal{V}^*S\mathcal{V}Y_t\|. \quad (\text{E.86})$$

Using Assumption 6.2(3):

$$|\langle \mathcal{V}X_t^F, S\mathcal{V}Y_t \rangle| \leq \|X_t - P_S X_t\|_{\mathcal{H}} \left(K_2 \|L_O|Y_t\|_{\mathcal{H}_S} + K_3 \sqrt{\mathcal{E}_{-|L_O|}(Y_t)} \right). \quad (\text{E.87})$$

This completes the proof of all three inequalities. \square

Theorem E.2 (Flow Poincaré Inequality for Ad Embed, cf. Theorem 6.3). *Let C_{AQF} be the constant from the Approximate Quadratic Form condition. Assume η is sufficiently small such that $1 - \eta C_{corr} > 0$, where $C_{corr} = C_{AQFS}(L_O)^{-1}c_1(T)$ is a correction constant derived in the proof. Under Assumption 6.2, for any $T > 0$ and initial state $X_0 \in \mathcal{F}^\perp \cap \text{Dom}(L)$, the trajectory $X_t = P_t X_0$ satisfies:*

$$\alpha_T(\eta) \|X_t\|_{T,\mathcal{H}}^2 \leq \mathcal{E}_{T,\mathcal{R}}(X_t), \quad (\text{E.88})$$

with

$$\alpha_T(\eta) = \left[\frac{2\tilde{A}_1(T, \eta)^2\gamma^2 + 4\tilde{A}_1(T, \eta)\tilde{A}_2(T, \eta)\gamma + 2\tilde{A}_2(T, \eta)^2}{(1 - \eta C_{corr})^2} + \frac{1}{\lambda_R} \right]^{-1}, \quad (\text{E.89})$$

where the η -dependent coefficients are:

$$\tilde{A}_1(T, \eta) = c_3(T) + \sqrt{\eta C_{AQFS}}(L_O)^{-1}c_1(T), \quad (\text{E.90})$$

$$\begin{aligned} \tilde{A}_2(T, \eta) &= K_1 c_2(T) + \lambda_R^{-1/2} (\|S\|^{1/2} c_4(T) + K_2 c_1(T) + K_3 c_2(T)) \\ &\quad + \sqrt{\eta C_{AQF}} K_1 s(L_O)^{-1/2} c_2(T). \end{aligned} \quad (\text{E.91})$$

Here, $c_i(T)$ are constants defined in Theorem 6.2.

Proof. Let $X_t = P_t X_0$ be the trajectory evolving under the generator $L = \gamma\mathcal{R} + \mathcal{V}$. We denote by P_S the orthogonal projection onto the slow subspace $\mathcal{H}_S = \ker(\mathcal{R})$, and let $X_t^F = (\mathbf{1} - P_S)X_t$ be the component in the fast subspace \mathcal{H}_F . By assumption, the projected path $P_S X_t$ lies in $L_{\perp}^2([0, T]; \mathcal{H}_S)$.

The proof strategy relies on decomposing the total norm $\|X_t\|_{T,\mathcal{H}}^2$ into slow and fast components and bounding each in relation to the dissipation $\mathcal{E}_{T,\mathcal{R}}(X_t) = \frac{1}{T} \int_0^T \mathcal{E}_{\mathcal{R}}(X_t) dt$. The orthogonal decomposition yields:

$$\|X_t\|_{T,\mathcal{H}}^2 = \|P_S X_t\|_{T,\mathcal{H}_S}^2 + \|X_t^F\|_{T,\mathcal{H}}^2. \quad (\text{E.92})$$

The fast component is controlled by the coercivity of \mathcal{R} on \mathcal{H}_F (gap $\lambda_R > 0$):

$$\|X_t^F\|_{T,\mathcal{H}}^2 \leq \frac{1}{\lambda_R} \mathcal{E}_{T,\mathcal{R}}(X_t^F) = \frac{1}{\lambda_R} \mathcal{E}_{T,\mathcal{R}}(X_t). \quad (\text{E.93})$$

The central task is to estimate the slow component $\|P_S X_t\|_{T,\mathcal{H}_S}^2$. We employ the auxiliary paths (Z_t, Y_t) solving the abstract divergence equation $\partial_t Z_t + |L_O| Y_t = P_S X_t$, as guaranteed by Theorem 6.2. Integrating by parts and applying the Inner Product Reduction Lemma E.1 leads to the identity:

$$\|P_S X_t\|_{T,\mathcal{H}_S}^2 = \langle \mathcal{A} P_S X_t, Z_t + S V Y_t \rangle_{T,\mathcal{H}} + R_{T,\eta}(P_S X, Y), \quad (\text{E.94})$$

where the remainder term satisfies $|R_{T,\eta}(P_S X, Y)| \leq \eta C_{AQF} \frac{1}{T} \int_0^T \|P_S X_t\|_{\mathcal{H}} \|Y_t\|_{\mathcal{H}} dt$. We decompose the inner product term using $P_S X_t = X_t - X_t^F$:

$$\langle \mathcal{A} P_S X_t, Z_t + S V Y_t \rangle_{T,\mathcal{H}} = \langle \mathcal{A} X_t, Z_t + S V Y_t \rangle_{T,\mathcal{H}} - \langle \mathcal{A} X_t^F, Z_t + S V Y_t \rangle_{T,\mathcal{H}}. \quad (\text{E.95})$$

Using $\mathcal{A} X_t = -\gamma \mathcal{R} X_t$ and $\mathcal{A} X_t^F = -\partial_t X_t^F + V X_t^F$, and performing integration by parts on the time derivative terms (while noting $\langle \mathcal{R} X_t, Z_t \rangle = 0$ and $\langle X_t^F, \partial_t Z_t \rangle = 0$), we arrive at the identity:

$$\begin{aligned} \|P_S X_t\|_{T,\mathcal{H}_S}^2 &\leq \gamma |\langle \mathcal{R} X_t, S V Y_t \rangle_{T,\mathcal{H}}| \quad (\text{Term 1}) \\ &\quad + |\langle V X_t^F, Z_t \rangle_{T,\mathcal{H}}| \quad (\text{Term 2}) \\ &\quad + |\langle X_t^F, \partial_t(S V Y_t) \rangle_{T,\mathcal{H}}| \quad (\text{Term 3}) \\ &\quad + |\langle V X_t^F, S V Y_t \rangle_{T,\mathcal{H}}| \quad (\text{Term 4}) \\ &\quad + |R_{T,\eta}(P_S X, Y)|. \end{aligned} \quad (\text{E.96})$$

Now we deal with all these terms one by one, using the explicit bounds from Lemma E.2. For Term 1, we note that $\|Y_t\|_{T,\mathcal{H}} \leq s(L_O)^{-1} c_1(T) \|P_S X_t\|_{T,\mathcal{H}_S}$. Thus:

$$\gamma |\langle \mathcal{R} X_t, S V Y_t \rangle_{T,\mathcal{H}}| \leq \gamma \sqrt{\mathcal{E}_{T,\mathcal{R}}(X_t) (\mathcal{E}_{T,-|L_O|}(Y_t) + \eta C_{AQF} \|Y_t\|_{T,\mathcal{H}}^2)} \quad (\text{E.97})$$

$$\leq \gamma \sqrt{\mathcal{E}_{T,\mathcal{R}}(X_t)} \left(\sqrt{\mathcal{E}_{T,-|L_O|}(Y_t)} + \sqrt{\eta C_{AQF}} \|Y_t\|_{T,\mathcal{H}} \right) \quad (\text{E.98})$$

$$\leq \gamma \sqrt{\mathcal{E}_{T,\mathcal{R}}(X_t)} \left(c_3(T) + \sqrt{\eta C_{AQF}} s(L_O)^{-1} c_1(T) \right) \|P_S X_t\|_{T,\mathcal{H}_S}. \quad (\text{E.99})$$

For Term 2, using $\|Z_t\|_{T,\mathcal{H}} \leq s(L_O)^{-1/2} c_2(T) \|P_S X_t\|_{T,\mathcal{H}_S}$:

$$|\langle \mathcal{V}X_t^F, Z_t \rangle_{T,\mathcal{H}}| \leq K_1 \sqrt{\mathcal{E}_{T,\mathcal{R}}(X_t)} \left(\sqrt{\mathcal{E}_{T,-|L_O|}(Z_t)} + \sqrt{\eta C_{AQF}} \|Z_t\|_{T,\mathcal{H}} \right) \quad (\text{E.100})$$

$$\leq K_1 \sqrt{\mathcal{E}_{T,\mathcal{R}}(X_t)} \left(c_2(T) + \sqrt{\eta C_{AQF}} s(L_O)^{-1/2} c_2(T) \right) \|P_S X_t\|_{T,\mathcal{H}_S}. \quad (\text{E.101})$$

For Term 3:

$$|\langle X_t^F, \partial_t(S\mathcal{V}Y_t) \rangle_{T,\mathcal{H}}| \leq \|S\|^{1/2} \lambda_R^{-1/2} c_4(T) \sqrt{\mathcal{E}_{T,\mathcal{R}}(X_t)} \|P_S X_t\|_{T,\mathcal{H}_S}. \quad (\text{E.102})$$

For Term 4:

$$|\langle \mathcal{V}X_t^F, S\mathcal{V}Y_t \rangle_{T,\mathcal{H}}| \leq \lambda_R^{-1/2} \sqrt{\mathcal{E}_{T,\mathcal{R}}(X_t)} (K_2 c_1(T) + K_3 c_3(T)) \|P_S X_t\|_{T,\mathcal{H}_S}. \quad (\text{E.103})$$

For the remainder term:

$$|R_{T,\eta}(P_S X, Y)| \leq \eta C_{AQF} \frac{1}{T} \int_0^T \|P_S X_t\|_{\mathcal{H}} \|Y_t\|_{\mathcal{H}} dt \quad (\text{E.104})$$

$$\leq \eta C_{AQF} \|P_S X_t\|_{T,\mathcal{H}_S} \|Y_t\|_{T,\mathcal{H}} \quad (\text{E.105})$$

$$\leq \eta C_{AQF} s(L_O)^{-1} c_1(T) \|P_S X_t\|_{T,\mathcal{H}_S}^2. \quad (\text{E.106})$$

Let's define $\eta C_{corr} = \eta C_{AQF} s(L_O)^{-1} c_1(T)$. Combining all estimates:

$$\|P_S X_t\|_{T,\mathcal{H}_S}^2 \leq (\gamma \tilde{A}_1(T, \eta) + \tilde{A}_2(T, \eta)) \sqrt{\mathcal{E}_{T,\mathcal{R}}(X_t)} \|P_S X_t\|_{T,\mathcal{H}_S} + \eta C_{corr} \|P_S X_t\|_{T,\mathcal{H}_S}^2, \quad (\text{E.107})$$

where $\tilde{A}_1(T, \eta) = c_3(T) + \sqrt{\eta C_{AQF}} s(L_O)^{-1} c_1(T)$ and $\tilde{A}_2(T, \eta)$ is the sum of the other coefficients. Rearranging, and assuming η is small enough that $1 - \eta C_{corr} > 0$:

$$(1 - \eta C_{corr}) \|P_S X_t\|_{T,\mathcal{H}_S}^2 \leq (\gamma \tilde{A}_1(T, \eta) + \tilde{A}_2(T, \eta)) \sqrt{\mathcal{E}_{T,\mathcal{R}}(X_t)} \|P_S X_t\|_{T,\mathcal{H}_S}. \quad (\text{E.108})$$

Dividing by $\|P_S X_t\|_{T,\mathcal{H}_S}$ (if non-zero, else trivial):

$$\|P_S X_t\|_{T,\mathcal{H}_S} \leq \frac{\gamma \tilde{A}_1(T, \eta) + \tilde{A}_2(T, \eta)}{1 - \eta C_{corr}} \sqrt{\mathcal{E}_{T,\mathcal{R}}(X_t)}. \quad (\text{E.109})$$

Plugging this into the decomposition $\|X_t\|_{T,\mathcal{H}}^2 = \|P_S X_t\|^2 + \|X_t^F\|^2$:

$$\|X_t\|_{T,\mathcal{H}}^2 \leq \left(\frac{\gamma \tilde{A}_1(T, \eta) + \tilde{A}_2(T, \eta)}{1 - \eta C_{corr}} \right)^2 \mathcal{E}_{T,\mathcal{R}}(X_t) + \frac{1}{\lambda_R} \mathcal{E}_{T,\mathcal{R}}(X_t) \quad (\text{E.110})$$

$$= \left[\frac{(\gamma \tilde{A}_1(T, \eta) + \tilde{A}_2(T, \eta))^2}{(1 - \eta C_{corr})^2} + \frac{1}{\lambda_R} \right] \mathcal{E}_{T,\mathcal{R}}(X_t). \quad (\text{E.111})$$

Defining $\alpha_T(\eta)$ as the inverse of the bracketed term yields the desired inequality. \square

Theorem E.3 (*T*-Average Convergence Lower Bound, cf. Theorem 6.4). *Let the generator $L = \gamma\mathcal{R} + \mathcal{V}$ satisfy the assumptions of Theorem 6.3. Assume η is sufficiently small such that $\alpha_T(\eta) > 0$. For any observation period $T > 0$, provided the effective rate ν_{eff} defined below is positive, any initial state $X_0 \in \mathcal{F}^\perp \cap \text{Dom}(L)$ exhibits time-averaged strict exponential decay bounded by:*

$$\frac{1}{T} \int_t^{t+T} \|P_s X_0\|_{\mathcal{H}}^2 ds \leq e^{-2\nu_{\text{eff}} t} \|X_0\|_{\mathcal{H}}^2, \quad (\text{E.112})$$

where the decay rate parameter ν_{eff} depends on γ, η, T as

$$\nu_{\text{eff}} = \nu_{\text{eff}}(\gamma, \eta, T) := \gamma\alpha_T(\eta) - \eta\|L_{\text{pert}}\|. \quad (\text{E.113})$$

Proof. The proof is a standard Grönwall-type argument based on Theorem 6.3. We begin by defining the T -averaged energy functional for a trajectory X :

$$E_T(t) := \frac{1}{T} \int_t^{t+T} \|X_s\|_{\mathcal{H}}^2 ds. \quad (\text{E.114})$$

Taking the time derivative and using the fundamental theorem of calculus, we have:

$$\frac{d}{dt} E_T(t) = \frac{1}{T} (\|X_{t+T}\|_{\mathcal{H}}^2 - \|X_t\|_{\mathcal{H}}^2) \quad (\text{E.115})$$

$$= \frac{1}{T} \int_t^{t+T} \frac{d}{ds} \|X_s\|_{\mathcal{H}}^2 ds \quad (\text{E.116})$$

$$= \frac{2}{T} \int_t^{t+T} \text{Re}\langle X_s, L X_s \rangle_{\mathcal{H}} ds. \quad (\text{E.117})$$

Note that $L = \mathcal{V} + \gamma\mathcal{R} = L_{\text{ham}} + \eta L_{\text{pert}} + \gamma\mathcal{R}$, and L_{ham} is skew-adjoint, we have:

$$\frac{d}{dt} E_T(t) = \frac{2}{T} \int_t^{t+T} \text{Re}\langle X_s, (\eta L_{\text{pert}} + \gamma\mathcal{R}) X_s \rangle_{\mathcal{H}} ds \quad (\text{E.118})$$

$$= \frac{2\eta}{T} \int_t^{t+T} \text{Re}\langle X_s, L_{\text{pert}} X_s \rangle_{\mathcal{H}} ds + \frac{2\gamma}{T} \int_t^{t+T} \langle X_s, \mathcal{R} X_s \rangle_{\mathcal{H}} ds. \quad (\text{E.119})$$

Selecting time interval $[t, t+T]$ in Theorem 6.3, we have:

$$- \int_t^{t+T} \langle X_s, \mathcal{R} X_s \rangle_{\mathcal{H}} ds = \mathcal{E}_{T,\mathcal{R}}(X_t) \geq \alpha_T(\eta) \int_t^{t+T} \|X_s\|_{\mathcal{H}}^2 ds = \alpha_T(\eta) T E_T(t). \quad (\text{E.120})$$

On the other hand, as for the perturbation, we note that:

$$\frac{2\eta}{T} \int_t^{t+T} \text{Re}\langle X_s, L_{\text{pert}} X_s \rangle_{\mathcal{H}} ds \leq 2\eta\|L_{\text{pert}}\| \frac{1}{T} \int_t^{t+T} \|X_s\|_{\mathcal{H}}^2 ds = 2\eta\|L_{\text{pert}}\| E_T(t). \quad (\text{E.121})$$

Plugging them into the time derivative:

$$\frac{d}{dt}E_T(t) \leq -2\gamma\alpha_T(\eta)E_T(t) + 2\eta\|L_{\text{pert}}\|E_T(t) = -2(\gamma\alpha_T(\eta) - \eta\|L_{\text{pert}}\|)E_T(t). \quad (\text{E.122})$$

Applying Grönwall's inequality, we have:

$$E_T(t) \leq E_T(0) \exp(-2\nu_{\text{eff}}t), \quad (\text{E.123})$$

where $\nu_{\text{eff}} = \gamma\alpha_T(\eta) - \eta\|L_{\text{pert}}\|$. By contractivity of the semigroup, $E_T(0) = \frac{1}{T} \int_0^T \|X_s\|_{\mathcal{H}}^2 ds \leq \|X_0\|_{\mathcal{H}}^2$. Thus:

$$\frac{1}{T} \int_t^{t+T} \|X_s\|_{\mathcal{H}}^2 ds \leq \exp(-2\nu_{\text{eff}}t) \|X_0\|_{\mathcal{H}}^2, \quad (\text{E.124})$$

as desired. \square

Corollary E.1 (Near-optimal Selection of γ , cf. Corollary 6.1). *Assume η is sufficiently small such that $\alpha_T(\eta) > 0$. Under the assumptions of Theorem 6.4, for any $T > 0$ and initial state $X_0 \in \mathcal{F}^\perp \cap \text{Dom}(L)$, the trajectory $X_t = P_t X_0$ satisfies the pointwise decay bound:*

$$\|X_t\|_{\mathcal{H}} \leq C_T e^{-\nu_{\text{eff}}t} \|X_0\|_{\mathcal{H}}, \quad (\text{E.125})$$

where the decay rate is $\nu_{\text{eff}} = \gamma\alpha_T(\eta) - \eta\|L_{\text{pert}}\|$ and the prefactor is $C_T = e^{\nu_{\text{eff}}T}$.

Furthermore, for a fixed T , the lower bound on the decay rate ν_{eff} is maximized by choosing γ near-optimally as

$$\gamma_{\text{opt}}(T) = \frac{1}{\tilde{A}_1(T, \eta)} \sqrt{\tilde{A}_2(T, \eta)^2 + \frac{(1 - \eta C_{\text{corr}})^2}{2\lambda_R}}, \quad (\text{E.126})$$

where $\tilde{A}_1(T, \eta)$, $\tilde{A}_2(T, \eta)$ and C_{corr} are the constants defined in the proof of Theorem 6.3. This choice yields the corresponding maximal rate lower bound:

$$\nu_{\text{opt}}(T) = \frac{1 - \eta C_{\text{corr}}}{2\sqrt{2}\tilde{A}_1 \left(\sqrt{2}\tilde{A}_2 + \sqrt{2\tilde{A}_2^2 + \frac{(1 - \eta C_{\text{corr}})^2}{\lambda_R}} \right)} - \eta\|L_{\text{pert}}\|. \quad (\text{E.127})$$

For compactness, let $\hat{A}_i = \frac{\sqrt{2}\tilde{A}_i}{1 - \eta C_{\text{corr}}}$, then $\nu_{\text{opt}}(T) = \frac{1}{2\hat{A}_1(\hat{A}_2 + \sqrt{\hat{A}_2^2 + \lambda_R^{-1}})} - \eta\|L_{\text{pert}}\|$.

Proof. Since the semigroup $\{P_t\}_{t \geq 0}$ is contractive, the function $s \rightarrow \|X_s\|_{\mathcal{H}}^2$ is non-increasing. Therefore, for all $s \in [t, t+T]$, we have $\|X_{t+T}\|_{\mathcal{H}}^2 \leq \|X_s\|_{\mathcal{H}}^2$. Integrating over $[t, t+T]$ yields:

$$\|X_{t+T}\|_{\mathcal{H}}^2 \leq \frac{1}{T} \int_t^{t+T} \|X_s\|_{\mathcal{H}}^2 ds \leq \exp(-2\nu_{\text{eff}}t) \|X_0\|_{\mathcal{H}}^2. \quad (\text{E.128})$$

We perform a time translation to obtain the hypocoercive bound. Set $t' = t + T$, namely $t = t' - T$, the inequality above gives:

$$\|X_{t'}\|_{\mathcal{H}}^2 \leq \exp(2\nu_{\text{eff}}T) \exp(-2\nu_{\text{eff}}t') \|X_0\|_{\mathcal{H}}^2. \quad (\text{E.129})$$

Taking the square root, we have:

$$\|X_t\|_{\mathcal{H}} \leq C_T \exp(-\nu_{\text{eff}}t) \|X_0\|_{\mathcal{H}}, \quad (\text{E.130})$$

where $C_T = \exp(\nu_{\text{eff}}T)$.

To compute the optimal γ , we maximize $\nu_{\text{eff}}(\gamma) = \gamma\alpha_T(\eta) - \eta\|L_{\text{pert}}\|$. It suffices to maximize $f(\gamma) = \gamma\alpha_T(\eta)$. Let $\widehat{A}_1 = \frac{\sqrt{2}\tilde{A}_1(T,\eta)}{1-\eta C_{\text{corr}}}$ and $\widehat{A}_2 = \frac{\sqrt{2}\tilde{A}_2(T,\eta)}{1-\eta C_{\text{corr}}}$. From Theorem 6.3, $\alpha_T(\eta)^{-1} = \widehat{A}_1^2\gamma^2 + 2\widehat{A}_1\widehat{A}_2\gamma + \widehat{A}_2^2 + \lambda_R^{-1}$. We maximize $f(\gamma) = \frac{\gamma}{\widehat{A}_1^2\gamma^2 + 2\widehat{A}_1\widehat{A}_2\gamma + \widehat{A}_2^2 + \lambda_R^{-1}}$. The maximum occurs at $\gamma_{\text{opt}} = \frac{\sqrt{\widehat{A}_2^2 + \lambda_R^{-1}}}{\widehat{A}_1} = \frac{1}{\widehat{A}_1(T,\eta)} \sqrt{\tilde{A}_2(T,\eta)^2 + \frac{(1-\eta C_{\text{corr}})^2}{2\lambda_R}}$. The maximal value is $f(\gamma_{\text{opt}}) = \frac{1}{2\widehat{A}_1(\widehat{A}_2 + \sqrt{\widehat{A}_2^2 + \lambda_R^{-1}})}$. Substituting this back into the expression for ν_{eff} gives the stated result. \square

Corollary E.2 (Strict Asymptotic Rate Scaling, cf. Corollary 6.2). *Let $s := s(L_O)$ denote the singular value gap of the target effective generator. Under the assumptions of Theorem 6.3, suppose the structural constants satisfy the scaling conditions $K_1, K_2, \lambda_R, \|S\| = \Theta(1)$ and $K_3 = \Theta(\sqrt{s})$. Assume further that the Approximate Quadratic Form constant scales inversely with the gap, $C_{AQF} = \Theta(s^{-1})$, and that the non-conservative perturbation strength is strictly subdominant to the squared gap, specifically:*

$$\eta = o(s^2) \quad \text{as } s \rightarrow 0. \quad (\text{E.131})$$

Then, by choosing the observation time optimally as $T_{\text{opt}} = cs^{-1/2}$ for some constant $c > 0$, the maximal convergence rate lower bound exhibits the strict asymptotic scaling:

$$\nu_{\text{opt}}(T_{\text{opt}}) = \Theta(\sqrt{s}) \quad \text{as } s \rightarrow 0. \quad (\text{E.132})$$

Moreover, the associated prefactor $C_{T_{\text{opt}}} = e^{\nu_{\text{opt}}T_{\text{opt}}}$ remains asymptotically bounded, $C_{T_{\text{opt}}} = \Theta(1)$.

Proof. We rigorously bound the terms in the expression $\nu_{\text{opt}}(T) = \frac{1-\eta C_{\text{corr}}}{D(T)} - \eta\|L_{\text{pert}}\|$.

First, we analyze the stability of the flow correction factor. Recall from Theorem 6.3 that $C_{\text{corr}} = C_{AQF}c_1(T)s^{-1}$. Using the premise $C_{AQF} = \Theta(s^{-1})$ and noting that at the optimal time scale $T_{\text{opt}} = \Theta(s^{-1/2})$, the energy constant satisfies $c_1(T_{\text{opt}}) = \Theta(1)$, the correction factor scales as:

$$C_{\text{corr}} = \Theta(s^{-1}) \cdot \Theta(1) \cdot s^{-1} = \Theta(s^{-2}). \quad (\text{E.133})$$

Under the assumption $\eta = o(s^2)$, the product $\eta C_{\text{corr}} = o(s^2) \cdot \Theta(s^{-2}) = o(1)$. This guarantees the strict positivity condition $1 - \eta C_{\text{corr}} = 1 - o(1)$, which is well-behaved asymptotically.

Next, we estimate the η -dependent coefficients \tilde{A}_1 and \tilde{A}_2 . For \tilde{A}_1 , recalling that $c_3(T_{opt}) = \Theta(s^{-1/2})$:

$$\tilde{A}_1(T_{opt}) = c_3(T_{opt}) + \sqrt{\eta C_{AQF}} s^{-1} c_1(T_{opt}) \quad (\text{E.134})$$

$$= \Theta(s^{-1/2}) + \sqrt{o(s^2)\Theta(s^{-1})} \cdot s^{-1} \cdot \Theta(1) \quad (\text{E.135})$$

$$= \Theta(s^{-1/2}) + o(\sqrt{s}) \cdot s^{-1} \quad (\text{E.136})$$

$$= \Theta(s^{-1/2}) + o(s^{-1/2}) = \Theta(s^{-1/2}). \quad (\text{E.137})$$

For \tilde{A}_2 , we utilize the assumption $K_3 = \Theta(\sqrt{s})$, which implies the unperturbed term $A_2(T_{opt}) = \Theta(1)$:

$$\tilde{A}_2(T_{opt}) = A_2(T_{opt}) + \sqrt{\eta C_{AQF}} K_1 s^{-1/2} c_2(T_{opt}) \quad (\text{E.138})$$

$$= \Theta(1) + \sqrt{o(s^2)\Theta(s^{-1})} \cdot \Theta(1) \cdot s^{-1/2} \cdot \Theta(1) \quad (\text{E.139})$$

$$= \Theta(1) + o(\sqrt{s}) \cdot s^{-1/2} \quad (\text{E.140})$$

$$= \Theta(1) + o(1) = \Theta(1). \quad (\text{E.141})$$

We now bound the denominator $D(T_{opt})$ appearing in the rate expression:

$$D(T_{opt}) = \frac{2\sqrt{2}\tilde{A}_1}{1 - \eta C_{corr}} \left(\frac{\sqrt{2}\tilde{A}_2}{1 - \eta C_{corr}} + \sqrt{\frac{2\tilde{A}_2^2}{(1 - \eta C_{corr})^2} + \frac{1}{\lambda_R}} \right) \quad (\text{E.142})$$

$$= \frac{\Theta(s^{-1/2})}{1 - o(1)} \left(\Theta(1) + \sqrt{\Theta(1) + \Theta(1)} \right) \quad (\text{E.143})$$

$$= \Theta(s^{-1/2}). \quad (\text{E.144})$$

Finally, substituting these asymptotic forms back into ν_{opt} :

$$\nu_{opt}(T_{opt}) = \frac{1 - o(1)}{\Theta(s^{-1/2})} - \eta \|L_{\text{pert}}\| \quad (\text{E.145})$$

$$= \Theta(\sqrt{s}) - o(s^2) = \Theta(\sqrt{s}). \quad (\text{E.146})$$

The perturbative decay term $\eta \|L_{\text{pert}}\|$ is negligible because $o(s^2)$ vanishes strictly faster than the lifting rate \sqrt{s} as $s \rightarrow 0$. The prefactor exponent is $\nu_{opt} T_{opt} = \Theta(\sqrt{s}) \cdot \Theta(s^{-1/2}) = \Theta(1)$, implying $C_{T_{opt}} = e^{\Theta(1)} = \Theta(1)$. \square